**Combustion of biomass in fluidized beds.**
**A review of key phenomena and future perspectives**

K.Y. Kwong*, E.J. Marek**
Department of Chemical Engineering and Biotechnology, University of Cambridge, UK
*kyk25@cam.ac.uk, **ejm94@cam.ac.uk

***Abstract***

This review presents recent advances in research on fluidized bed combustion of solid biomass. While the main focus is on thermochemical processes occurring in fluidized beds, applicable investigations on biomass combustion from other research areas are also described as they often provide fundamental insight about the processing of biomass, applicable also in the context of fluidized beds. This review aims to summarize lessons learned and indicate some remaining gaps in the existing body of knowledge. The paper discusses combustion in separate stages: drying, pyrolysis, homo- and heterogeneous combustion, and characterizes how fluidized beds affect combustion, discussing heat and mass transfer, material segregation, and bed agglomeration. Finally, advances in new research trends and the prospects for technology development are considered, highlighting the chemical-looping technology with its inherent potential for carbon capture, scale-up of advanced computational models, and progress in spectroscopic and tomographic studies applied to combustion.

*Keywords:* biomass combustion, fluidized bed, energy generation, chemical looping, modeling, review

## *1. Introduction*

### 1.1. *Fluidized combustion technologies for future utilization of biomass*

Biomass is the oldest carbonaceous fuel used by humankind and the only solid fuel that is sustainable. Combustion of biomass has been gaining attention again because of its potential for power generation with significantly reduced $CO_2$ emissions.[1] The advantages of biomass utilization through combustion include a straightforward production of high-temperature heat that can be employed in generating high-pressure steam for power production, chemical industry, healthcare (*e.g.* sterilization). Recent reviews highlight that the potential of biomass is not fully exploited.[2] Industrial thermochemical processes other than combustion, such as pyrolysis and gasification, can bring further benefits by decreasing the level of exergy destruction, providing higher-value products (bio-oils, carbon nanotubes), and further lowering $CO_2$ emissions However, combustion of biomass is most mature technologically, with solutions commercially available at all scales, from micro-devices to GW-scale power plants. With only moderate requirements for retrofitting (especially in fluidized bed boilers),[3,4] biomass can readily replace coal in existing installations; hence, even if used temporarily, biomass can significantly ease the pathway towards net-zero emission targets. Combustion is also the easiest and the most socially acceptable method of utilizing problematic biomass, such as waste or sewage sludge.

Among available technologies, combustion in fluidized beds is particularly well-fitted for biomass and wastes because it works well with a variety of fuels, including fuels with high moisture content, varied composition, inhomogeneous or mixed. The idea of combustion in fluidized beds is feeding a stream of fuel into a hot bed of largely inert material, usually sand, and providing an oxidizing gaseous medium, usually air, that flows with a velocity high enough to fluidize the fuel and bed particles. Because of the constant movement of the solid particles, fluidized beds offer good mixing of solids and, hence, fast heat redistribution, minimizing potential problems with local hot spots and thermally induced pollutants, such as $NO_x$. In contrast, gas mixing is obstructed by solids, with a fraction of the oxidizer channeling through the bed in bubbles and another fraction moving with the solid particles in an emulsion phase. Mass transfer between the bubbles and the emulsion phase is limited; thus, most mixing of the gas takes place in the freeboard (above the fluidized bed).

The advantage of fluidized beds with good mixing of solids and their long residence times assures high conversions, a relatively low environmental impact, and offers the potential of *in-situ* removal of $SO_x$.[5] In comparison to other combustion technologies, disadvantages include high capital and operating costs, increased emission of particulates, accumulation of ash and the resulting potential maintenance problems, *e.g.* bed defluidization.[5,6]

The design of a fluidized bed depends primarily on the required fluidization regime, depending on the gas velocity. When fluidized in the bubbling regime, the bed will be largely stationary (net flux of solids ~ 0 kg/m$^2$). Alternatively, in the churn-turbulent or core-annulus regimes, the bed material will be transported upwards (net flux > 0 kg/m$^2$) and out of the combustor.[7] The stationary approach is realized industrially in Bubbling Fluidized Beds (BFB) comprising distinct bed and freeboard zones, as shown in Fig. 1(a); the transporting approach is realized in Circulating Fluidized Beds (CFB), where the transported solids are separated from the gas in cyclones, to be circulated back to the main reactor, as illustrated in Fig. 1(b).

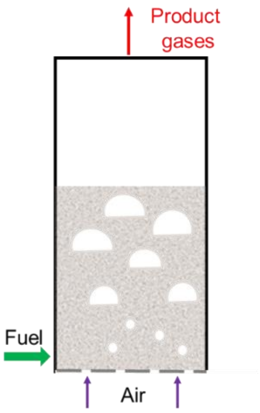


(a) Bubbling Fluidized Bed

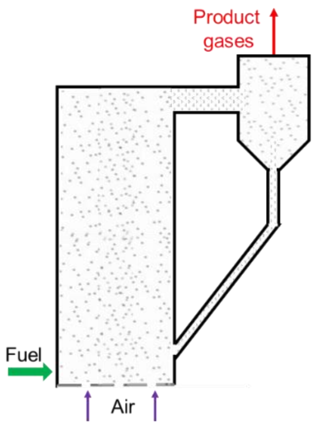


(b) Circulating Fluidized bed

**Figure 1: Schematic diagram of (a) Bubbling fluidized bed and (b) Circulating fluidized bed.**

The development of the first fluidized bed installations for chemical industries started in the 1940s, and later for energy conversion in the 1960s.[6] While originally fluidized bed combustors were developed for burning coal, co-feeding of coal and biomass is possible.[8]

CFBs have several advantages over BFB, such as higher efficiency for combustion and sulfur capture, both important primarily in large-scale installation and fuels with high sulfur content. Thus, CFB is the preferred technology for coal-powered systems, especially for coals with high sulfur content or lower reactivity. For biomass, bubbling beds are more common because the efficiency of combustion for a reactive fuel like biomass is satisfactory, and the sulfur capture is not essential in the combustion of plant-based biomass with low S-content.[9] Because of lower capital costs, BFB is also preferred for smaller-scale units, which are the preferred option for biomass and waste usage in distributed power production with locally-available resources, for which fuel transportation may be uneconomical. Nevertheless, large and middle-scale fluidized beds combusting solely biomass also have been developed. A list of recently commissioned biomass combustors was presented by Mladenovic et al.9 Small scale reactors, with a thermal capacity of 1-10s of MW, are used for heat production. In contrast, large scale installations, of the order of 100s MW, usually co-produce heat and electricity.[10] An overview of practical issues arising during biomass combustion in large-scale fluidized systems was presented by de Jong and Van Ommen.[6]

### 1.2. *Focus and methods*

A keyword search through the Web of Science databases indicates that despite a well-established fundamental understanding of biomass burning in fluidized beds, the number of papers on this subject has been increasing, clearly aligning with the policy changes and the global quest towards more sustainable power generation.

This review aims to compare classically used methods when discussing biomass combustion (models, experiments), concluding about remaining research gaps. The secondary aim is to highlight new research trends, identify emerging ideas and capabilities, and discuss future research directions. Throughout the paper, we summarize areas already well described in the literature, providing readers with references to extensive topical reviews. To avoid overlaps with previous reviews, we focus on a critical evaluation of the most common approaches without fully explaining the intricacies and the assumptions. For that, we direct the readers to the selected and recommended literature, provided in Table 1.

Table 1. Selected reviews on combustion of biomass and fluidized beds.

| *Topic* | *Reference* | *Main scope* | *Year* |
|---|---|---|---|
| Fluidized bed combustion | [10] | Bubbling fluidized bed combustion, covering theoretical aspects and practical insights into the technology, arising from over 30 years of applied research in FBC in Eastern Europe.<br>*Key topics*: historical review, fuel type, pollutants, heat transfer | 2003 |
| Scale-up of biomass combustion in fluidized beds | [6] | Comparison of CFB and BFB for biomass applications; scaling analysis for process scale-up and development, emissions and agglomeration phenomena<br>*Keywords*: dimensionless analysis, practical problems | 2009 |
| | [11] | Problems arising from large-scale biomass combustion in FB.<br>*Keywords*: pollutants, agglomeration, corrosion, trace metals | 2009 |
| Fundamentals of biomass combustion and gasification | [12]<br>(extensive review) | Combustion and gasification of biomass chars, discussing the published experimental results, and the influence from process conditions (temperature, pressure, heating rate, type of biomass, ash)<br>*Keywords*: heterogeneous reactions, char yield, kinetics and rate expressions | 2009 |
| Modeling biomass gasification in fluidized beds | [13]<br>(extensive review) | An extensive summary of existing modeling approaches for fluidized beds, primarily focused on gasification but applicable to other processes. Detailed description of all | 2010 |

| | | | |
|---|---|---|---|
| | | main phenomena encountered during thermal processing of biomass.<br>*Keywords*: fluidization models, heat and mass transfer, attrition, kinetics | |
| Pollutants from burning biomass | [14] | Chemical mechanisms of creation of main pollutants in biomass combustion and co-combustion. Comparison to other technologies.<br>Keywords: pollutants, emissions, modeling pollutant formation, control methods | 2012 |
| Combustion and gasification of biomass in fluidized beds | [15]<br>(extensive review) | One of the most comprehensive overviews of fundamentals of fluidization and energy technologies with fluidized and circulating beds.<br>*Key topics*: fundamental research, advances in industrial atmospheric and pressurized FB, gasification, carbon capture technologies | 2013 |
| Chemical details of biomass combustion | [16] | Chemical reactions characteristic to biomass treatment in energy technologies. Research gaps in understanding chemical details of reactions with biomass.<br>*Keywords*: particle conversion, catalytic properties of ash, creation of pollutants, agglomeration, ash deposits | 2017 |
| Physical properties of biomass and their change during combustion | [17]<br>(extensive review) | Modeling thermal degradation of biomass, including transient changes in biomass physical and chemical properties. Comparison of single particle models. Application in fixed bed technologies.<br>*Keywords*: thermally thick particles, 1D, 2D, 3D models | 2017 |
| Combustion of non-woody biomass | [18] | Comparison of properties and composition of non-woody biomass. Single particle combustion, drop tube furnace experiments. Application in pulverized combustion.<br>*Keywords*: models, non-woody biomass fuels | 2018 |

The paper is structured as follows: introduction to the topic and its importance in Section 1; fundamental phenomena of biomass combustion and, more generally, biomass thermal treatments in Section 2; phenomena specific to fluidization in Section 3. Each section starts with a general discussion, moving to the mathematical descriptions and experimental procedures. Section 4 highlights new methodologies and future directions. Section 5 lists research challenges and gaps, and Section 6 main conclusions, reiterating the identified research needs, in light of new research methods.

## *2. Combustion of biomass – phenomena*

When exposed to thermal treatment, particles of biomass undergo a series of phenomena involving physical processes and chemical reactions. Upon heating, biomass particle first starts to lose moisture, initially present in the material as loosely bound free water in pores or as strongly bound moisture adsorbed in biomass cells and fibers.[19] Upon further heating, the organic structure of biomass starts to thermally decompose, producing pyrolytic gases and a solid residue known as char. Drying and pyrolytic reactions in fluidized beds are usually fast, resulting in a local pressure increase and convective transport of the gases outwards from the biomass particle. The efflux of moisture and volatiles shields the char from the oxidizing

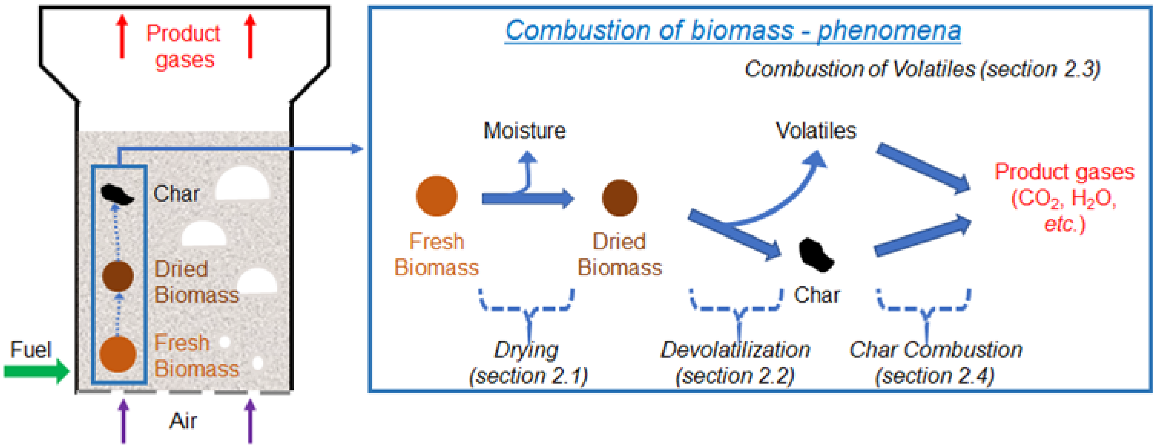


**Figure 2: Simplified visualization of phenomena occurring during combustion of biomass in fluidized beds.**

medium; hence, combustion of the solid residue usually occurs as the last step in the sequence of relatively independent phenomena. Visualization of the phenomena in the context of fluidized bed is presented in Fig. 2.

### 2.1. *Drying*

Evaporation of water from a particle, which is usually in equilibrium with the ambient air, starts as soon as the temperature of the particle increases, with the expected highest rate around the boiling point of water at ~100ºC. Because of high heating rates in fluidized beds, water evaporation is usually limited by heat transfer, as energy is needed to overcome the latent heat of vaporization. Biomass heating and drying are relatively short, at least in comparison to the longest step: char combustion; but the variability of drying might be significant because the moisture content in biomass can span from a few percent to 40% in a plant-type biomass,[20] and higher in a waste-type of fuels.

Pyrolysis and combustion have been extensively studied at the fundamental level, whilst drying is usually limited to measuring rates and duration, rather than rigorously describing the involved physical phenomena and their influence on the fuel particle, fluidization, and overall combustion. However, the importance of moisture release is significant because the convective flux of moisture from within the particle results in the creation of endogenous bubbles, which then rise in the fluidized bed, dragging the fuel particle towards the surface - a phenomenon discussed in Section 3.4. Furthermore, the presence of $H_2O$ in the bed affects the homogeneous combustion of CO and heterogeneous reactions with char, as discussed in Section 2.

Accurate modeling of biomass drying is difficult because it ought to account for hydrodynamics of the flow of free water in pores, diffusion of the bound water within the cell walls, alongside the phase change and transport of the produced steam.[21] Additionally, coupling of the heat and mass transfer, their dependence on the fiber saturation point (FSP), and the anisotropic structure of biomass complicate the modeling to the level that cannot be solved analytically.[22] Three of the most common methods for describing biomass drying are (1) the heat sink approach, (2) the Arrhenius approach, (3) the equilibrium approach.[23] Comparison of advantages and disadvantages of the three modeling approaches is given in Table 2. Extensive discussion, although not in the context of fluidized beds, can be found in reviews by Haberle *et al.*[17] and Hosseini *et al.*[24]

*The heat sink approach*

In most published studies on biomass combustion, the drying process is simplified by assuming that biomass particles are isotropic, and the overall rate of drying is limited solely by heat transfer. The latter is realized when the temperature in the particle reaches the boiling point, at which all further heat supplied to the particle is used to evaporate the water, following a so-called heat sink model.[23] The model is applicable and useful in fluidized beds because even though heat transfer in the bed is fast, the heat transfer limitation often concerns the internal resistances within the dried section of the fuel particle.

With these assumptions, the exact analytical solutions of drying for a spherical fuel particle at a pseudo-steady state was first proposed by McIntosh for coals of high moisture content.[25,26] As long as the main simplifications and assumptions remain unchanged, the same approach for the heat sink models can be used for biomass. McIntosh calculated the amount of moisture remaining in the particle by using an empirical approximation for the rate of drying, related to the heat-sink assumptions.

Agarwal extended the heat sink model, demonstrating that drying-induced shrinkage of a fuel particle does not affect the dynamics and timescale of moisture removal.[27] To account for the transient effect, a non-steady-state model of heat conduction with a convective flux at a particle surface was proposed by Agarwal *et al.*[28] to simulate drying of low-rank coals in a fluidized bed. They assumed that the overall rate was limited by heat transfer and that the drying occurred at a surface of a receding wet core, a situation shown in Fig. 3. To represent the surface of the wet core, the model used a moving boundary condition obtained using a heat balance. Agarwal's model was validated against experimental results using two approaches. In the first, the physical properties appearing in the analytical solution (*e.g.* thermal diffusivity) were varied to obtain the same total drying time as in one of the performed experiments. Based on these fitted thermo-physical parameters, drying profiles for the same fuel in other experimental conditions were predicted correctly. In another approach, pre-determined thermo-physical parameters were used in Agarwal's model,[29] resulting in reasonable predictions for fuels with high moisture content but overpredictions otherwise. Komatina *et al.* proposed an empirical coefficient that corrects the heat sink

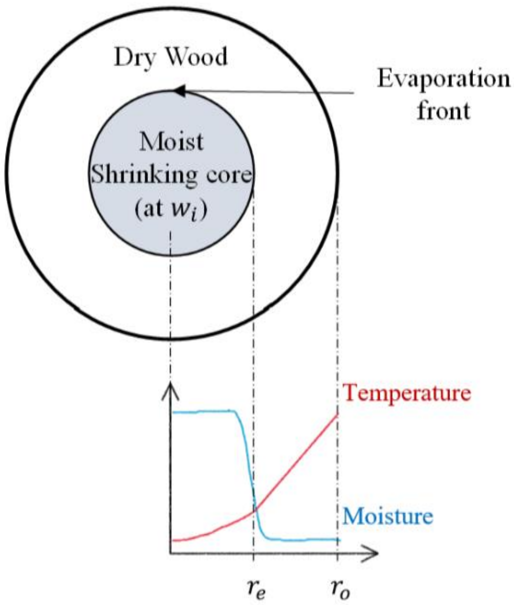


**Figure 3: Schematic diagram of a partially dried wood particle with a wet core and dry external shell.**

approach, noting that a classical model, such as the one derived by Agarwal, ignores superheating of the generated steam and is highly sensitive to the external heat transfer coefficient.[29] Other phenomena that can affect the rate of drying include the mass flux of steam that leaves the particle, making the convective fluxes in energy balance non-negligible (similar to transpiration cooling),[30] the capillary pressure affecting the boiling point of water,[31] or particle cracking and fragmentation under the thermal stresses experienced during drying.[21,32]

A more advanced approach to drying limited by heat transfer was presented by Thunman *et al*.[33] in their work focused on fuels with high moisture content. Besides the heat transfer limitation, they assumed that, during drying of a particle placed in a hot environment, (a) an infinitely thin evaporation front within the particle is created; (b) the unaffected section of the particle resembles a shrinking core, and, in consequence, inside the core, the moisture level does not change, while in the region outside the core, the moisture content is zero; (c) the temperature of the core does not change, *i.e.* $T(r < r_e) = T_{initial}$. Despite additional assumptions, the approach can be still represented by Fig. 3. For a heat transfer–limited process, the rate of evaporation, $\dot{m}_g$, can be related to the rate of heat transfer to the core interface, $r_e$, located between the wet core and dry shell,

$$\dot{m}_g = \frac{c_1 r_e^n \kappa_s}{\Delta H_e} \frac{\partial T}{\partial r}\bigg|_{r_e} \tag{1}$$

where $c_1 r_e^n$ is the surface area of the core, (*e.g.* $c_1 = 4\pi$ and $n = 2$ for a sphere, $c_1 = 2\pi$ and $n = 1$ for a cylinder per unit length), $\kappa_s$ is the thermal conductivity of the dry section, and $\Delta H_e$ is the heat of vaporization of water. The position of the drying front, $r_e$, changes from the particle radius, $r_o$, at the beginning of drying to $r$ =0, when the particle is dry. Hence, $r_e$ can be related to the overall level of "conversion" as:

$$r_e = X_e^{1/(1+n)}\, r_o \tag{2}$$

where $X_e$ is the fraction of moisture remaining in the particle, and $n$ is the shape factor, defined earlier.

In the region outside the core ($r_o > r > r_e$), the temperature of the dried particle can be evaluated from the heat balance:

$$\rho_s C_{p,s} \frac{\partial T}{\partial t} = \frac{1}{r^n} \frac{\partial}{\partial r}\left(r^n \kappa_s \frac{\partial T}{\partial r}\right) - \frac{1}{r^n} \frac{\partial}{\partial r}\left(r^n U_g \rho_g c_{p,g} T\right) \tag{3}$$

with a boundary condition at the surface of the particle, $r = r_o$ obtained from equating the external convective and internal conductive heat fluxes:

$$-k_s \frac{\partial T}{\partial r}\bigg|_{r_o} = h_{\mathrm{eff}}\left(T_{r_0} - T_\infty\right) \tag{4}$$

and another boundary condition at the evaporation front, $r = r_e$, specifying the temperature:

$$T = T_e \tag{5}$$

In Eq.(3), $U_g$ is the velocity of the efflux of the vapour (*i.e.* $\dot{m}_g = U_g \rho_g c_1 r^n$), $\rho_g$ is the density of the vapour, $C_{p,g}$ is the specific heat capacity of the vapour, $T_\infty$ is the ambient temperature. In Eq. (4), $h_{\mathrm{eff}}$ is the effective heat transfer coefficient between the particle and the fluidized bed (see Section 3.1), and in Eq. (5), $T_e$ is the temperature at which liquid water and its vapor are in equilibrium.[34] The value of $T_e$ can be higher than the saturation temperature at a flat interface (*e.g.* 373 K at 1 bar) due to the capillary forces (for free water)[21,31,35] and sorption enthalpy (for bound water)[21,33,35–37]. Consequently, the equilibrium temperature can vary with the type of biomass. As reviewed by Haberle *et al*., studies, which account for the transpiration effects of the efflux of moisture, allow for the elevated boiling point of water, or differentiate between the free and bounded water are still rare.[17] Successful implementation of an empirically correlated $T_e$ in the modeling of drying of a biomass particle was recently demonstrated by Kung and Ghoniem.[38]

As proposed by Thunman *et al*., the moving boundary problem of the evaporation front can be simplified with a pseudo-steady state assumption.[33] After eliminating the transient term from Eq.(3) and performing a scaling analysis, Thunman *et al.*[33] showed that the convective flux can be neglected if the following criterion is satisfied:

$$\frac{x_e^n C_{p,g}(T_\infty - T_e)}{\Delta H_e} \frac{\partial\theta}{\partial x}\bigg|_{x_e} \ll 1 \tag{6}$$

Here, $x_e$ is the dimensionless evaporation front, $r_e/r_o$, and the derivative term $\frac{\partial\theta}{\partial x}\Big|_{x_e}$ describes the dimensionless temperature gradient at the evaporation front. For Eq. (3) at steady state, Thunman *et al.*[33] provided an analytical solution, which ought to be solved iteratively unless the efflux term can be ignored, simplifying Eq. (3) further. Without the steady-state assumption, Eq. (3) can be readily modelled and solved numerically after coupling with mass transfer, as was demonstrated, for example, for a cylindrical geometry,[39] or a slab geometry.[22]

*The pseudo-kinetic approach*

Despite drying being a physical process, the rate of drying is often modelled as a zero-order reaction[25,32,40,41] with a rate constant, $k_d$, calculated using the Arrhenius expression for the temperature dependency: $k_d = A_d \exp\left(-\frac{E_d}{RT}\right)$, where $A_d$ and $E_d$ are pseudo-kinetic parameters representing the pre-exponential constant and activation energy of drying, respectively.

The pseudo-kinetic approach can be only understood as an empirical description of drying because the fitted kinetic parameters have no physical meaning[42] and tend to underestimate the drying rate significantly.[43] To overcome the drawbacks of modeling using this method, the reaction engineering approach (REA) was introduced. REA considers evaporation and re-condensation of water as two competitive reactions with different rate constants.[32,44,45] The imposed difference in the kinetics can be explained intuitively by the fact that evaporating water requires energy input to overcome the latent heat of vaporization (analogous to the activation energy), whereas condensation occurs without an associated energy barrier. While REA has been used to model drying at a relatively low temperature (< 200°C),[45] there has been no attempt to apply REA to biomass drying in fluidized beds under combustion heat fluxes. When a biomass particle is exposed to a high temperature in an environment with fast heat and mass transfer, such as in fluidized bed combustors, re-condensation of the water vapor inside the wood matrix might be insignificant, which means that a single Arrhenius-type rate equation might be sufficient.

The pseudo-kinetic approach offers simplicity at the cost of an accurate physical description of drying. It can be easily implemented in numerical models for biomass combustion; however, in consequence, the involved phenomena are lumped into a single expression, which can only be calibrated empirically. Hence, this simplified approach ought to be used with caution and applied in a range of drying temperatures for which the model was experimentally calibrated.

*Equilibrium models*

The third approach commonly applied to describe drying is based on equilibrium models.[35,45–47] The main hypothesis of the equilibrium-based approach is that, within a fuel particle, the water vapor and the liquid moisture are in equilibrium. The equilibrium is defined by the local temperature modelled *via* the heat balance equation similar to Eq. (3). However, instead of having a set of separate heat balance equations before and after the evaporation front, the particle is modelled as a continuum, ranging from the particle's center to its external surface. Then, the rate of evaporation is calculated by simultaneously solving mass conservation equations for water and balancing fluxes. Therefore, the equilibrium approach relaxes the assumption of an infinitely thin evaporation front, making the model applicable to a wide range of systems but at the cost of more complex numerical calculations.

Recently, Borujerdi *et al.* applied the equilibrium approach to model the drying of a biomass slab and found that, at a high radiant heat flux (40 kW $m^{-2}$), the evaporation front inside the moist slab was distinct and thin.[23] This confirms that the heat sink models might be sufficiently accurate for describing the drying of biomass in fluidized bed combustors and explains why the equilibrium models are not very common in the area of combustion. However, a dedicated study focusing solely on the suitability of the equilibrium models for fast, high-temperature drying could still provide valuable insight about how the physics of biomass drying affects the main process characteristics (timescales, front movement, *etc.*).

Table 2: Advantages and drawbacks of most common approaches for describing drying.

| Modeling Approaches | Example of application | Advantages | Drawbacks |
|---|---|---|---|
| Heat sink model | [38,48–50] | Simple.<br>Has an analytical solution at steady state. Can incorporate devolatilization kinetics. | Valid only when the evaporation front is thin.<br>Probable numerical instabilities caused by a step function applied to describe drying. |
| Arrhenius kinetic model | Pseudo-kinetic[20,51,52]; REA[53] | Numerically stable.<br>Simple to incorporate as a step in devolatilization and combustion. | Semi-empirical approach requiring calibration or checking between cases.<br>Physically less realistic (can result in substantial evaporation below the boiling point).[23] |
| Equilibrium model | [23,36] | Applicable in a broad range of situations. | Computationally expensive |

## 2.2. *Devolatilization*

Devolatilization is the release of volatile components that leaves behind a porous solid known as char. For biomass, the thermally induced decomposition and the release of gases results in a significant mass loss (~80 wt% dry basis), aligning with the high volatile content assessed with standard methods for proximate fuel analysis.[54–56] Hence, devolatilization is a crucial step during the thermal usage of biomass, regardless of the application. Comprehensive reviews of biomass pyrolysis were given by Di Blasi[57] and Anca-Couce[58], with updates in many recent reviews, covering both experimental and theoretical developments[59–61], or focusing mainly on modeling[62–65].

Pyrolysis, the thermally induced release of volatiles, is important when discussing the combustion of biomass in fluidized beds because it affects (1) the yields and composition of the released gases, (2) the yield and properties of the resulting solid char, (3) the hydrodynamics of fluidization (*e.g.* release of endogenic gas bubbles, separation of fuel particles and their floating on top of the bed material). So far, a lot of effort has been devoted to the first two topics and significantly less to the mechanics of the gas release in a bed of fluidizing particles.

Nowadays, information about the composition and yields of pyrolytic gases can be obtained quite precisely, but this level of detail is often not essential when discussing biomass combustion. In fact, for combustion applications, pyrolytic gases are often discussed using a lumped composition of combustibles volatiles (*i.e.* $C_nH_mO_p$),[66] and more attention is paid evaluating the total time of pyrolysis and, associated with this task, rates of the process. Because pyrolysis as a thermally induced process requires a continuous heat input, the estimation of its rate often involves a discussion about chemical kinetics and heat transfer.

*Kinetics of biomass pyrolysis*

The structure of woody and herbaceous biomass can be separated into natural polymers: cellulose, hemicellulose, lignin, and each of them decomposes differently, as demonstrated in studies that looked at their separate and combined pyrolysis.[67] For waste and inhomogeneous biomass (refused-derived fuel, sewage sludge), the composition is usually unknown, and primary information about the fuel comes from their proximate and ultimate analysis, as well as, experiments or practical operations. Hence, despite significant progress in the research on biomass pyrolysis, there is no single approach to describe the rate of involved chemical reactions.

The simplest approach is to assume that biomass, no matter the origin, can be treated as a single homogenous species. One of the most popular models following this approach was firstly proposed by Shafizadeh and Chin,[68] who described pyrolysis of wood as three parallel first-order reactions, which transform wood into gas, char and tars, as shown in Fig. 4. A number of published studies followed, providing the kinetic parameters for each reaction determined for various types of biomass (*e.g.* oak saw dust,[69] sweet gum hardwood,[70] pine,[71] waste wood,[72] beechwood[73]) and using different experimental systems (such as isothermal tube furnaces,[69] screen heaters,[70] and thermogravimetric analyzers[71]). The global rate constant, $k$, taken as a summation of the rate constants of individual reactions, is particularly useful when the products of the pyrolysis are not of interest, but rather the conversion of the starting fuel is. Another consequence is that the expression for the rate of pyrolysis is then simplified to a single, first-order reaction.

Di Blasi[57] reviewed and examined the global rate coefficients from published studies, classifying the obtained activation energies, $E_a$, by the temperature range at which the experiments were conducted. Values of $E_a$ were low (69 – 91 kJ mol$^{-1}$) for experiments in high-temperature reactors (up to 1400 K), likely because of the endothermic pyrolysis, which progressed as the particle heats up, was limited by heat transfer, and that affected the observed rate. For experimental arrangements at low-temperatures (below 700 – 800 K), two ranges of $E_a$ were noted: 56 – 106 kJ mol$^{-1}$ and 125 – 174 kJ mol$^{-1}$, where the lower values of $E_a$ arose from averaging the rate of pyrolysis over the entire duration of the process, whereas the higher values of $E_a$ resulted if only the central part of the weight loss curve was considered.[73] Hence, the two groups demonstrate the effect of conversion on the intrinsic rates.[74] Kinetics derived using the latter approach led to a better agreement with experimental results, especially for temperatures higher than 700 – 800 K, so beyond the temperature range used in deriving those kinetic coefficients.

The problematic influence of heat transfer, when investigating the kinetics of pyrolysis, is relatively well-known. When biomass particle is quickly exposed to a high temperature, the rate of reaction approaches the rate of heat transfer but cannot exceed it because of the endothermicity of pyrolysis. Another common problem in studies focused on kinetics concerns the dependency of the rate expression on conversion models, which are often assumed *a priori*. The final effect concerns an isokinetic relationship between the preexponential factor, $A$, and the activation energy, $E_a$. The isokinetic problem represents a situation when the same value for the rate can be obtained with multiple pairs of $A$ and $E_a$. Consequently, a low value of $E_a$ can be compensated by a low value of $A$, because of the logarithmic nature of the Arrhenius expression.[75] To overcome the compensation effect in pyrolysis, results should be gathered from experiments at varied conditions (*e.g.* heating rates, temperature programs) to avoid repeating systematic errors. The compensation effect was discussed in Di Blasi's review,[55] followed by a few recent studies for specific types of biomass.[76–78]

Going beyond the three primary decomposition reactions, Di Blasi proposed a set of secondary reactions that describe cracking and repolymerization of tars into lighter gases and char,[57] as shown in Fig. 4, with kinetic parameters available in literature.[57,79] The secondary transformation of tars is highly relevant in biomass gasification and flash pyrolysis applications, affecting the composition of product streams. During combustion, tars should oxidize to CO and $CO_2$, but their polymerization leads to the emissions of polycyclic aromatic hydrocarbons (PAH) and volatile organic compounds (VOC) from fluidized beds.[80,81]

Modeling biomass particle as a homogenous solid is a crude but often effective simplification. As noted earlier, woody biomass comprises cellulose, hemicellulose and lignin, with a typical content of the listed components of 42, 27, 28 wt%, respectively for softwood, and 45, 30, 20 wt%, respectively for hardwood[82,83]). In experiments with low heating rates, decomposition of those natural polymers is relatively easily discernible, with each reaction occurring in a separate, although partially overlapping, temperature range: 498 – 598 K for hemicellulose, 598 – 648 K for cellulose, and 523 – 773 K for lignin.[84] At higher heating rates, significant degradation rates will be obtained by all the components simultaneously, and so all three reactions will overlap, creating an illusion of one global process, thus, justifying the applicability

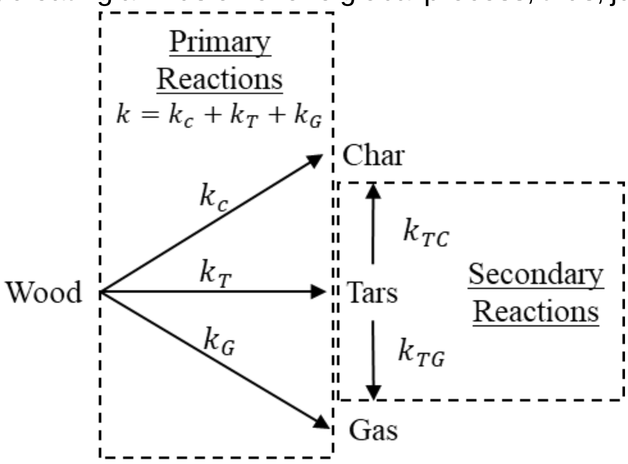


**Figure 4: One-component mechanism of the primary wood pyrolysis proposed by *Shafizadeh and Chin*[68] and secondary reactions by Di Blasi.[57]**

of the homogenous kinetic model. That said, at high heating rates, pyrolysis can quickly become limited by heat transfer; thus, the extraction of kinetic parameters would require decoupling kinetics from the heating effects.

By assuming no interaction between pyrolysis of the three polymers, the kinetics for three separate decomposition reactions can be obtained by performing experiments at low heating rates, generally below 10 K min$^{-1}$, and using three homogenous kinetic models. For example, Gronli *et al.* described pyrolysis of wood using three independent and parallel 1$^{st}$ order reactions, with all kinetic constants expressed in the Arrhenius form.[85] With experiments at 5 K min$^{-1}$, they found the activation energy for pyrolysis of hemicellulose, cellulose and lignin to be 80 – 116 kJ mol$^{-1}$, 195 – 286 kJ mol$^{-1}$ and 18 – 65 kJ mol$^{-1}$, respectively. Another common approach is to use more than three 1$^{st}$ order reactions, ascribing a few reactions to the decomposition of each of the three polymers.[86] In addition to fitting the experimental results better, the multiple reactions approach might be more appropriate for polymers that are amorphous or can take different structures (*e.g.* hemicellulose of deciduous woods contains mainly xylan, whereas coniferous woods contain mannan).

Other approaches to describe pyrolysis using multi-component mechanisms exist; for instance, Miller and Bellan used nine reactions, three for each of the polymers, proposing that, in each set, the first reaction was to activate the component, while the second and third were to describe the component's decomposition into gas, char and tars.[87] Another similar approach is the bio-chemical percolation devolatilization (bio-CPD) model, where a labile bridge is firstly activated to form an intermediate form of a reactive bridge, and, consequently, a char bridge (with gas) and a side-chain, which can convert into a light gas (analogous to the secondary reaction of tars into gas).[88,89] In bio-CPD, instead of a single value of activated energy, a distribution of activation energy describes the kinetics of each transformation. The argument of adding more reactions is supported by microchemical studies of pyrolysis of cellulose, which decomposes into a wide range of intermediate and final products, with reaction mechanisms and associated kinetics available in the literature.[90,91]

A further extension from the multiple-reaction models is the distributed activation energy model (DAEM), in which pyrolysis involves an infinite number of reactions, described with a continuous distribution of the activation energy. A comprehensive review of DAEM and its application to pyrolysis of lignocellulosic biomass was given by Cai *et al.*[92] In DAEM, the mass of remaining volatiles that will be released in a reaction with the activation energy between $E$ and $E + \mathrm{d}E$ at a given time, $t$, is $m(E,t)\mathrm{d}E$;[93] hence, the mass of all unreleased volatile components can be obtained by integrating over all possible values of $E$. Then, the mass fraction of the volatiles remaining in the solid, $M_v(t)/M_{vo}$ arises as:

$$\frac{\overbrace{M_v(t)}^{\int_0^\infty m(E,t)\mathrm{d}E}}{M_{vo}} = \int_0^\infty g(E) \times \exp\left[-A(E)\int_0^t \exp(-E/RT)\,\mathrm{d}t\right]\mathrm{d}E \tag{7}$$

where $A(E)$ is the pre-exponential factor accompanying a given activation energy, $E$, while $g(E)$ is the distribution of the activation energies[93]. For the case where $g(E)$ and $A(E)$ are known, the yield of volatiles can be determined using Eq. (7) even though the calculations will be relatively computationally demanding.[93] For the inverse situation, *i.e.* determining $A(E)$ and $g(E)$ from pyrolysis experiments, the problem is mathematically ill-posed, thus, unsolvable, except for simplified cases where the number of reactions is finite, and the reactions are independent and do not overlap, as discussed by Scott *et al.*[93] One of the common approaches to overcome the ill-posed problem is to assume the type of the distribution that describes $g(E)$; for instance, often, a Gaussian distribution is taken, adjusting the mean and the standard deviation of $g(E)$ to fit the model to measurements.[64,92,94–97] As a side note, the CPD model described earlier usually implements a Gaussian distribution as well.[98] For DAEM and its application for determining pyrolysis kinetics, an algorithm was developed by Scott *et al*.[93], and demonstrated on pyrolysis of sewage sludge in a fluidized bed,[99] and later in a range of various types of unconventional, so often difficult to handle and model, fuels, such as date palm waste[100] or microalgae[101]. Recently, a two-dimensional DAEM was developed by considering the pre-exponential factor, $A$, as a separate variable, independent of $E$, and the distribution function is two-dimensional, $g(A,E)$, depending both on $A$ and $E$. The justification is that the relationship between $A$ and $E$ is unclear; hence, treating them independently will help overcome problems with 1-D DAEM, caused, for example, by the compensation effect.[102]

Some of the developed multi-component models allow for parallel, competitive, or interdependent pyrolysis reactions. For example, Renzi *et al.*[103] proposed a set of 29 pyrolytic primary and secondary reactions, now known as a CRECK group model. The work was later extended to 32 reactions and analyzed in a metastudy of ~250 pyrolysis experiments from 30 papers.[104] The distinctive characteristic of this model is the feasibility of predicting the composition and characteristics of all products, including the generated solid residue, char.

Finally, some recently published work analyzed pyrolysis on a molecular level using quantum mechanics calculations, for example, applying density functional theory (DFT). Because of the heavy computational load involved in DFT simulations, most published studies focused on reaction pathways and energy requirements during pyrolysis of a model compound, such as cellulose.[91] Recent progress in the application of quantum chemistry for biomass pyrolysis was given by Hu e*t al*.[105]

*Particle scale modeling*

For a devolatilizing particle of a solid fuel, the following differential equations describe the heat and mass balances:

Heat balance (assuming gas and solid are in local thermal equilibrium):

$$\rho_s(r)C_{p,s}(r)\frac{\partial(T)}{\partial t}=\frac{1}{r^n}\frac{\partial}{\partial r}\left(r^n\kappa_s(r)\frac{\partial T}{\partial r}\right)-G_d(r)\Delta H_{py}-F(r)c_{p,v}\frac{\partial T}{\partial r} \tag{8}$$

And mass balance (solid particle):

$$\frac{\partial\rho_s(r,t)}{\partial t}=-G_d(r) \tag{9}$$

where $n$ is the shape factor (0, 1 or 2 for slab, cylinder or sphere, respectively), $G_d$ is the rate of release of volatiles per unit volume, described using a suitable kinetic model, $\Delta H_{py}$ is the heat of pyrolytic reaction, and $F$ is the flux of volatiles, so that, the last term of Eq. (8) describes the enthalpy of volatiles leaving the particle. A simplified mass balance in Eq. (9) ignores any effects of intra- and extra-particle mass transfer because during pyrolysis and drying the influence of heat transfer is much more significant than of mass transfer.[106]

The flux of volatiles can be calculated from volatiles conservation equation in the gas phase, assuming a quasi-state situation with negligible transient and diffusional terms, hence, obtaining:

$$F(r) = \frac{1}{r^n} \int_0^r r^n G_d(r)\, dr \tag{10}$$

As in the drying models, the cooling effect from the efflux term is sometimes neglected,[107] but in other cases was found important (*i.e.* high Peclet number, as expected during pyrolysis[108,109]). For simplification, the contribution from the efflux of volatiles is sometimes accounted for by introducing a correction factor.[110]

One of the common approaches to simplify Eq. (8) is to determine limiting factors, which then leads to reduced models of thermally thin or thick particles. For example, Bryden *et al.*[32] modelled the pyrolysis of a wood slab using Eq. (8) and then classifying considered cases into four pyrolysis regimes: (1) thermally thin and limited by slow chemical reactions, (2) thermally thin and heat transfer limited, (3) thermally thick, and (4) a thermal wave regime, in which devolatilization follows a shrinking core model. The first three regimes were earlier identified by Pyle and Zaror,[106] who performed a scaling analysis on Eq. (8), and determined the limiting criteria using the Biot number, *Bi* and pyrolysis number, *Py* (all dimensionless numbers are provided in the nomenclature). However, as mentioned by Bryden *et al.*[32], those transition criteria required updating between low and high temperatures; otherwise, the simplified approach led to significant errors. The influence of temperature and of heat of pyrolysis were later addressed by Scott *et al.*,[99] who proposed a third dimensionless group called a heat release number, *Hr*. With $Hr \gg 1$, the enthalpy of pyrolysis is considered significant. Under some circumstances (*e.g.* the particle is sufficiently large so that $Bi \gg 1$ and $Hr \gg 1$), the devolatilization problem in fluidized beds can be solved with an analytical solution based on the shrinking core approach, as shown by Chern and Hayhurst.[13,111–113]

Drying and pyrolysis can be considered as separate processes induced by thermal treatment,[31,114,115] or, alternatively, drying can be incorporated as a pseudo-reaction in the pyrolysis model.[32,116,117] Agarwal *et al.* analyzed situations in fluidized beds where drying and pyrolysis overlap, assuming no chemical interaction between moisture and volatiles, and noting that the answer depends on the thermophysical properties of the system and the fuel,

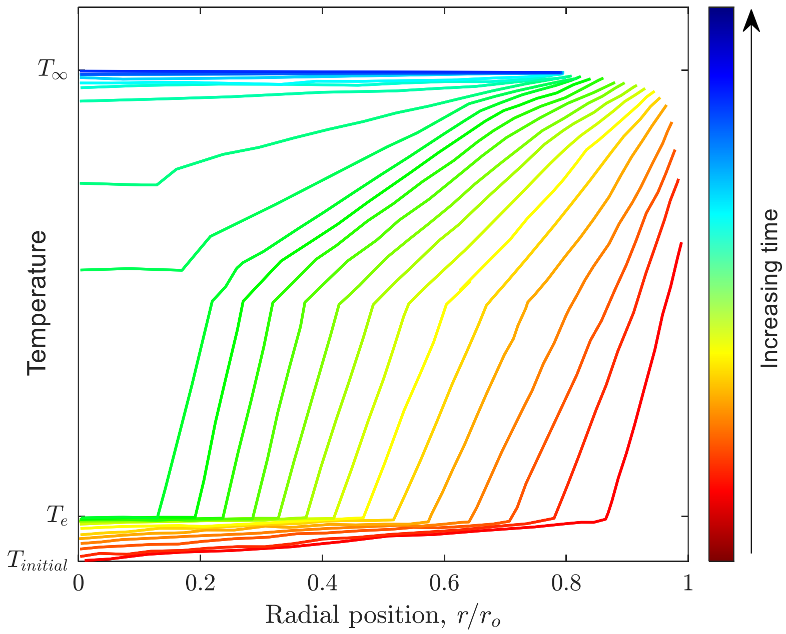


**Figure 5: Typical temperature profiles inside a thermally thick wood particle during drying and devolatilization in a fluidized bed. Results recreated using input information from Storm and Thunman.[121]**

such as the Biot number ($Bi$), the temperature of the bed, moisture content.[118] At a low bed temperature and when $Bi \ll 1$, the particle can be considered isothermal, and, in consequence, no devolatilization would occur as long as the heat sink (moisture) is present. Hence for $Bi \ll 1$, drying and devolatilization can be modelled as separate, sequential processes. In contrast, for a thick particle ($Bi \gg 1$), pyrolysis begins well before the moisture evaporation is completed, meaning that both processes should be considered simultaneously, and that propagation fronts of drying and pyrolysis will be observed.[39,119] In this situation, typical temperature profiles are demonstrated in Fig. 5.[120] For thermally thick particles, the governing equations might differ to Eqs. (8-9), depending on the regions inside the particle. As a qualitative measure of a possible overlap, a dimensionless parameter, called the drying number, *Dr*, which compares the kinetic rate of devolatilization to the rate of drying, was proposed by Thunman *et al.*[33] If *Dr* is small ($< 10^{-1}$), then drying and devolatilization can be modelled separately.[33] The analysis was further extended using three dimensionless numbers, *Dr*, *Bi* and the Damköhler number, *Da*, and the discussion was summarized by Gomez-Barea and Leckner.[13]

### 2.3. *Combustion of volatiles*

The timescale of pyrolysis is significantly shorter than the timescale of char combustion, mainly because combustion is usually limited by slow kinetics (at low temperatures) or oxygen transport (at high temperatures), while the release of volatiles is controlled by heat transfer, which, in fluidized beds, is typically fast (see Section 3.1). Nevertheless, the fate and reactions of the released volatiles significantly affect the overall performance of fluidized bed reactors because a significant portion of biomass is transformed into volatiles, and its combustion represents ~ 50-60 % of the total energy in the fuel.[121] Hence, the burning of volatiles affects the temperature distribution, overall efficiency of combustion, composition of the off-gas, and the formation of temperature-sensitive pollutants (*e.g.* $NO_x$).

Gas released from a biomass particle surrounds it, forming an endogenous bubble, which later detaches and raises to the top of the bed.[122,123] Depending on the effectiveness of gas mixing between the bubble and the emulsion phase, some fraction of the volatiles burns within the bed, but the dominating share of volatiles combusts once the bubble bursts, accessing oxygen in the splash zone and the freeboard. Furthermore, the moving particles of the bed material act as a flame arrestor, hindering gaseous reactions by quenching radicals, which are intermediate species, essential for sustaining homogenous burning. Experimental studies demonstrated that the homogenous combustion of CO and hydrocarbons ($CH_4$ or $C_3H_8$) in beds of fluidizing inert particles ($SiO_2$) was significantly inhibited.[124–126] As a result, ignition occurred at higher temperatures than the spontaneous ignition temperature observed in premixed or diffusive flames. Interestingly, very little work was done on $H_2$ combustion in fluidized beds, except for a study by Baron *et al.*, who noticed that $H_2$ burned in the bubble phase at a temperature ~100 K lower than predicted by kinetic models.[127] The authors explained that this surprising result was caused by the catalytic effect of Ni-containing steel tubes feeding the fuel to the reactor.

Depending on the temperature, gas velocity ($U/U_{mf}$), and the type and size of the fluidized bed, homogeneous combustion will occur firstly in the freeboard, then in the bubbles, and finally in the emulsion phase.[128] Scala and Salatino modeled biomass combustion in a fluidized bed, noting that at 850°C, less than 10% of the volatile matter combusted in the bed, while the rest burned in the splash zone and freeboard.[121] This result is indicative of possible problems when burning biomass, as a non-negligible heat release can occur above the bed (~ 55% of the total heat release in the described simulation[121]). Because of the density difference between biomass and the bed material and the lift from the endogenic bubble of volatiles, the biomass particles tend to separate and float at the top of the bed (see Section 3.4). In that case, the volatiles are released directly to the freeboard with very little mixing with the particulate phase. Some recent studies focused on analyzing the main operational parameters that would help burn volatiles in the bed in a “flameless” mode;[123,129] others proposed simple, dedicated devices to keep the biomass particles submerged and help distribute volatiles in the bed.[130,131]

During biomass combustion, the main homogeneous reactions are the oxidation of volatiles, the water–gas shift reaction, the burning of CO (see Section 2.3), and secondary reactions of hydrocarbons. In some cases, while the particle scale modeling can neglect homogenous combustion, modeling of fluidized bed combustion of biomass at a reactor scale should include homogenous combustion in the freeboard, and ideally also in the bed. Mixing and reactions in the freeboard for both bubbling and circulating beds have been extensively studied and reviewed before,[13,15] and a range of similarities can be found when compared with homogeneous combustion above a fixed bed in moving grate combustors.[24]

Mathematical modeling of combustion of volatiles should account for the described phenomena, such as segregation of the fuel and the volatiles,[123] reaction inhibition by the particulate phase, and the distribution of the volatile components. However, most publications introduce some significant simplifications, such as representing the released volatiles as a single species of a lumped composition. The reaction quenching by the fluidizing particles is also rarely addressed.[13] Instead, the same combustion kinetics are often applied across the whole model. In such cases, the kinetic rates of homogeneous burning are usually modelled with global expressions, eliminating the possibility of flame retardation by the solids, unless the kinetics were determined empirically for the required conditions and bed materials. As noticed by Gómez-Barea and Leckner,[13] most of the used kinetic expressions give significantly different results. Worryingly, studies referenced as the source of the applied kinetic expressions are rarely the original work; hence, the details about the applicability of those commonly used kinetics become obscure.

As an alternative approach, two sets of kinetic parameters can be considered, one for combustion in the bed, and another for the freeboard, as demonstrated by Dounit *et al*.[132] for premixed combustion of methane in a fluidized bed of sand. To highlight the issue with kinetics further, Wu *et al.* compared three commonly used types of kinetics for methane combustion, taken from different experimental setups: laminar flow, turbulent flow, and jet-stirred reactors, demonstrating that only the last one gave a result that allowed reasonable predictions of combustion of $CH_4$ bubbles in a fluidized bed.[133]

### 2.4. *Char combustion*

After devolatilization, the solid residue, char, combusts and gasifies in heterogeneous reactions with an oxidizing gas. The yield, reactivity and internal structure of char depend on the fuel properties (type of biomass, particle size, pre-treatment) and the conditions of devolatilization (heating rate, reactor type, temperature history).[134] Char properties can be characterized by their level of carbonization, which indicates how much the original structure of biomass was reorganized in pyrolysis. Carbonization comes from cross-linking and molecular rearrangement, occurring simultaneously with the breakage of weak bonds, releasing light components to the gas phase. The level of carbonization depends on the final temperature of pyrolysis and, if the temperature is high enough, all chars will have a similar structure, regardless of the origin of biomass.[135] Their reactivity can still differ, likely because of the differences in the content of catalytically active inorganic elements, especially alkali and alkaline earth metals.[134]

Process conditions during pyrolysis also influence the yield and composition of the released volatiles; high heating rates and moderate temperatures promote the production of oils, high temperatures increase the yield of light gases, and low heating rates and low temperatures improve the yield of chars. Further discussion and a graphical summary of product yields from published experiments in fluidized beds were presented by Di Blasi.[12]

If the char is prepared *ex-situ* and then introduced to a fluidized bed, secondary devolatilization can be observed, caused by a thermally induced reorganization of the char structure. The process is accompanied by a small weight loss and release of light gases (*i.e.*, CO, $CO_2$, $CH_4$). The overall impact of the secondary devolatilization on combustion in fluidized beds should not be significant. However, qualitative evaluation of that impact has not been broadly researched, with the process obscured by char combustion.

Among all the discussed processes of biomass conversion in fluidized beds, the heterogenous reactions with char last the longest. Besides being the slowest step, char oxidation is also readily limited by the delivery of the oxidizing gaseous components. For highly porous biomass chars at low temperatures, combustion will be affected by the reaction kinetics, but a moderate increase in the temperature will speed up the kinetics sufficiently to use up the oxygen close to the particle surface. This is when combustion as a process becomes limited by intraparticle mass transfer of the gaseous oxidizer and the reaction products through the char matrix. Further increases in the char temperature (caused by, for example, the exothermic nature of combustion) accelerate the rate, so that oxygen becomes further depleted within the char particle and also its surrounding gas. The rate is then controller by the transfer of oxygen from the bulk. These three situations are often referred to as Regime I (kinetic control), Regime II (intraparticle diffusion control), and Regime III (interparticle diffusion control); although, for combustion, Regime II can also indicate a situation where the reaction takes place in a thin external shell within the char particle,[136] so that the observed rate is influenced by both internal and external transport.

Because the combustion of char strongly affects the overall duration of biomass conversion, the approach of modelling char combustion significantly affects the accuracy of the overall engineering prediction for biomass combustion. Burning of char is often described as a steady-state process; however, experiments show that the rate of combustion changes with conversion (usually increases), which is ascribed to the changes in the internal structure: an increase in the char porosity, a higher number of active sites on the developed surface, and a higher concentration of catalytic metals (K, Ca) per carbon atoms. Previous reviews provide a further overview.[12,57] Beyond the listed factors, the reactivity of char is also manifested through the combustion products, CO and $CO_2$. Assuming the same rate for oxygen delivery in the mass transfer-controlled regimes, if the combustion produces only CO, then the burnout time is half the time expected if combustion produced $CO_2$ instead. The discussion about the final products is still open in the literature, and, in the case of biomass research, recent works provide some new insight (see Fig. 6).

*Primary CO to $CO_2$ ratio from char combustion*

Carbon can be oxidized to either CO or $CO_2$ following reactions [R1] and [R2], respectively.

$$\mathrm{C_{(s)}} + \frac{1}{2}\mathrm{O_2} \rightarrow \mathrm{CO} \qquad \Delta_r H^\circ(298\,K) = -110\ \mathrm{kJ/mol} \qquad \text{[R1]}$$

$$C_{(s)} + O_2 \rightarrow CO_2 \qquad \Delta_r H°(298\,K) = -393\ \mathrm{kJ/mol} \qquad [R2]$$

$$C_{(s)} + \frac{\xi+2}{2(\xi+1)} O_2 \rightarrow \frac{2\xi}{2(\xi+1)} CO + \frac{2}{2(\xi+1)} CO_2 \qquad \Delta_r H°(298\,K) = -\frac{1}{\xi+1}(\xi \times 110 + 393)\ \mathrm{kJ/mol} \qquad [R3]$$

where $\xi$ is the $CO/CO_2$ molar ratio.

As mentioned earlier, the burnout time of chars depends on the primary $CO/CO_2$ ratio, defined as the ratio of the two products created from the reaction at the particle surface.[135–137] As pointed out by Scala, any additional $CO_2$ from the combustion of CO at, or near, the surface of the carbon particle will be difficult to separate from the "primary $CO_2$". Because the effect of that additional CO combustion is similar to effect of the "primary $CO_2$" (total heat release and oxygen consumption), from the practical point of view, its input might be as well included in the "the primary $CO_2$" population.[137]

Both surface combustion reactions (R1-2) are usually described using the Langmuir-Hinshelwood mechanism, although the proposed steps of the mechanisms can differ.[140,141] The starting point always involves $O_2$ adsorption using an active carbon site $C()$ on the char surface, and a subsequent formation of a carbon-oxygen complex, $C(O)$. The surface complex can then desorb, producing gaseous CO or $CO_2$, or participate in a reaction with a gaseous $O_2$ molecule, also giving off CO or $CO_2$.[140,142] An alternative scenario, where the heterogeneous reaction results primarily in CO, was also discussed.[143] In that case, $CO_2$ would be created solely from CO oxidation in the gas phase.

The primary $CO/CO_2$ ratio conveys important information about the combustion and the associated heat release. Reaction [R2] is more exothermic than [R1]; therefore, if the $CO/CO_2$ ratio is low, meaning $CO_2$ is the primary product of char combustion, then the released heat is significant, causing an increase in the char temperature, and consequently faster combustion. Research on $CO/CO_2$ ratio has been primarily carried out for coal char, with only a few studies reporting on the $CO/CO_2$ ratio in biomass combustion.[136] This is quite a significant gap in research because biomass chars are frequently described as more reactive, which should directly connect to the distribution in the combustion products. Even though the same fundamental understanding is expected to apply for biomass and coal chars, dedicated research is needed to fully support this argument and add to the discussion on the combustion mechanisms.

Measurements of the primary $CO/CO_2$ ratio in fluidized beds are difficult because CO can be oxidized in the bed far from the burning particle, although in some cases inert sand can effectively quench CO combustion through recombination of radicals.[124,144] In another scenario, if $CO_2$ is present close to the char surface, then it will react through the reversed Boudouard reaction [R4], producing additional CO.

$$C_{(s)} + CO_2 \rightarrow 2CO \qquad \Delta_r H°(298\,K) = 173\ \mathrm{kJ/mol} \qquad [R4]$$

For clarity in discussing $CO/CO_2$ ratios in char combustion, these two additional reactions (1) the oxidation of CO in the emulsion phase away from the char particle, and (2) char gasification through [R4] are referred to as secondary reactions.

To avoid the influence of secondary reactions, various strategies have been implemented, *e.g.* by adding $POCl_3$ to the gas stream with the intent to inhibit the secondary oxidation of CO.[145] In another study, high flow rates of gas were used to minimize the gas residence time and, hence, the secondary reactions.[146] *In-situ* gas sampling close to the surface of the char particle has also been attempted, with the intent of minimizing the contribution of CO combustion in the emulsion phase.[147] Additionally, the fluidizing gas was dried before its introduction into the bed. The goal was to remove any trace of moisture and, hence, any OH radicals, which are vital for effective CO combustion.[147]

The $CO/CO_2$ ratio changes with the char temperature, with a dependency that is usually represented in Arrhenius form, *viz.*

$$\frac{[\mathrm{CO}]}{[\mathrm{CO_2}]} = A \exp\left(-B/T_p\right) \tag{11}$$

where $A$ and $B$ are constants and $T_p$ is the temperature of the burning particle.[145,146,148]

Equation (11) indicates that the primary $CO/CO_2$ ratio increases with temperature. Some studies, however, demonstrated that during combustion in fluidized beds, this dependence might not be monotonic. Linjewille *et al*.[147] discussed that at low temperatures, oxygen is able to penetrate into the bulk of a char particle, and the combustion results largely in CO. Outside of the particle, the rate of the homogeneous oxidation of CO at low temperatures and in fluidized beds is negligible but increases with temperature, as does the measured $CO/CO_2$ ratio. With a further increase in the temperature, CO starts to combust already in the char pores, which leads to a depletion of $O_2$ in the char matrix and a decrease in the $CO/CO_2$ ratio. At very high temperatures, the heterogenous reaction becomes confined to the external surface of the char particle. Additionally, the CO produced cannot oxidize in the boundary layer because of quenching by the surrounding bed particles. Consequently, the $CO/CO_2$ ratio again increases.

The uncertainty of experimentally evaluated $CO/CO_2$ ratios is especially high for methods based on analyzing the off-gas composition because even if the sampling line is positioned close to the surface of the char particle, the measurements could still be affected by gas mixing and reacting downstream of the sampling point. To overcome this problem, determination of the gaseous products should ideally be done *in-situ*, at the particle surface. While this has not yet been explicitly reported, the future studies will surely implement advanced surface sensitive techniques, investigating the transient surface species and the combustion products. Some initial studies examined oxide species from *ex-situ* prepared fuel samples, although so far only for coal chars.[149]

Other methods for determining $CO/CO_2$ ratios without gas analysis were also proposed. For example, Hayhurst and Parmar[128] carried out combustion experiments using single graphite spheres with a thin thermocouple inserted into the sphere to measure its temperature. From the collected temperature profiles, they performed an energy balance, determining how much of the available carbon oxidized in reaction [R2]. The results indicated that the $CO/CO_2$ ratio decreased as the temperature of the bed increased, reaching a value of 1 at 900°C. Hayhurst and Parmar[128] concluded that solid carbon burns exclusively *via* reaction [R1], producing CO, which later combusts in the gas phase. The quenching influence of the fluidized bed material was the main reason why CO was the only product below 800°C. The authors later argued that with increasing the bed temperature, the CO in small bubbles started to combust. At 900°C, combustion in the particulate phase occurred; therefore, the CO has now oxidized already in the vicinity of particle. As suggested by Mao,[150] the observations might be skewed because the assumption about the heat distribution might not be valid in fluidized beds. Namely, the heat from char combustion was assumed to be used for heating the particle, and the rest of the heat was transferred to the bed by radiation and convection; however, other complexities could have been involved, *e.g.* the heat being fed back by the particle motion in the emulsion phase.

Scala proposed another method of determining the primary $CO/CO_2$ ratio by burning a single sphere of char in a bed fluidized by a gas mixture with low $O_2$ content.[137] By using a low concentration of $O_2$ in the gas, combustion will be readily controlled by $O_2$ transfer to the char particle. Additionally, the heat release will be relatively slow, so the temperature of the char particle will remain close to the temperature of the bed. Thus, the gas properties in the particle boundary layer can be still evaluated using the temperature of the bed, with a negligible error. Under external diffusion control (to the surface of the char particle), the rate of combustion per unit external surface area of char particle, $R_p$ (mol m$^{-2}$ s$^{-1}$), can be expressed as:

$$R_p = \lambda k_g c_{O_2} \tag{12}$$

where $\lambda$ is the molar ratio between the consumed carbon and oxygen; from the stoichiometry in [R3], $\lambda$ is equal to $(1+\xi)/(1+(\xi/2))$, with $\xi$ being the molar ratio of $CO/CO_2$. Furthermore, $k_g$ is the mass transfer coefficient within the boundary layer and $c_{O_2}$ is the molar concentration of $O_2$ in the particulate phase. The value of $k_g$ can be determined through a Sherwood number[151], which itself comes from semi-empirical correlations, for example:

$$Sh = 2.0\varepsilon_{mf} + 0.70\left(Re_{mf}/\varepsilon_{mf}\right)^{1/2} Sc^{1/3} \tag{13}$$

where $\varepsilon_{mf}$ is the bed voidage at the minimum fluidization conditions, $Re_{mf}$ is the Reynolds number calculated using the minimum fluidization velocity, and *Sc* is the Schmidt number. Equation (12) can be used to solve for $\lambda$ by combining mass balances in emulsion and bubble phases, and by knowing the extent of particle conversion, $X$.

Another method of determining the $CO/CO_2$ ratio was recently proposed by Hu *et al.*,[139] using thermogravimetric measurements. The evaluation of $CO/CO_2$ ratios was done by comparing the rate of combustion of carbon, measured from the mass change, with the rate of oxygen transfer, determined in an experiment with a reference material, in their case, through the oxidation of particles of Cu ($Cu+1/2\ O_2 \leftrightarrow CuO$). Both reactions were studied at a high enough temperature to assure full mass transfer control. If the resulting rates were equal, the main product of char combustion would be CO because all the delivered $O_2$ must have been consumed in [R1]. If the rate of combustion was lower than the rate of Cu oxidation, the gaseous products would contain $CO_2$, as expected from the stoichiometry of [R2]. Hu *et al.*[139] found that in an atmosphere of ~1% $O_2$, between 700 and 900°C, a graphite produced only $CO_2$, whereas a lignite char, up to 850°C, produced a mixture of CO and $CO_2$, with the proportion of CO increasing with temperature. Above 850°C, only CO was produced. The same method was recently applied to determine the $CO/CO_2$ ratio from the combustion of birch char. The char was prepared in a fluidized bed, but the combustion experiment was carried out in a thermogravimetric analyzer. Kwong *et al.*[136] demonstrated that the birch char combusted with a $CO/CO_2$ ratio between 0 to 4.0, changing with the experimental temperature between 700 and 900°C.

Most of the published studies on $CO/CO_2$ ratio considered chars derived from coals, and only a limited number of studies provided results for biomass chars. For example, Anna-Couce *et al.* gave $CO/CO_2$ ratios from the combustion of straw, spruce and miscanthus char, measured with a gas analyzer downstream from a single-particle reactor.[152] Similarly, Morin *et al*. and Peterson and Brown looked into the outlet gas composition when burning chars derived from biomass in a fluidized bed reactor.[153,154] In those studies, the influence of secondary reactions was not evaluated, so the measured product ratios might not be fully representative of the primary $CO/CO_2$ ratios. Interestingly, the temperature range in Morin *et al.*'s study was relatively lower than in other combustion experiments, as summarized in Table 3. At low

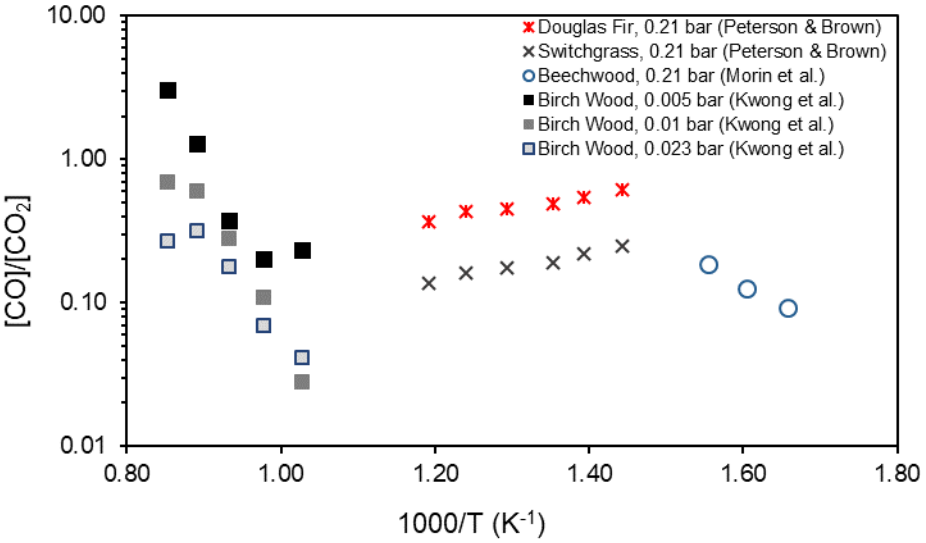


**Figure 6: Ratio of CO to $CO_2$ from combustion of various types of biomass chars at different temperatures.[154,155,164] Experiments in air ($pO_2$ = 0.21 bar), unless stated otherwise.**

temperatures, the secondary reactions, especially in fluidized beds, might have been insignificant.[155] Additionally, the outlet gas was sampled at the bed surface, and, hence, the influence of reactions in the freeboard was minimized. Morin *et al.* found that the CO/$CO_2$ ratio from the combustion of char particles from beech wood increased with temperature,[153] as shown in Fig. 6, in agreement with the trend observed by Kwong *et al*. for birch char,[136] and others for non-biomass chars (Table 3). However, CO/$CO_2$ ratios found by Peterson and Brown for other biomass-derived chars decreased with temperature. This is probably the effect of the secondary reactions inside the bed or, more importantly, in the freeboard, as the gas was sampled at the outlet of the reactor.[154]

Comparing Peterson and Brown's results for different types of biomass chars, the char derived from herbaceous biomass produced more CO, giving a higher CO to $CO_2$ ratio, compared to woody biomass, as shown in Fig. 6. The observed CO/$CO_2$ ratio and the combustion rate were found to correlate with the total ash content in char, the overall content of metals, and the content of potassium in the ash.[154] Potassium is believed to enhance the production of $CO_2$ by facilitating faster transport of oxygen from the gaseous phase to the adsorbed oxygen at a carbon reactive site.[156] Conclusions about the catalytic role of potassium in Peterson and Brown's work was further consolidated by burning char particles after an acid-wash. With potassium being removed, the char particles burned with a lower rate and higher CO/$CO_2$ ratio.[154]

Experimental results for primary CO/$CO_2$ ratios for a range of fuels are summarized in Table 3. The ratio changes with temperature but the exact dependency varies from fuel to fuel. Additionally, the CO/$CO_2$ ratio depends on the concentration of $O_2$ in the system, but the form of this dependency is rarely reported. For a detailed description of biomass combustion, the CO/$CO_2$ ratio should be determined for an expected $O_2$ concentration, prior to constructing the particle-scale models.

Table 3: Summary of published work discussing the $CO/CO_2$ ratio from burning various fuels.

| Experimental System | Ref. | Fuel type | Temperature (K) | Vol % $O_2$ | [CO] / [$CO_2$] |
|---|---|---|---|---|---|
| Flow system | [145] | Coal char and graphite | 730 – 1170 | 5 – 25 | 2510exp(-6240/*T*) |
| | [146] | Electrode carbon | 790 – 1690 | 5 – 25 | 1860exp(-7200/*T*) |
| | [157] | Vitreous carbon | 770 – 920 | 3 – 15 | 25.7exp(-2000/*T*) |
| | [152] | Straw, Spruce, Miscanthus | 773 - 1273 | 5.6 | 0.09 – 0.99 |
| Fluidized bed | [158] | Graphite | 985 – 1110 | 20 | 0.17 – 0.50 |
| | [158] | Petroleum coke | 850 – 970<br>970 – 1220<br>1220 – 1650 | 21 | 1240exp(-7640/*T*)<br>0.00472exp(4500/*T*)<br>12.4exp(-5060/*T*) |
| | [128] | Graphite | 1080 – 1400 | 21 | 4.0 – 0.0 |
| | [138] | Bituminous | 1073 – 1173 | 0.5 – 8.0 | ~ 0 |
| | [150] | Active carbon | 973 – 1173 | 21 | 5.3 – 19 ([1]) |
| | [153] | Beech wood | 603 - 643 | 5 – 21 | 6309exp(-6724/*T*) |
| | [154] | Douglas fir, Pine, Red Oak, Willow, Switchgrass, Corn stover | 693 - 839 | 21 | Herbaceous: 0.0071exp(2440/*T*)<br>Woody: 0.038exp(1800/*T*) |
| Thermogravimetric methods | [160] | Soot | 670 – 890 | 5 – 100 | 120exp(-3200/*T*) |
| | [161] | Highly-pure carbon | 900 – 1600 | 40 – 100 | 600exp(-8000/*T*) $(\rho Y_{O_2})^{-0.24}$ ([2]) |
| | [139] | Graphite,<br>Lignite | 973 – 1173 | 1 | ~ 0<br>From 0 (at 973K) to only CO (at 1173K) |
| | [162] | Coal char | 873 – 1173 | 4,10,20 | 0.95 – 1.4 |
| | [163] | Birch char | 973 – 1173 | 0.57 – 2.3 | 1290exp(-14350/*T*) $P_{O_2}^{-1.08}$ ([3]) |
| Static system | [164] | Graphon | 798 – 948 | 1 – 21 | *A*exp(-3220/*T*), where *A* varies from 140 to 200 |
| Electrodynamic balance | [148] | Spherocarb char | 670 – 1670 | 5 – 100 | 50.0exp(-3040/*T*)$P_{O_2}^{-0.21}$ ([4]) |

([1]) Some of the values of $CO/CO_2$ ratios were negative due to the uncertainty in the experiments. Those were excluded from the summary in Table 3.
([2]) $\rho$ is the density of gas (kg m$^{-3}$) and *Y* is the mass fraction of $O_2$.
([3]) *P* in bar.
([4]) *P* in atm.

Recently, Shaddix *et al.*[165] looked into the existing work on the $CO/CO_2$ ratio, analyzing several studies listed in Table 3.[145,146,148,157,160,161] They concluded that the expression for the $CO/CO_2$ ratio proposed by Tognotti *et al.*[148] gives the most accurate results, applicable for large-scale modeling of combustion of coal chars, because Tognotti *et al.* considered the effect of partial pressure of $O_2$ and performed experiments in a broad temperature range.

Besides the discussed experimental studies, some authors tried to predict the $CO/CO_2$ ratio numerically using various approaches, for example, a mechanistic oxidation model that employs multistep semi-global kinetics.[142,166–168] The proposed reaction pathways have been used to explain the impact of the temperature[168] or partial pressure of $O_2$[169] on the $CO/CO_2$ ratio. Another investigation looked into the influence of metallic elements, although the analysis was mainly qualitative.[169] Quantum mechanics calculations were performed using a DFT modeling to explain the mechanism of formation of $CO_2$ when burning pure carbon (*e.g.* graphene)[170], but, again, the results were only qualitative. Theoretical studies on the $CO/CO_2$ ratio produced specifically from the oxidation of biomass chars are yet to come.

To conclude, the information about the primary $CO/CO_2$ ratio could be summarized as follow:

1. The ratio depends on the temperature, oxygen partial pressure, presence of ash (metallic impurities), and the nature of the carbon (amorphous/ graphitic).[153]
2. Most studies indicate that the $CO/CO_2$ ratio increases with the combustion temperature.
3. There is no consensus about the effect of partial pressure of $O_2$.
4. For the same type of fuel, a higher content of mineral matter favors the formation of $CO_2$; however, clear indication about which elements facilitate the reaction is lacking.

*Kinetics of char oxidation*

The simplest approach to describe the rate of char oxidation is to express the global kinetics as an empirical $n^{th}$ order power law with respect to oxygen:[171,172]

$$R_p = k_{ap} c_{O_2,s}^n = A_{ap} \exp\left(-\frac{E_{ap}}{RT}\right) c_{O_2,s}^n \tag{14}$$

Here, $R_p$ (mol m$^{-2}$ s$^{-1}$) is the rate of combustion per unit of the external surface area of the char particle, $k_{ap}$ is the apparent kinetic coefficient of combustion, which can be expressed using the Arrhenius equation with $E_{ap}$ and $A_{ap}$ for the apparent activation energy and pre-exponential factor, respectively. Then, $c_{O_{2,s}}$ is the concentration of oxygen at the external surface of the char particle.

As char particles are highly porous, a more accurate approach for describing such a heterogeneous combustion reaction is to define the intrinsic kinetic coefficient, $k_i$:

$$R_p = \frac{1}{A_p} \int_0^{V_p} k_i S_{\mathrm{eff}} c_{O_2}^n \, \mathrm{d}V = \frac{1}{A_p} \int_0^{V_p} A_i \exp\left(-\frac{E_i}{RT_p}\right) S_{\mathrm{eff}} c_{O_2}^n \, \mathrm{d}V \tag{15}$$

where $A_p$ is its total external surface area, $V_p$ is the volume of char particle, $S_{\mathrm{eff}}$ is the effective surface area per volume of char particle, $A_i$ and $E_i$ are the Arrhenius parameters for $k_i$; $T_p$ is the particle temperature, and $c_{O_2}$ is the local concentration of $O_2$ within a differential volume, $\mathrm{d}V$.

Sometimes Eqs. (14) and (15) include an $f(X)$ function, which describes how the reactivity of the fuel changes with conversion $X$. The meaning of this addition is to account for the structural changes in the char matrix, as the reaction progresses. The form of the $f(X)$ function usually depends on an assumed conversion model, and a summary of various rate expressions, which account for the structural contribution was presented by Di Blasi.[12] Alternatively, experimentally determined $f(X)$ might be proposed, for example, directly accounting for the changes in the available surface area in the burning or gasifying particle.[173,174]

As mentioned in the review by Haberle *et al.*,[17] the kinetics of char combustion are among parameters that significantly add to the uncertainty in modeling of biomass combustion. The kinetics of oxidation of biomass char vary significantly among the published studies because (1) most of the existing research is focused primarily on the apparent kinetics, $k_{app}$, which vary between studies because of the differences in chemical and physical properties of chars (porosity, reactive surface area, $CO/CO_2$ ratio during combustion); (2) only a limited number of papers report on kinetics, covering relatively wide, but often not overlapping, ranges of biomass types (from grape residues[175] to woody biomass[154,176]); (3) different char preparation methods are used; and, hence, the resulting chars have different reactivities.

Overcoming these listed issues in the research on combustion kinetics will be especially helpful in biomass studies, where a lot of uncertainty also comes from the heterogeneous nature of biomass fuels, their variation in seasons, geographical origin, *etc*. Another gap specific to biomass char is the lack of intrinsic kinetics, as presented in Eq. (15). In this case, the analysis would need to be clearly decoupled from the effects of variable char properties, such as the structure or the effect of catalytic alkaline metals, so that the results could be applicable to many types of biomass. If such intrinsic kinetics were known, only a minimum amount of information about the char would be required to model its combustion, for example, the BET surface area or some enhancement factor describing the catalytic influence from the ash. Intrinsic kinetics for biomass chars might be lacking because experiments with such reactive fuels become affected by mass transfer at lower temperatures than with less reactive fuels.

For a variety of chars (mainly coal chars and graphites), Smith[171] performed a meta-analysis of results gathered from other researchers, coming up with the order of reaction and a set of intrinsic kinetic parameters, giving the values of $n$, $A_i$ and $E_i$ to be 1, $470\ T_p$ and 179.4 kJ mol$^{-1}$, respectively. Because of the lack of similar studies gathering information on biomass chars, Kwong *et al.* successfully applied Smith's intrinsic kinetics when analyzing the combustion of birch char in a fluidized bed, in the presence of active bed materials that release $O_{2(g)}$ in chemical looping oxygen uncoupling experiments.[136] Applying the kinetics of coal char in modeling the combustion of biomass is debatable, as biomass chars are more reactive than high-rank coal chars; the difference in the combustion rates reaches up to 5 orders of magnitude.[177] However, Al-Qayim *et al.*[178] found that if biomass chars burn in Regime I (kinetic control), the resulting activation energy for intrinsic kinetics was close to the one given by Smith. When the rates of burning biomass chars were imposed on Smith's meta-Arrhenius plot, they overlapped closely with the results for more active, low-rank coal chars.

Most of the published work on biomass char combustion focuses on apparent kinetics, Eq. (14), usually accounting for structural changes with $f(X)$. Di Blasi[12] reviewed the published studies up to 2009, summarizing that $E_{ap}$ found in the literature ranges between 76 and 229 kJ mol$^{-1}$. This section gives an overview of recent investigations in apparent kinetics for biomass char combustion.

Shen *et al.*[176] studied the thermal degradation of four wood species in a thermogravimetric analyzer in a flow of air. The obtained mass loss profiles were divided into two regions, one corresponding to pyrolysis and another to combustion. By fitting the differential thermogravimetric results from the second stage, $E_{ap}$ was found, ranging from 89 to 220 kJ mol$^{-1}$, depending on the heating rate and the type of biomass. The results for $E_{ap}$ overlap with the range given in Di Blasi's review; however, the experimental sections analyzed by Shen *et al.*[176] started at relatively low temperatures of ~ 400ºC, where the thermal degradation of lignin is still possible, as mentioned in Section 2.2. Hence, the resulting $E_{ap}$ most likely corresponded to two overlapping reactions, a situation that was observed in a similar study by Varhegyi *et al.*[179]

Recari *et al.*[180] studied the combustion of a spruce char, prepared at various pyrolysis temperatures (623 to 723 K) and pressures (0.1 to 2.0 MPa). Kinetic parameters were extracted at conditions indicating the kinetically controlled regime (< 723 K, 5 vol% $O_2$) from recorded conversion profiles. Chars produced at higher temperatures combusted with lower rates than chars from low-temperature pyrolysis, resulting in higher values for $E_{ap}$ (~97 kJ mol$^{-1}$ for chars prepared at 723 K *vs* 65 kJ mol$^{-1}$ for chars obtained at 623 K). The trend, in which char reactivities decrease with increasing pyrolysis temperature, was well described by Di Blasi,[12] and recently revisited in a few other studies, including the work by Morin *et al.*[181] They found that as the devolatilization temperature increases, the ratios of H/C and O/C in a beech char decrease, probably due to the decomposition of aliphatic groups and a more pronounced tar polymerization, which produces a secondary char. The secondary char structures are less reactive, alter the primary char porosity, and, consequently, the overall reactivity of the final char.[182]

Mian *et al.*[181] and Morin *et al.*[181] found that chars from biomass pellets have a lower $E_{ap}$ than chars from raw biomass. Mian *et al.*[183] proposed that the compact structure of pellets helps suppress deoxygenation of biomass and prevents polymerization of tars, resulting in chars that have high reactivity. Additionally, pelleted chars had a higher ash content, which also affects their reactivity.[181] Peterson and Brown[154] analyzed kinetics for chars originated from various biomass species and found that the value of $k_{ap}$ strongly correlated with the total content of metals and the potassium content in ash. The apparent activation energy, $E_{ap}$ ranged from 94 to 129 kJ mol$^{-1}$, and the lower values corresponded to the higher potassium content, indicating its catalytic influence.

To conclude, the reactivity of chars is important for correctly describing the combustion of biomass. Very little information is available to discuss the intrinsic kinetics of combustion of biomass chars. Most of the published work focuses on apparent reaction rates and factors influencing char reactivity. However, as discussed by Vallejos-Burgos *et al.*,[184] no single one of the relevant parameters, including the char surface area, H/C ratio, ash content, *etc.*, can be expected to be a 'very good index' of char reactivity if analyzed in isolation.

## 3. *Influence of fluidized bed on combustion*

Combustion in fluidized beds differs from other technologies, mainly because of the constant movement of the fluidizing material, which supports good mixing of the solids and, thus, the heat distribution in the bed, but not the mixing of gases; hence, the combustion of chars and volatiles are decoupled. Additionally, fuel properties change with time and the history of thermal treatment. In an ideal system, the biomass particles mix well in the bed, but because of the relatively low density of the fuel compared to the common bed materials, solid segregation is a common issue. Finally, ash can react with the bed material leading to operational problems, for example, bed defluidization and elutriation.

### 3.1. *Heat transfer*

Heat transfer in fluidized bed reactors affects how the particle of fuel heats up, dries and devolatilizes. During combustion, the extraction of heat from a combusting particle also influences the observed rate; in Regime I, the temperature of the particle strongly influences the combustion kinetics, while in Regimes II and III, the rate is affected by the temperature mainly through the coupling of heat and mass transfer in the particle matrix. Thus, correct information about heat transfer to and from a reactive fuel particle is essential for the design of combustors and the prediction of fuel behavior in fluidized bed reactors.

The effective heat transfer coefficient, $h_{\mathrm{eff}}$, for describing heat transfer to and from a freely moving fuel particle in a fluidized bed offers a convenient way to account for different mechanisms of heat transfer simultaneously. In fluidized beds, $h_{\mathrm{eff}}$ includes (1) gas convection/conduction in the particulate phase, $h_{gc}$, (2) particle convection/conduction in the particulate phase, $h_{pc}$, (3) convection with the gas phase flowing as bubbles, $h_b$, (4) radiation, $h_r$.[185,186] Further overview was given by Natale *et al*.[186] and Abdelmotalib *et al*.[187]

The effective heat transfer coefficient changes with the operating conditions in the bed, following the input from all involved mechanisms. It also depends on the relative size of the fuel particle, $d_f$, to the size of the bed particle, $d_p$, as shown in Fig. 7.[188,189] If $d_f/d_p \geq 3$, which is expected in biomass combustion, $h_{\mathrm{eff}}$ is small in the packed bed region ($U < U_{mf}$) but increases sharply (a discontinuity) when $U \geq U_{mf}$, affected by the onset of particle convection, where heat is transferred by frequently replaced bed particles in contact with the fuel particle. The heat transfer coefficient increases with the gas velocity as fluidization becomes more vigorous. It reaches a maximum and drops because, with a further increase in the gas velocity, the fuel particle starts to be covered by gas bubbles, which are less effective in heat distribution than the bed particles.

In bubbling fluidized beds, the heat transfer coefficient of convection/conduction with the gas phase flowing as bubbles, $h_b$, is often neglected because its contribution is small.[190] The input from gas-convection and particle-convection in the particulate phase ($h_{gc}$ and $h_{pc}$) can be

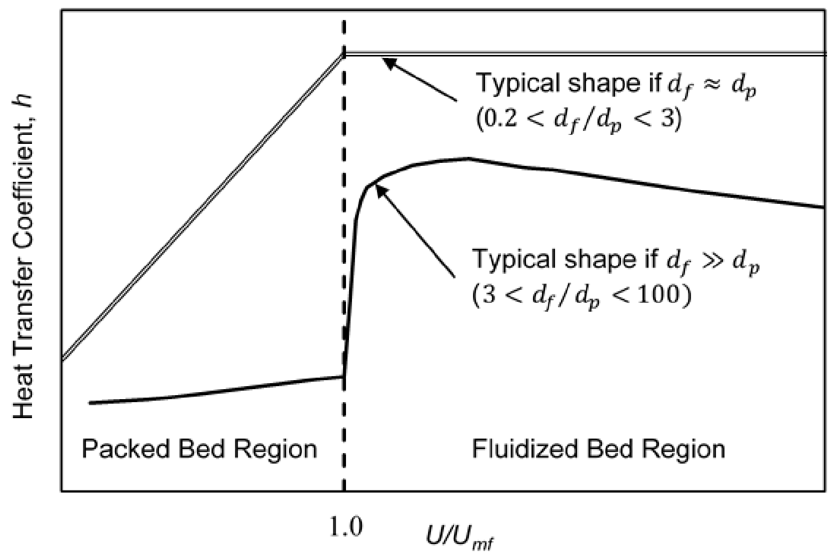


**Figure 7: Heat transfer coefficient in fluidized beds in relation to the superficial gas velocity**.[189,190]

determined separately or as a lumped coefficient.[185] The gas convective component was given by Agarwal as:[190]

$$h_{gc} = \frac{\kappa_g}{d_f}\left\{2\frac{\kappa_{\mathrm{eff},p}}{\kappa_g} + 0.693\left(\left[1 + Re_p Pr\right]^{1/3} - 1\right)\left(\frac{C_{d\varepsilon} Re_p}{8}\right)^{1/3}\left(\frac{q}{\varepsilon_{mf}}\right)^{2/3}\right\} \tag{16}$$

where $\kappa_g$ is the thermal conductivity of the gas, $\kappa_{\mathrm{eff},p}$ is the effective thermal conductivity of the particulate phase, $C_{d\varepsilon}$ is the porosity dependent drag coefficient for the heat transfer surface, $q$ is the tortuosity for the flow of gas through the emulsion phase of porosity $\varepsilon_{mf}$. Similarly to the convective heat transfer with bubbles, the gas-convective contribution in the emulsion phase, $h_{gc}$, is often small, becoming insignificant for systems with fine bed material.[186,190]

The particle-convective heat transfer coefficient, $h_{pc}$, can be determined using the surface-renewal theory:[185,190,191]

$$\frac{1}{h_{pc}} = \frac{d_p}{\phi\kappa_g} + 0.5\sqrt{\frac{\pi\tau_c}{\kappa_{\mathrm{eff},p}\rho_p C_p}} \tag{17}$$

where $d_p/\phi$ represents the thickness of the gas film, $\tau_c$ is the contact time between the fluidized particles and the fuel particle, $\rho_p$ is the density of the particulate phase, and $C_p$ is the specific heat capacity of particles of the bed material. The first term in Eq. (17) represents resistance to conduction between the fuel particle and the bed particles in the gas film. The second term represents resistance across the emulsion phase.[185]

For typical fluidization conditions, Agrawal,[190] and Parmar and Hayhurst[185] predicted the values of $h_{\mathrm{eff}}$ using Eqs. (16) and (17). Parmar and Hayhurst[185] validated the model with experiments of heating spheres of phosphor bronze. The use of inert spheres is beneficial because it eliminates any additional assumptions needed when discussing reactive particles. For example, when heat transfer is deduced from temperature measurements of a combusting char particle, a common experimental approach,[158,192,193] the analysis of the heat transfer coefficient directly relies on the assumptions about mass transfer and the $CO/CO_2$ ratio in the system.[190] On the other hand, inert particles lack the ability to mimic the effect of gas ejection from a reactive particle when the jet of gas prevents the fuel particle from direct contact with the fluidized bed. Hence, for biomass combustion, there is also a need to describe how the heat transfer changes during devolatilization, when the particle ejects a significant amount of gas and segregates from the bed material, *e.g.* floating at the surface of the bed (see Section 3.4).

The described surface renewal model (Eq. 17) is valid when the time needed for the fuel particle to reach a uniform temperature is longer than the time constant for the "renewal" of the bed particles; hence, it applies only if the thermal boundary thickness, $\delta_t$ is small.[194] Additionally, the particulate phase is treated as a continuum which will be invalid if the time constant to heat/cool the bed particle is longer than the contact time with the fuel particle. The surface renewal model was recently revisited by Chao *et al.*, who proposed describing the thermal resistance from the particulate phase as the sum of thermal resistances (*i*) of surface contact and (*ii*) through penetration into the emulsion phase.[195] Other heat transfer models, based on different methods,[13,196] exists, but some do not consider the influence of operating parameters such as fluidization velocity.[158] Von Berg *et al*. implemented different heat transfer models into an existing single-particle model developed by Anca-Couce *et al.*[197] They found that predictions from the model, which considers fluidization velocity, gave results in agreement with experiments; however, some deviation was still observed when the fluidization velocity was close to the $U_{mf}$.[196]

During combustion, the size of the fuel particle decreases, decreasing the $d_f/d_p$ ratio. When the ratio falls <3, for example, when the fuel particle fragments into smaller pieces, the heat transfer coefficient becomes independent of the gas velocity at $U > U_{mf}$, as shown in Fig. 7. Because of a smaller external surface, the number of bed particles in contact with a small fuel particle is smaller than for a larger fuel particle, resulting in a diminishing heat transfer from the particle convection and more pronounced gas convective transfer from the gas flow in the emulsion phase. The behavior for $h_{\mathrm{eff}}$ for small $d_f/d_p$ ratios was confirmed experimentally,[198] giving an expression for the Nusselt number in the fluidized bed, $Nu$, defined with the thermal conductivity of the gas, $\kappa_g$,

$$Nu = \frac{hd_f}{\kappa_g} = 2 + 0.90\, Re_{mf}^{0.62}\left(d_f/d_p\right)^{0.2} \tag{18}$$

where $Re_{mf}$ is the Reynolds number at the onset of fluidization.

Further discussion on heat transfer to active particles in fluidized beds can be found in a few recent studies and previous reviews.[13,15,196,199] For example, a comparison of published correlations for heat and mass transfer was recently given by Leckner,[199] with a discussion separately covering particles of small and large $d_f/d_p$ ratios.

As mentioned earlier, heat transfer in fluidized beds is fast, which helps redistribute heat from a reactive particle. Hence, the values for $h_{\mathrm{eff}}$ are typically large[185], ~300 ± 40 W m$^{-2}$ K$^{-1}$, but reduce to ~220 ± 40 W m$^{-2}$ K$^{-1}$ when the active particle releases gas (as analyzed with 4.6 mm diameter spheres of graphite and dry ice at $U/U_{mf}$ of ~ 1.5[194]). Garcia-Gutierrez *et al.* found that while the model proposed by Chao *et al.*[195] can predict the heat transfer coefficient of a subliming particle (of dry ice) at moderate and high fluidization velocities, it overestimates the heat transfer coefficient at low $U/U_{mf}$ because the buoyancy effects are significant and the active particle can exhibit a flotsam behaviour.[200] Further information about the changes in heat transfer coefficient during the full history of biomass thermal treatment would be beneficial, allowing to extract the influence of the gas release during drying and devolatilization; however, experimental complications arise as decomposition of biomass affects its shape, density, thermal conductivity, *etc*.

### 3.2. *Mass transfer*

Mass transfer during combustion usually boils down to the delivery of oxygen from the bulk to the combusting particle, and the removal of the combustion products away from the particle surface. In contrast, in fluidized beds, the mass transfer supporting combustion involves at least two processes, each described with a separate mass transfer coefficient. The first one is the inter-phase transfer (*i.e.* between phases or regions) in a fluidized bed, for example, between the bubble and emulsion phase; described with an associated inter-phase mass transfer coefficient, $K$ (or specifically $K_{be}$, for the given example). The second mechanism describes the mass transfer between the combusting particle and the oxidizing gas, described with the particle-gas transfer coefficient, $k_g$. As mentioned by Di Natale *et al.*,[186] the analogy between heat and mass transfer does not hold in fluidized beds; hence, the form of correlations for the Sherwood number and the Nusselt number usually vary. A number of previous studies and reviews provide expressions for *Sh* in a fluidized bed, including Prins *et al.*,[201] Agarwal *et al.*,[202] and, more recently, an extensive review by Di Natale *et al*.[186]

Experimental investigations on the particle-gas coefficient, $k_g$, usually involve a chemical reaction, which, naturally, is constraint by stoichiometry. If the process is controlled by mass transfer, then, at a steady-state, the constraint dictates the relationship between mass fluxes. Hence, the effect of the chemical reaction on the resulting magnitude of $k_g$ should be evaluated. This is especially important for non-diluted cases and situations involving non-equimolar counter diffusion (non-EMCD), as encountered during char combustion to CO, in reaction [R1]. Appropriate correction factors are available for combustion in air, often accompanied by a sensitivity analysis for their applicability (*e.g*. Hayhurst,[203] Fortsch *et al.*,[204] Scala[205]). Based on the analytically-derived correction factor from Scala[205], the EMCD mass transfer coefficient in air combustion of chars can lead to errors up to 10%. It is also worth mentioning that the investigations on the correction factors usually ignored the possibility of homogenous reaction of CO and $O_2$ in the boundary layer, assuming the reaction was negligible or, the opposite, rapid (*e.g.* the 'two-film' model from Hayhurst[203]).

As mentioned by Di Natale *et al.*,[186] recently, only few investigations looked into interphase mass transfer. Thus, the usually encountered expression for $K_{be}$ remains the one proposed by Sit and Grace,[206] expressed per unit volume of bubble as:[207]

$$K_{be} = \frac{1.5U_{mf}}{d_b} + 12\left(\frac{\mathcal{D}_G \varepsilon_{mf} U_b}{\pi d_b^3}\right)^{0.5} \tag{19}$$

where $d_b$ is the diameter of the bubble, $\mathcal{D}_G$ is the diffusivity of gas, and $U_b$ is the velocity of the bubble. The first term in Eq. (19) represents the convective throughflow of gas through the bubble and the second term describes the diffusion between phases derived from the penetration theory. Interestingly, the coefficient in the convective term is sometimes reported to be 2 rather than 1.5 (*e.g.* in Scala[205]), probably because of the difference between the throughflow velocity and the minimum fluidizing velocity.[208]

Other correlations for $K_{be}$ were summarized by Medrano *et al*.,[209] who also measured $K_{be}$ at room temperature using a non-invasive IR technique. They found that predictions using the correlation by Davidson and Harrison[210] agreed with the experimental results well, apart from the case when the bed particles were large. Similarly, Wu *et al.* reported good agreement between the correlation of Sit and Grace and results from high-temperature experiments of combusting bubbles of methane.[211] In another study, a CFD - DEM approach was used to investigate $K_{be}$ between a hot and non-isothermal bubble and a bed at room temperature. While the mass transfer mechanism seems to be similar to the isothermal condition, higher temperatures of bubbles reduces $K_{be}$, and mainly its convective component.[212]

### 3.3. *Transient change of fuel properties*

The effect of the thermally induced processes depends on the applied conditions, such as the heating rate, pressure, final temperatures, and specifically for fluidized beds, the fluidization regime, the size of bubbles, *etc*. The progress of all the expected phenomena also depends on the type of biomass, its structure, physicochemical properties, or pre-treatment.

While the influence of the process conditions has been extensively investigated, the effect of the fuel itself is more elusive because of the anisotropic nature of biomass. However, changes in the biomass particle undergoing thermal treatment are significant, including the variation in its shape and changes in the physicochemical and mechanical properties. For example, during pyrolysis $\rho_s$, $C_p$ and $k_s$ denoting the material's density, heat capacity and thermal conductivity change with time and position in the particle. When comparing the thermal diffusivity, $\alpha = \kappa/\rho C_p$), between wood and its chars, the difference ranges an order of magnitude; as shown by Redko *et al.*, $\alpha_{char}/\alpha_{wood}$ = 15 for spruce and its char prepared at 600°C in a fluidized bed[213]. This change in the physical parameters depends on the thermal treatment and can be expressed using empirical correlations, which vary with experimental conditions and the type of biomass.[17] The variability of lignocellulosic fuels, their physical and mechanical properties, and correlations and interactions between those properties were recently summarized by Yan *et al.*[214] The review describes established and new methodologies for characterizing lignocellulosic feedstocks for their rheological properties, grindability, chemical composition, functional groups analysis, or surface properties (*e.g.*, texture and free energy). Haberle *et al*.[17] provided an extensive overview of key physical parameters, which are often not measured explicitly but rather correlated or extrapolated, such as specific heat capacity, shape, heat conductivity, or shrinkage.

While research on biomass combustion often requires some idealization, sensitivity investigations into the influence of biomass anisotropy and changes in the physicochemical parameters are scarce. Recently, Gentile *et al*. developed a general computational framework to investigate pyrolysis of 3D, fully resolved particles of biomass, accounting for the starting anisotropy and thermally-induced, non-uniform changes in the shape and properties.[215] With examples for three particle geometries and varied boundary conditions, the authors demonstrated deformations in the shape and the movement of pyrolysis fronts. The simulations results agreed with available experimental information, although the latter was limited, similarly to the thermal and physical input parameters that would be needed in the model.

Non-uniform efflux of volatiles during pyrolysis creates a structurally non-uniform char; hence, a classification of biochar structures was recently proposed by Lester *et al*.[216] Anisotropy of chars affects their reactivity in gasification[217] and combustion[218]; however, it is rarely included in combustion models. Instead, the expression of combustion rates often contains a fitted parameter or a conversion model, which aims to describe pore and surface evolution (see Section 2.4). Dongyu and Singer demonstrated that pore-resolved information is required to correctly model combustion limited by intraparticle mass transfer. They proposed to improve reactor-scale models by including distributions of particles, their morphologies, and a corresponding distribution of effectiveness factor models.[219] Supporting their conclusions, recent results with *in-situ* and *ex-situ* tomography of pyrolyzed particles demonstrated that the pore distribution throughout char particles is non-uniform and significantly differs for chars made from various types of biomass and at different temperatures.[220]

When a biomass particle undergoes thermal treatment, it shape changes significantly; for example, for birch wood particles, it is associated with 45-70% volume shrinkage.[221] In the simplest approach, the change in the particle volume is linked to the mass loss by linearly reducing the main dimensions of the particle. However, experimental results show that, the shrinkage is not clearly pronounced at high heating rates until ~20% of the mass is lost.[221] Additionally, some investigations report thermally-induced swelling of biomass particles, but the effect diminishes at high heating rates.[222,223]

Shrinkage of biomass is still not well understood, and *a priori* predictions, without any experimental evidence, might be incorrect. For example, despite similar nature and composition, almond shell particles shrink much more than walnut shell particles, the former simultaneously losing mass and volume, the latter losing mass but gaining in porosity.[220] Hence, some studies provide fitted empirical correlations.[224] More advanced models link shrinkage with compressive and tensile stresses the biomass particles experiences during pyrolysis.[225] The computational framework of Gentile *et al*. enables modeling of localized, non-uniform shrinkage without fitted coefficients but, instead, applying dynamic meshing of a reacting 3-D particle. Despite the recent progress, shrinking remains among the fundamental challenges of biomass-focused research.[226]

### 3.4. *Segregation and mixing*

Mixing of solids in fluidized combustors affects the performance and efficiency of the combustion system. Uniform distribution of fuel particles over the cross-section of the bed (horizontal mixing) and throughout the height of the bed (vertical mixing) promotes a uniform fuel conversion, oxygen distribution, and heat and gas release from the fuel.[227]

If a fuel particle floats at the bed surface, it will experience different rates of heat and mass transfer than a particle immersed in the bed. For example, Qin *et al*. showed that the Sherwood number of floating particles is 35% lower than the Sherwood number of immersed particles.[228] The results were obtained in a cold model; hence, a follow-up investigation, validating the effect on biomass combustion, would be useful, especially when considering that the surface of the bed might be exposed to more significant radiation from flames created in gaseous combustion in the splash zone. The effectiveness of horizontal and vertical mixing of biomass particles depends on various factors, such as the density of the fuel, gas velocity $(U/U_{mf})$, bubble fraction, gas release by the fuel particles, *etc*. Hence, investigations into solid mixing usually involve some simplifications (such as cold models), followed by probability analysis of the special distribution of biomass particles.[229] Out of the listed factors, the influence of the jet forces, which are created when volatiles escape the solid particle, are rarely discussed. However, in the effect of those jetting forces, the biomass particles rise to the surface of the bed, and often remain there.[230] The floating particles will also experience slower lateral mixing than the particles submerged in the emulsion phase.[231]

Experimental techniques applied to study the effectiveness of solid mixing usually involve various imaging methods, *e.g.*, X-ray,[232] magnetic particle tracking,[229,231,233] camera probe,[234,235] thermographic camera.[236] In lateral mixing, an increase in the particle size, decrease in the fluidizing velocity and decrease in the pressure drop over the air distributor reduces the extent of the mixing.[236] For axial mixing, the situation depends primarily on the biomass density and the fluidizing velocity. Thus, three fuel segregation regimes can be identified, transitioning with the increase in the gas velocity from a flotsam regime, through a transition regime, to a developed regime.[229] The positive effect of the gas velocity comes from the exogenous bubbles of air, which grow larger and rise faster through the bed, carrying more solid material in their wake, and that induces vigorous axial mixing and reduces the tendency of the biomass particle to segregate to the bed surface. The transition velocities between the axial mixing regimes depend on the bed height and the density of the biomass particle.[230,237] Kohler *et al.* modelled the axial mixing of a biomass particle in a fluidized bed during drying, devolatilization and combustion, considering the change in the size and density of the fuel particle.[230] While the model provides essential insight about the location of biomass particle throughout combustion, the discussion about the influence of the jetting devolatilization of the fuel particle is missing. The probability of segregation of gas-emitting particles is different than from inert particles of the same density;[235] and, according to Solimene *et al*., the mixing models developed for non-emitting particles might be inadequate.[238]

Fiorentino *et al.* reported that emissions of volatiles from biomass fuels lead to the formation of endogenous bubbles, which surround the fuel particle and lift it when travelling towards the bed surface. This segregation phenomenon involves two mechanisms. Either the bubble of volatiles alone lifts the gas-emitting fuel particle, in so-called single bubble segregation (SBS), or the fuel particle moves upwards in a stepwise manner, resulting from a cooperative action of multiple bubbles, in multiple bubble segregation (MBS).[122,239] Whether the segregation progresses depends on the force balance on fuel particle, including its weight, buoyancy force, drag from the fluidizing gas in the particulate phase, and lift from the bubble of volatiles.[238] The magnitude of the lift force was found to depend on the rate of gas emission and the fuel particle size, *i.e.*, for fuel particles coarser than the bed solids, the significance of the lift force is larger than for smaller fuel particles.[238]

The problem of biomass segregation in fluidized systems has been studied extensively and reviewed earlier.[13,15,123] However, some significant gaps in the knowledge remain. Future studies, including advanced modeling with a detailed description of solid movements (*e.g.* DEM modeling, Section 4.1), may shed more light on the specific issue of the gas-emitting particle. Further experimental work validating models at operating reactor temperatures will also be essential. As discussed in Section 2.2, to overcome the problem with biomass segregation, novel concepts to trap the fuel particles in the particulate phase have been proposed.[130,131]

### 3.5. *Bed agglomeration and attrition*

Although biomass usually has a low ash content, some types of biomass contain significant amounts of sodium, potassium or phosphorous, which makes their combustion in fluidized beds challenging.[16] Frequently, biomass combustion results in a deposition of the ash onto the particles of the bed material. This new, ash-originated layer (so called “particle layer” [240]) often leads to operational problems, causing the particles of the bed material to adhere and agglomerate into large chunks, or, the opposite, causing particles to fragment into smaller pieces, which can be easily elutriated out of the reactor. Recent reviews on the interaction between biomass ashes and common bed materials thoroughly summarize the current state of the knowledge, discussing the mechanisms of the observed phenomena and methods of their detection.[16,240,241]

Locally, bed agglomeration leads to the formation of hotspots, and, with time, to defluidization of the whole bed. The mechanisms of agglomeration and the formation of particle layer depend on various factors, *e.g.*, the chemical composition of the bed material, the chemical nature of the biomass ash, the operating temperature. Thus, the effect and scale of possible interaction between the ash and bed particles is difficult to predict.[240,241]

The particle layer leads to agglomeration through one of the two main routes: coating-induced (most often associated with K and Ca) or melting-induced (usually involving P).

Coating-induced agglomeration is caused by the formation of a sticky, viscous layer of alkali salts, created in the reaction between the ash components and the bed material. The mechanism was first noticed in experiments with silica sands, where the sticky coatings were made of low-melting, alkali-rich silicates. Melting-induced agglomeration does not involve the bed material, so, instead, the sticky layer arises as a product of interaction between different ash components. For combustion of woody biomass (rich in K and Ca), the coating-induced agglomeration often starts with a creation of a particle layer made of potassium silicate, which is later penetrated by calcium, lowering the melting point of the layer and also increasing its thickness.[242] Because Ca diffuses towards the melt- particle interface, its accumulation induces microstructural stress, which after prolonged time results in the formation of cracks, both within the bed particle and the particle layer.[243] Cracks create new points of access for the ash elements, now able to attack the internal structure of the bed particle. When the cracks

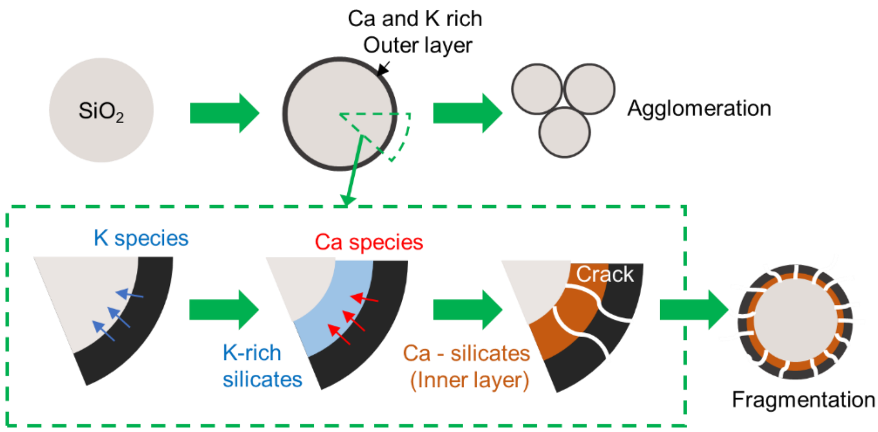

**Figure 8: Mechanism of coating-induced agglomeration and fragmentation of bed particles.**

propagate, the probability of the destruction of the affected particle increases; hence, agglomeration can be accompanied by particle fragmentation,[240] as shown in Fig. 8.

The mechanism of agglomeration is more complicated when the bed material is active, *i.e.* participates in the combustion. This is a characteristic feature of a family of chemical looping (CL) technologies, including the highly promising application of CL for bioenergy and carbon capture (BECCS). Imtiaz *et al.* looked into CuO-based bed materials,[244] which at high temperatures can reversibly release $O_{2(g)}$, supporting combustion. Although their study did not focus on the interaction with biomass ash, the results demonstrate possible problems of material sintering and agglomeration. The authors found that under redox conditions, Cu diffuses through some supporting materials (*e.g.* $ZrO_2$), which leads to agglomeration, but not through others (MgO), which prevent agglomeration. Since agglomeration in CL reactors arises from the redox cycles and chemical activity of the bed material, dedicated studies on CL with biomass are clearly needed. Corcoran *et al.* investigated the fate of biomass ash in "oxygen carrier aided combustion", where the bed material is active, but the main source of oxygen is still the air used for fluidization. They noted that ilmenite interacts with potassium and calcium from biomass ash, with both species diffusing with time towards the core of the main particle.[245] The spread in the size distribution and the average size of the bed particles increased throughout 364 h of biomass burning but with no operational problems caused by agglomeration or defluidization of the bed.

The ash-induced problems have a significant impact on the operation of fluidized beds; hence, even qualitative predictions are essential. The proposed modeling approaches are usually based on equilibrium phase calculations, for predicting what thermodynamically stable phases can form from reactions between the ash and bed material.[246] The thermodynamic calculations can be further expanded by adding a diffusion model[242], or even modeling the particle coating using discrete element models.[247] Alternatively, predictions can be based on empirical correlations.[248] Models that account for the fragmentation of bed particles are lacking.

Possible remedies for preventing ash-induced agglomeration were reviewed by Khan *et al.*[11], Morris *et al.*[249], Bartels *et al*.[250] and include: introduction of anti-agglomeration additives (such as clays, carbonates, hydroxides), multi-fuel co-combustion (*e.g.* sewage sludge helps mitigate the agglomeration behavior of wheat straw[251]), alternative bed materials (dolomite, magnesite, ferric oxide, alumina[250]). Another approach could be to remove the problematic ash components prior to combustion. Vassilev and Vassileva reviewed the effectiveness of water leaching, which, as a pre-treatment method, removes the water-soluble fraction of biomass ash.[252] This fraction can represent from ~ 4 to 61 wt% of the total mass of ash (usually ~ 21-27 wt%), removing a significant fraction of components responsible for corrosion and agglomeration (Cl, S, K, Na, P).[252]

## 4. *New research frontiers*

### 4.1. *Progress in reactor-scale modeling*

A single particle model for drying, pyrolysis and combustion can be readily extended into a simple reactor scale model by accounting for processes external to the particle, such as heat transfer, hydrodynamics in a fluidized bed, or tar cracking.[110,253] The reactor-scale models can be classified by their dimensionality, from zero to three dimensions. A comprehensive review of the common models was given by Gomez-Barea and Leckner.[13] The 0D-types of models, also called the black-box models, simulate the heat and mass balance over the whole system without considering the processes within the reactor. Empirical correlations (*e.g.* a simple kinetic model) can be included into the overall heat and mass balances to predict the performance of combustion. Because of simplicity, zero-dimensional models have been often used in techno-economic analyses for estimations of the reactor's performance, comparisons of different technologies or operating conditions.[254,255] However, the empirical correlations developed from operations of a particular reactor might result in a poor predictability in others conditions and configurations.[13]

Another popular modeling approach, described in every textbook on fluidization, is the one-dimensional phenomenological model. Here, the hydrodynamic effects in the reactor are considered by introducing two (sometimes three) phases or regions, *i.e.* the bubble phase and the emulsion phase. A number of comprehensive reviews describe the assumptions and fundamentals of this model and further its applicability to combustion, *e.g.* Yates,[207] Kunii and Levenspiel[256]. The 1-D models most commonly applied in combustion research is the two-phase model developed by Davison and Harrison (D-H model)[210] and a three-phase model by Kunii and Levenspiel (K-L model)[257,258]. For instance, the D-H model has been used to derive an analytical expression of the burnout time of char particles in a fluidized bed.[144,259] The K-L model differs from the D-H model by considering a wake phase and its interaction with gas in bubbles and solids from the emulsion phase.[256] For combustion research, those 1D modeling approaches provide a good compromise between the accuracy and numerical complications; they are sufficient in describing the main characteristics of fluidization while avoiding the details of complex gas-solid dynamics. Besides the operational predictions, 1D models have been recently used in techno-economics assessments of biomass combustion in fluidized beds, *e.g.* in BECCS systems.[260,261]

More complex phenomenological models of fluidized reactors can also be constructed. For example, Di Blasi *et al.* constructed a 2D reactor model by including unsteady heat and mass transfer for the solid and gas phase, and a simplified momentum transfer described by Darcy's law. Despite considering only a single continuous phase, the simulated conversion of biomass agreed with the results of the experiment conducted at a pilot scale.[262]

More advanced reactor scale-models propose detailed descriptions of solids and gas flows, as both phases are constantly moving in fluidized bed configurations. There are two dominating approaches, one using a multiphase model, often realized within Computational Fluid Dynamics (CFD), the other using combined discrete element models (DEM) for the movement of solids and CFD for the gas. An overview of modeling strategies for gas-solid fluidized beds was summarized by van der Hoef *et al*.[263]

In the Eulerian–Lagrangian models, the solid particles are traced, and particle movements and collisions are modelled using Newtonian laws of motion; separately, the gas phase is solved as a continuous medium, following the Eulerian approach. Hence, in the CFD-DEM models, the expected overall accuracy is higher than in the Eulerian-Eulerian models because the mechanics of the particle movement is correct. However, the interaction between the solids and the gas in the momentum balance is still based on empirical correlations. Linking of the two phases is usually done through the drag force, appearing in the particle Newtonian momentum balance, and, with the opposite sign, in the fluid's Navier-Stokes momentum balance. As each solid particle is tracked in the Lagrangian approach, a more detailed information about the particle behavior and transformations can be incorporated in the model, *e.g.* particle shrinkage and breakage.

On the downside, tracking of a large number of particles requires significant computational efforts, for example, a simulation of 10 s of physical time of a system containing 0.8 million particles took 87 days with a 192-core 2.3 GHz computational machine.[264] To reduce the computational power, some simplifications have been proposed. For example, Papadikis *et al.*[265,266] modelled sand particles as a pseudo-fluid with the Eulerian approach, but tracked all biomass particles with the Lagrangian approach. Alternatively, the number of tracked particles can be reduced by replacing them with parcels of particles but keeping the overall mass unchanged.[267] To preserve the physical nature of the system with parcels, some key parameters, such as gas viscosity or coefficients in the particle contact forces, need to be scaled proportionally to the scaling factor applied when replacing the solid particles.[268] Recently, a char combustion model in a CFD-DEM setup was presented and the results agreed with the experimental findings.[269] Altogether, the detailed modeling of the movement of solid particles that can participate in reactions (biomass particle, char) is a promising and quickly developing field of research. Moreover, single-particle models, described in Section 2, can be readily applied in more advanced models, such as CFD-DEM; for example, a model of a shrinking combusting particle and a model of a thermally thick particle were successfully implemented when modeling combustion of a single particle of fuel using the Eulerian-Lagrangian approach.[270,271]

The insight gained from the recently published studies confirms that DEM and multiphase simulations can reveal interesting new information about processes in fluidized beds. For example, the movement of bubbles can cause non-uniform distribution of the char particles in the horizontal direction while promoting axial mixing. This uneven char distribution affects the gas profiles, *e.g.* the concentration of $O_2$ is lower near the wall where more char particles can be found. For larger particles or fuels of higher density, the horizontal distribution is more uniform than for small or lighter fuel particles, resulting in a more uniform gas profile. However, the explanation for the observed temperature profile is more complex because it involves heat release both from the char and CO combustion. With well-distributed (*e.g.* smaller) char particles, combustion of char close to the wall dominates the heat release in the bed. If the distribution of char particles is not uniform (*e.g.* large particles), the importance of CO combustion, primarily in bubbles, increases, resulting in a more uniform temperature profile.[272]

In addition to the use of CFD-DEM for modelling chemical reactions such as combustion[269,272,273] and gasification[274], CFD-DEM has been used to study fundamental mechanisms of heat and mass transfer in fluidized beds. Patil *et al*. incorporated various mechanisms of heat transfer such as gas-particle, particle-particle, gas-wall, particle-wall into a CFD-DEM simulation, and compared the results with a combined infrared-particle image velocimetry-digital image analysis.[275] They found that an unaccounted form of heat transfer, namely heat transfer across less mobile, dense-phase regions near the wall, caused a deviation between the simulations and experimental results. However, modelling of heat transfer in this region was found challenging because the thermal boundary layer affecting heat transfer near the walls is typically smaller than the grid size in CFD simulations.[276] Modelling of bed-to-wall heat transfer in CFD-DEM can be realized by following a thermal boundary condition approach or a particle-wall conduction model; both were reviewed and studied by Liu *et al.,* who recommend the lumped particle-wall conduction model due to its robustness.[276]

### 4.2. *Spectroscopic and tomographic studies*

With the progress in experimental techniques, new studies offer further insight into thermal processing of biomass, providing fundamental information about factors affecting the quality and reactivity of biochars,[181] the level of carbonization,[135] catalytic effect of metals in ash,[277] and more. This section describes advances in researching combustion achieved using Raman spectroscopy, X-ray micro-tomography, and X-ray photoelectron spectroscopy. Other, more advanced and possibly less available spectroscopic techniques and their applications in combustion have been recently described by Fatehi *et al*.[61]

Among the available relatively new techniques, Raman spectroscopy has been successfully implemented in *in situ* and *ex situ* studies, offering a non-destructive way of characterizing all pyrolysis and combustion products (gas, oils, chars). Recent reviews give an overview of the fundamentals of the technique, characteristic results for cellulose and lignocellulose materials,[278] and notes on its application in thermal processing of solid fuels.[279] When researching chars, Raman spectroscopy can be afflicted by problems with fluorescence and because the interpretation of results is based on advanced peak deconvolution, the informed analysis needs experience.[280]

Recently, Raman micro-spectroscopy was used to investigate the content of lignin in woody biomass, demonstrating an attractive and simple method of quantifying lignin that does not require time-consuming pre-treatment of biomass samples.[281] Raman spectroscopy can inform about the degree of structural order in carbonaceous materials.[282] The change in the char structure (level of carbonization, graphitization[283]) was correlated with reactivity for cellulose chars, prepared at various temperatures.[284] The analysis of the char surface was further demonstrated to correlate well with an (O+H)/C ratio, informing about the level of heteroatoms in the structure, thus, also about the expected reactivity of the fuel.[285] Most of the described investigations were conducted *ex situ*, *i.e*. after quenching the char sample to room temperature. Recently, *in operando* Raman spectroscopy was used to characterize the evolution of the coal structure during pyrolysis and gasification.[286,287] It has been found that the presence of mineral matter promotes the formation of chars with a more disordered structure.[287] It can be expected that *in situ* work dedicated to biomass chars will follow shortly.

In another approach, X-ray micro-tomography (micro-CT) has been used to image the variation in biomass structure and particle shape during pyrolysis at varied temperatures. First, *ex situ* experiments demonstrated the development of microporosity, highlighting the capability of 3D reconstruction of the pore network.[288] The information obtained from the micro-CT scans was then used in pore-resolving simulations to study the effect of the char morphology on gasification and combustion.[219,289] The results, although for coal chars, highlighted the impact of structural anisotropy, indicating that global effectiveness factors fail to describe the effect of intraparticle mass transfer in chars with complex network morphology. *In situ* micro-CT revealed time-resolved information about the evolution in shape and porosity during the pyrolysis of shell-types of biomass, showing that two similar materials can behave markedly differently during the same thermal treatment.[220] In a most recent study, through the combination with X-ray absorption and fluorescence, *in situ* micro-CT was used to track the fronts of pyrolysis and combustion during smoldering of cuboids of oak.[290] The progress of pyrolysis was clearly influenced by the grain structure of the wood, resulting in an irregular 3D plane of the pyrolysis front. The observed 3D features were distinct, demonstrating that shrinking core models might be too idealized in describing the front of pyrolysis in anisotropic fuels. Similarly, the combustion front followed, showing that the least dense regions were consumed first, and that led to particle cracking and fragmentation.

Another technique that has been used in combustion research is X-ray photoelectron spectroscopy (XPS), which offers quantitative information about elements at the sample surface, including their chemical environment. The technique requires skilled deconvolution of the collected spectra; while straightforward in evaluation of metals and heteroatoms, the analysis of C1s spectra for carbons requires informed peak deconvolution, with support or validation from theoretical studies, *e.g.* employing quantum mechanics.[291] Nevertheless, XPS grows in popularity, offering a new insight into the chemical structure of carbonaceous fuels and their evolution upon thermal treatment. For example, non-uniform distribution of elements between the bulk and surface of coal char samples was noted, with the surface enriched in Si and Al, but depleted in Fe, aligning with a non-uniform presence of the mineral matter.[292] In a wood char, the surface-analysis allowed the quantification of the increasing degree of graphitization, noting that the amount of aromatic carbon increased with the temperature of pyrolysis.[293] Interesting information from this surface-sensitive technique came from looking at partially oxidized samples. At low temperatures, a pre-oxidized char surface is predominantly covered by singly-bonded C-O, but at >250ºC, when the sample starts to measurably lose mass, a marked presence of carboxyl groups is observed.[292] More recently, Levi *et al.*[294] demonstrated that a further increase in the oxidation temperature results in the creation of other surface oxides, including epoxy, ether and carbonyl-carboxyl groups. The same group of researchers analyzed pre-oxidized samples, noting that epoxy structures are metastable but, at high temperatures, transform into the “edge” groups, namely the carbonyl-carboxyl and ether groups.[295] When those pre-oxidized samples were heated in $N_2$, the oxide species desorbed as CO and $CO_2$.[149] The $CO/CO_2$ ratio increased with the temperature of pre-oxidation, correlating with a higher ratio of edge to epoxy groups. Summarizing, the existing XPS research, although mainly focused on coal chars, provides an invaluable and new mechanistic insight about the oxidation of carbon. Further work should include biomass chars, and ideally ash-free samples to exclude catalytic effects. *In situ* XPS studies with varied $pO_2$ are yet to come, but will clearly broaden our understanding, adding to the discussion on $CO/CO_2$ ratios.

### 4.3. *Experimental techniques during fluidization*

Magnetic resonance imaging (MRI), electrical capacitance tomography (ECT), electromagnetic tomography or X-ray tomography, to name a few, are non-invasive imaging techniques, which can shed more light on transient behavior and structure of fluidized beds. While not yet applied to biomass combustion, three-dimensional imaging can provide information that can help explain the role of drying and devolatilization on the floating and sinking behavior of biomass particles during combustion. For example, ECT enables measurements of electrical permittivity and conductivity in the bed. As the bubbles and the dense phase exhibit different permittivities, ECT can be used to characterize the 3-D distribution of gas and solids in a fluidized bed, providing information about a bubble size, void fraction, bubble velocity, or describing how does a gas jet impinge into a fluidized bed[296–298]. Measurements with ECT have been recently used to study gas-solid interactions in bubbling and slugging beds. Obtained images informed about the bed structure, providing means for comparison with CFD results and for validating drag models used in Eulerian-Eulerian two-phase simulations.[299] ECT has also been used to investigate the segregation behavior between a fluidized material, silica sand, and wood pellets and chips in a cold bubbling fluidized bed.[300] Although the study confirmed that the biomass particles and sand segregate at room temperature mainly because of the density difference, the work demonstrates that 3-D tomography can be potentially an interesting technique in researching biomass and fluidization, once combined with hot experiments.

Another interesting trend in fluidization research includes micro-fluidized beds. Micro-beds have small volumes, are usually shallow and contained in narrow reactors. Microfluidized experiments have become increasingly popular because of enhanced heat and mass transfer between solid and gas phases and limited back-mixing.[301,302] Although the hydrodynamic behavior during fluidization of micro-beds differs from beds at medium and large scale, the simplicity of microfluidized experiments explains their popularity in researching reaction kinetics, gasification, catalytic effects, *etc*.[302,303] For example, a multistage *in situ* reaction analyzer based on a micro fluidized bed (MFB-MIRA) was developed and applied to determine the reaction order, $n$, of char combustion in $O_2$.[301] The bed was made of 3 to 6 g of $SiO_2$ sand, with a static height of 4 to 10 mm. Experiments gave comparable results ($n$ ~0.9) to the one obtained in larger beds.

Another interesting experimental capability has been demonstrated after combining a microfluidized bed with a thermogravimetric analyzer (MFB–TGA), thus, allowing to measure a mass change of the micro-bed system during the studied reactions. In a traditional fluidized bed, where experiments are primarily based on the analysis of the evolved gas products, the concentration signals could be influenced by gas mixing downstream to the reactor. In MFB–TGA with a real-time weight measurement, the mixing problem can be avoided. MFB–TGA reactors were successfully used in researching kinetics of char gasification[304] or measuring reduction and oxidation kinetics of solid metal oxides used in chemical looping technologies (see Section 4.4), including materials based on manganese and iron oxides,[305] calcium oxide for $CO_2$ capture,[306] or perovskites.[307] Because of the small scale, MFB can be relatively easily combined with other experimental techniques and at a lower cost than would be required from larger fluidized beds. For example, Geng *et al.*[308] carried out combustion experiments in an MFB reactor in conjunction with isotopic labelling. By tracing $^{18}O$ atoms, the authors demonstrated the extent of the $CO_2$ gasification during oxy-fuel char combustion. Overall, the advantages of microfluidized beds are undeniable. Unsurprisingly, the smaller size of fluidized beds becomes more and more attractive as the sensitivity of analytical methods for measuring gas composition or imaging the bed structure improves.

### 4.4. *Chemical looping for biomass combustion and BECCS*

Combustion of biomass provides an opportunity for heat and power production at reduced $CO_2$ emissions[1]. If the $CO_2$ produced during combustion is captured and stored (as in BECCS) rather than released, the process becomes net-negative with respect to $CO_2$ emissions.[309,310] Out of the available BECCS options, chemical looping combustion (CLC) of biomass appears to be the most attractive one, with the lowest costs for $CO_2$ capture.[311] Figure 9 presents the timeline of chemical looping research, highlighting key milestones, while Table 4 provides summary of recent reviews.

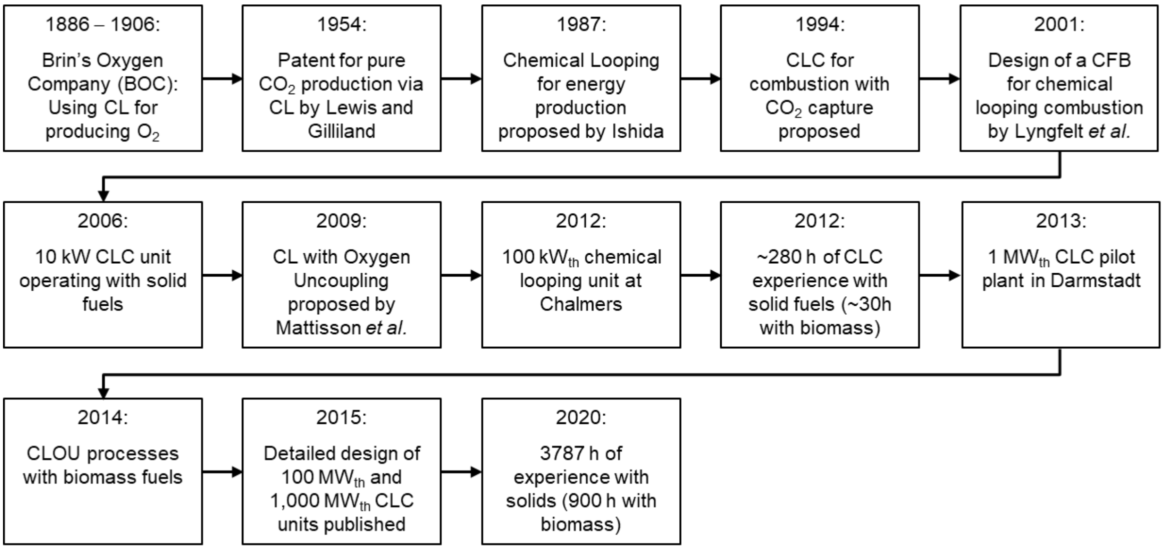


**Figure 9: Timeline and key milestones of CLC research**[312–321].

Chemical looping combustion and related technologies (calcium looping, sorption enhanced reforming, gasification) have been extensively studied in the last 30 years. Lyngfelt summarized the collective operative experience from 49 CLC pilots (300 $W_{th}$ to 1 $MW_{th}$), arriving at 11,000 hours of operation; of these, 700 hours involved CLC powered with biomass.[321,322] The full BECCS sequence from CLC is yet to be demonstrated.

In a typical CLC process, fuel is provided to a fuel reactor (FR), filled with an active bed material, which is fluidized by an air-free stream (*e.g.* $CO_2$). The solid particles of the bed material donate oxygen needed for combustion, and afterwards, are directed to an air reactor (AR) for regeneration with air. Because the bed material effectively transports lattice oxygen between the two reactors, it is commonly referred to as an oxygen carrier (OC). Materials suitable for the cyclic release and uptake of oxygen, as required from oxygen carriers, are mainly mono- or multi-metallic oxides.

In CLC, oxygen transfer involves the OC particles; thus, air and fuel never mix, so flue gas from the FR contains a highly concentrated stream of $CO_2$ in a mixture with readily removable $H_2O$. In the FR, to enable combustion of solid fuel with oxygen from a solid carrier, two approaches have been employed: *in-situ* gasification chemical looping combustion (iG-CLC) and chemical looping combustion with oxygen uncoupling (CLOU).

In iG-CLC, the solid fuel undergoes devolatilization, and the remaining char is gasified in the reaction with the fluidizing gas, *i.e.* $CO_2$ or $H_2O$. As a result, the solid fuel gradually transforms into a gaseous fuel, CO and $H_2$, which can then readily combust by extracting the lattice oxygen from the solid OC. Here, the two heterogeneous reactions, gasification of the solid fuel and combustion on the solid oxide, influence each other. Marek *et al.* demonstrated that active bed materials enhance the gasification rate, shifting the process from being mass transfer controlled back to kinetically controlled.[323] While the result is expected, because the reaction with OC effectively adds to the pool of gasifying medium and removes from the pool of combustible products, the authors provided a method to quantify and predict the enhancement effect for any combination of char fuels and active OCs.

In CLOU, the situation is reversed, as this time, the OC particles release oxygen to the gas phase, $O_{2(g)}$. The molecular oxygen readily reacts with solid fuel particles.[324] Here, again, the two reactions are interconnected. Kwong *et al.* demonstrated that the presence of a CLOU-type OC enhances the rate of combustion of birch char, significantly exceeding the rates observed in an analogous (the same $pO_2$) experiment but with inert bed material.[136] The authors provided an analytical model for predicting the time of complete combustion in CLOU, and, thus, the means of estimating the expected enhancement in the combustion rate.

In industrial operation for BECCS, which would aim at maximizing the $CO_2$ capture and efficiency of energy conversion, the CLC performance can deviate from ideal cases in several manners. The combustible gases (volatiles, products from gasification) should react completely in the FR unit, either in the bed of the active material or in the freeboard. If this is not achieved, then the off-gas requires further processing in an additional operational unit and with purified oxygen to prevent diluting the $CO_2$ stream. Mei *et al.* investigated the effectiveness of a post-combustion unit added to a 100 $kW_{th}$ FR in an iG-CLC configuration, showing that the gas conversion improved from less than 0.9 to nearly 1.0.[325] However, the need for purified oxygen in off-gas processing significantly adds to the operational cost of the plant; Lyngfelt and Leckner estimated that this will represent about 33% of the total cost of $CO_2$ capture.[319] To remedy the issue, a more reactive oxygen carriers can be implemented, such as CuO-based materials releasing $O_{2(g)}$ in a CLOU operation.[318,326] Another problem concerns unconverted particles of char, which can be carried over with the main OC stream from the fuel reactor to the air reactor. Once in the AR, the stream of OC and char is exposed to air, so any remaining char burns achieving full conversion, but the produced $CO_2$ is not captured. To circumvent losses caused by the unburnt char, a separation unit, such as a carbon stripper, might be required, where fuel is separated from the OC stream and returned to the FR.[327]

Oxygen carrier-aided combustion, a concept strongly related to CLC, also involves active materials, but the main gas medium for fluidization is still air, as in regular combustion units. Switching from inert sand to an active material improves the oxygen distribution in the combustor and reduces the concentration of unburnt components in the off-gas.[328] Additionally, this approach leads to lower NO emissions because the active material promotes fuel conversion within the bed, minimizing flame combustion in the freeboard.[329] Oxygen carrier-aided combustion can be readily implemented in the existing combustors if the hydrodynamics with the new bed material can match the design specification. The attractiveness of this approach also arises from the application of inexpensive carriers, such as ilmenite,[328,330] steel converter slag,[301] or natural ores.[332]

Table 4: Recent reviews on chemical looping combustion.

| *Topic* | *Year* | *Reference* |
|---|---|---|
| Chemical looping combustion (extensive review) | 2012 | [317] |
| Fundamentals, oxygen carriers, reactor designs of CLC (extensive books) | 2015, 2019 | [333,334] |
| Chemical looping combustion of solid fuels (extensive review) | 2018 | [336] |
| Reactor design and operation of chemical looping combustion | 2018 | [337] |
| Chemical looping with oxygen uncoupling | 2013, 2019 | [337–339] |

| | | |
|---|---|---|
| Biomass utilization with chemical looping technologies | 2017, 2018 | [310,340] |
| Challenges and outlook of chemical looping | 2019, 2020 | [321,341] |

## *5. Challenges, Research Gaps and Perspectives*

Combustion of biomass has been extensively research. However, with the increasing role of biomass in the future energy systems, the interest in the topic and the need to address the remaining research gaps are justified. As discussed in Section 4, the emerging new experimental and modelling capabilities can offer new insight, explaining the reasons for the observed combustion behavior that is influenced by the type of biomass fuel. For example, the transient changes in the physicochemical and mechanical properties of the fuels significantly affect combustion. The existing relationships of main properties usually link them with temperature or the composition and conversion of the fuel particle. Because of the anisotropic nature of biomass, the thermally induced changes are non-uniform, affecting the shape and speed of the process fronts (drying, pyrolysis, combustion). Describing the relationship between all the multidimensional changes remains a challenge. Simple and generalized methods that can model the spatial and temporal changes realistically, including the change in particle shape, are still needed.

Drying is a well-known process, but because biomass contains a significant amount of chemically bound water, a physically justified description of water release from biomass particles is missing. The classical and commonly used models with heat-sinks and empirical kinetic models remain the go-to approach when detailed information about drying is not crucially important, for example, when drying is fast. However, a full understanding of drying and its effects on biomass remains in the research perspectives. Recently, promising progress has been driven by the equilibrium models, which are computationally expensive but are more accurate. For integration into combustion simulations, a new, hybrid approach, compromising between accuracy and complexity, would be valuable. Bountiful information has also been published on pyrolysis, but often the discussion neglects heat transfer limitations, the influence of conversion, or the compensation effect in kinetics.

With recent developments in computational capabilities and methods allowing for advanced multiphase models, the progress in simulating fluidized beds has significantly accelerated. However, in combustion research, most of the implemented kinetics for homogeneous reactions does not account for the quenching influence of the moving solids. Experimental validation of the popularly used kinetic parameters is required. Furthermore, fuel segregation from the bed material and the impact of the gas emission from the fuel particle has not been fully researched but clearly affects the quality of combustion in fluidized beds. Perspective research and modelling should account for the gas efflux from biomass particles, as well as all phenomena observed during fluidization.

As described in Section 2.4, there is a gap in determining intrinsic kinetics for the combustion of biomass chars, with the biggest challenge concerning a clear description of the effect of char physical properties. In an ideal scenario, a set of kinetics, independent of the type of biomass, can be obtained, similarly as it was done by Smith for coal chars[171]. Since the variety of biomass is vast, the perspective research can turn into new data analysis techniques, for example, employing machine learning, which has been demonstrated useful in other areas of combustion research, such as predicting heating values of biomass,[342] or the product yields from devolatilisation.[343]

Information on the primary $CO/CO_2$ ratios from biomass combustion is scarce; hence, most researchers use correlations obtained from coal chars. This is clearly a significant research gap, since biomass and coals differ significantly in the ash content, and metals in ash are known catalysts of combustion, it would be expected that the $CO/CO_2$ ratio also differs. Furthermore, mechanistic insight into the role of ash in combustion products is still incomplete. Other chemical details affecting combustion, including the catalytic effects from inorganic minerals, are well researched but not implemented in combustion models. A discussion on research needs and challenges concerning chemical details was also presented by Hupa *et al.*[16]

Combustion is often limited by mass transfer; however, the transition between regimes when burning biomass is often not discussed but rather assumed *a priori*. The recent research using micro-CT casts doubt on the validity of using a uniform effectiveness factor in char combustion. While mainly discussed for coal char, perspective research with biomass chars, which are more reactive, would be even more interesting, adding further to the discussion.

## *6. Conclusions*

The topic of biomass combustion in fluidized beds is vast and overlapping with research in other areas (*e.g.* gasification, pyrolysis, heat and mass transfer); hence, the presented critical review is naturally limited to only a few key subtopics. Instead of providing a full overview of the fundamental knowledge in combustion, the intention of this paper was to focus on recent studies and identify research gaps. The readers are strongly encouraged to look for detailed discussions in extensive reviews listed in Table 1. Although the subject is vast, gaps in the existing body of knowledge have been recognized and discussed.

This review focused on selected topics, so it is useful to highlight research areas that were omitted. The pollutants from combustion were not discussed, but the issue was extensively covered by Khan *et al.*[11], Williams *et al.*[14], or Gulyurtlu *et al*.[344] More information on mass transfer, and specifically on gas mixing in fluidized beds was given by Gomez-Barea and Leckner[13] and Di Natale *et al.*[186] The review also omitted the topic of particle fragmentation - one of the most important phenomena affecting the burnout time in fluidized beds. The burning char particle can fragment into smaller pieces due to numerous reasons, such as thermal stress, weakening of the char structure due to gasification and combustion, or attrition because of impact with the fluidizing material. While this topic is not discussed here, it was reviewed by Scala *et al*.[345] Attrition can be modeled with a particle population balance,[346] or an attrition function, which depends on the particle conversion and fitted structural parameters.[347] Char gasification with $H_2O$ or $CO_2$ was only mentioned here, but it is expected that gasification plays a significant role at high temperatures where oxygen transport limits the rate of combustion. Gasification is also highly relevant when discussing combustion in atmospheres with a high $CO_2$ and $H_2O$ content, such as oxy-fuel combustion[348,349] or iG-CLC[323]. The topic of gasification has been reviewed, for example, by Di Blasi,[12] Gomez-Barea and Leckner[13].

In conclusion, thermochemical processing including combustion remains an active field of research, with new challenges arising with the application of new types of fuels, for example, organic wastes. The review described recent progress and some remaining gaps with the intention to inspire primarily young researchers.

**Acknowledgements**

K.Y. Kwong acknowledges the financial support from the Cambridge International Scholarship received from the Cambridge Trust.

**Nomenclature**

Letters

| | |
|---|---|
| A | Pre-exponential constant |
| $A_p$ | External surface area |
| $c$ | Molar concentration |
| $c_1$ | Coefficient for calculating particle surface area |
| $C_p$ | Specific heat capacity |
| $d_f$ | Diameter of fuel particle |
| $d_p$ | Diameter of bed particle |
| $E$ | Activation energy |
| $h$ | Heat transfer coefficient |
| $\Delta H$ | Change in Enthalpy |
| $k$ | Rate constant |
| $k_g$ | Mass transfer coefficient |
| $K$ | Interphase mass transfer coefficient |
| $m$ | Mass |
| $M_v$ | Total mass of volatiles |
| $n$ | Power index (due to shape factor or $n^{th}$ power law) |
| $r$ | Radius, radial coordinate |
| $R$ | Universal gas constant |
| $R_p$ | Rate of combustion per unit of external surface area |
| $S$ | Particle specific surface area |
| $t$ | Time |
| $T$ | Temperature |
| $U$ | Fluid velocity |
| $V$ | Volume |
| $w$ | Weight fraction |
| $X$ | Conversion/ fraction |

Greek letters

| | |
|---|---|
| $\alpha$ | Thermal diffusivity |
| $\varepsilon$ | Voidage |
| $\kappa$ | Thermal conductivity |
| $\mu$ | Viscosity |
| $\rho$ | Density |
| $\tau$ | Characteristic time |

| | |
|---|---|
| $\xi$ | Molar ratio of CO to $CO_2$ |

Dimensionless numbers

| | |
|---|---|
| Bi | Biot number, $Bi = rh/k$ |
| Da | Damköhler number, $Da = \tau_{mass\ transfer}/\tau_{reaction}$ |
| Dr | Drying number, $Dr = \tau_{drying}/\tau_{devolatilization}$ |
| Hr | Heat release number, $Hr$ compares heat release in reaction to heat removal *via* conduction or convection, see Scott *et al.*[99] |
| Pe | Peclet number, $Pe = rU/\alpha$ |
| Pr | Pyrolysis number, $Pr = \tau_{devolatilization}/\tau_{heat\ up}$ |
| Re | Reynolds number, $Re = \rho Ur/\mu$ |
| Sc | Schmidt number, $Sc = \mu/\rho D$ |
| Sh | Sherwood number, $Sh = rh/D$ |

Subscripts

| | |
|---|---|
| b | bubbles |
| eff | effective |
| f | Fuel particle |
| mf | Minimum fluidizing condition |

Abbreviations

| | |
|---|---|
| AR | Air Reactor |
| BECCS | Bioenergy with Carbon Capture and Storage |
| BET | Brunauer-Emmett-Teller |
| CFD | Computational Fluid Dynamics |
| CL | Chemical Looping |
| CLC | Chemical Looping Combustion |
| CLOU | Chemical Looping Combustion with Oxygen Uncoupling |
| CPD | Chemical Percolation Devolatilization |
| CT | Computed Tomography |
| D-H | Davidson and Harrison |
| DAEM | Distributed Activation Energy Model |
| DEM | Discrete Element Modelling |
| DFT | Density Functional Theory |
| EMCD | Equimolar Counter Diffusion |
| FSB | Fiber Saturation Point |
| FR | Fuel Reactor |
| iG-CLC | in-situ Gasification Chemical Looping Combustion |
| K-L | Kunii and Levenspiel |
| MBS | Multiple Bubbles Segregation |
| OC | Oxygen Carrier |

| | |
|---|---|
| PAH | Polycyclic Aromatic Hydrocarbons |
| REA | Reaction Engineering Approach |
| SBS | Single Bubble Segregation |
| VOC | Volatile Organic Compounds |
| XPS | X-ray Photoelectron Spectroscopy |

## References


(1) Sterman, J. D.; Siegel, L.; Rooney-Varga, J. N. Does Replacing Coal with Wood Lower $CO_2$ Emissions? Dynamic Lifecycle Analysis of Wood Bioenergy. *Environmental Research Letters* **2018**, *13* (1), 015007. https://doi.org/10.1088/1748-9326/aaa512.

(2) Fushimi, C. Valorization of Biomass Power Generation System: Noble Use of Combustion and Integration with Energy Storage. *Energy & Fuels* **2021**, *35* (5), 3715–3730. https://doi.org/10.1021/acs.energyfuels.0c04414.

(3) Variny, M.; Varga, A.; Rimár, M.; Janošovský, J.; Kizek, J.; Lukáč, L.; Jablonský, G.; Mierka, O. Advances in Biomass Co-Combustion with Fossil Fuels in the European Context: A Review. *Processes* **2021**, *9* (1), 100. https://doi.org/10.3390/pr9010100.

(4) Roni, M. S.; Chowdhury, S.; Mamun, S.; Marufuzzaman, M.; Lein, W.; Johnson, S. Biomass Co-Firing Technology with Policies, Challenges, and Opportunities: A Global Review. *Renewable and Sustainable Energy Reviews* **2017**, *78*, 1089–1101. https://doi.org/10.1016/j.rser.2017.05.023.

(5) Spliethoff, H. *Power Generation from Solid Fuels*; Power Systems; Springer-Verlag: Berlin Heidelberg, 2010. https://doi.org/10.1007/978-3-642-02856-4.

(6) Jong, W.; Van Ommen, J. R. Scale-up in Fluidized Bed Biomass Combustion; 2009; pp 33–60.

(7) Davidson, J. F. Circulating Fluidised Bed Hydrodynamics. *Powder Technology* **2000**, *113* (3), 249–260. https://doi.org/10.1016/S0032-5910(00)00308-9.

(8) Gayan, P.; Adanez, J.; de Diego, L. F.; García-Labiano, F.; Cabanillas, A.; Bahillo, A.; Aho, M.; Veijonen, K. Circulating Fluidised Bed Co-Combustion of Coal and Biomass. *Fuel* **2004**, *83* (3), 277–286. https://doi.org/10.1016/j.fuel.2003.08.003.

(9) Leckner, B. Atmospheric (Non-Circulating) Fluidized Bed (FB) Combustion. In *Fludised bed technologies for near-zero emission combustion and gasification*; Scala, F., Ed.; Woodhead Publishing, 2013; pp 641–668.

(10) Oka, S. *Fluidized Bed Combustion*, 1st ed.; Anthonly, E. J., Ed.; Marcel Dekker Inc.: New Tork, Basel, 2004.

(11) Khan, A. A.; de Jong, W.; Jansens, P. J.; Spliethoff, H. Biomass Combustion in Fluidized Bed Boilers: Potential Problems and Remedies. *Fuel Processing Technology* **2009**, *90* (1), 21–50. https://doi.org/10.1016/j.fuproc.2008.07.012.

(12) Di Blasi, C. Combustion and Gasification Rates of Lignocellulosic Chars. *Progress in Energy and Combustion Science*. Pergamon April 1, 2009, pp 121–140. https://doi.org/10.1016/j.pecs.2008.08.001.

(13) Gómez-Barea, A.; Leckner, B. Modeling of Biomass Gasification in Fluidized Bed. *Progress in Energy and Combustion Science* **2010**, *36* (4), 444–509. https://doi.org/10.1016/j.pecs.2009.12.002.

(14) Williams, A.; Jones, J. M.; Ma, L.; Pourkashanian, M. Pollutants from the Combustion of Solid Biomass Fuels. *Progress in Energy and Combustion Science* **2012**, *38* (2), 113–137. https://doi.org/10.1016/j.pecs.2011.10.001.

(15) Scala, F. *Fluidized Bed Technologies for Near-Zero Emission Combustion and Gasification*; Elsevier, 2013.

(16) Hupa, M.; Karlström, O.; Vainio, E. Biomass Combustion Technology Development – It Is All about Chemical Details. *Proceedings of the Combustion Institute* **2017**, *36* (1), 113–134. https://doi.org/10.1016/j.proci.2016.06.152.
(17) Haberle, I.; Skreiberg, Ø.; Łazar, J.; Haugen, N. E. L. Numerical Models for Thermochemical Degradation of Thermally Thick Woody Biomass, and Their Application in Domestic Wood Heating Appliances and Grate Furnaces. *Progress in Energy and Combustion Science* **2017**, *63*, 204–252. https://doi.org/10.1016/j.pecs.2017.07.004.
(18) Rabaç, M.; Pereira, S.; Mário Costa, M. Review of Pulverized Combustion of Non-Woody Residues. **2017**. https://doi.org/10.1021/acs.energyfuels.7b03258.
(19) Bellais, M. Modelling of the Pyrolysis of Large Wood Particles. **2007**.
(20) Yashwanth, B. L.; Shotorban, B.; Mahalingam, S.; Lautenberger, C. W.; Weise, D. R. A Numerical Investigation of the Influence of Radiation and Moisture Content on Pyrolysis and Ignition of a Leaf-like Fuel Element. *Combustion and Flame* **2016**, *163*, 301–316. https://doi.org/10.1016/j.combustflame.2015.10.006.
(21) Perré, P.; Keey, R. B. Drying of Wood Principles and Practices. In *Handbook of Industrial Drying*; Mujumdar, A. S., Ed.; CRC Press, 2006; pp 822–880. https://doi.org/10.1201/b17208.
(22) Zhao, J.; Fu, Z.; Jia, X.; Cai, Y. Modeling Conventional Drying of Wood: Inclusion of a Moving Evaporation Interface. *Drying Technology* **2016**, *34* (5), 530–538. https://doi.org/10.1080/07373937.2015.1060999.
(23) Rahimi Borujerdi, P.; Shotorban, B.; Mahalingam, S.; Weise, D. R. Modeling of Water Evaporation from a Shrinking Moist Biomass Slab Subject to Heating: Arrhenius Approach versus Equilibrium Approach. *International Journal of Heat and Mass Transfer* **2019**, *145*, 118672. https://doi.org/10.1016/j.ijheatmasstransfer.2019.118672.
(24) Hosseini Rahdar, M.; Nasiri, F.; Lee, B. A Review of Numerical Modeling and Experimental Analysis of Combustion in Moving Grate Biomass Combustors. *Energy and Fuels*. American Chemical Society October 17, 2019, pp 9367–9402. https://doi.org/10.1021/acs.energyfuels.9b02073.
(25) McIntosh, M. J. Mathematical Model of Drying in a Brown Coal Mill System. 1. Formulation of Model. *Fuel* **1976**, *55* (1), 47–52. https://doi.org/10.1016/0016-2361(76)90069-7.
(26) McIntos, M. J. Mathematical Model of Drying in a Brown Coal Mill System. 2. Testing of Model. *Fuel* **1976**, *55* (1), 53–58. https://doi.org/10.1016/0016-2361(76)90070-3.
(27) Agarwal, P. K.; Genett, W. E.; Lee, Y. Y. Pseudo Steady State Receding Core Model for Drying with Shrinkage of Low Ranked Coals. *Chemical Engineering Communications* **1984**, *27* (1–2), 9–21. https://doi.org/10.1080/00986448408940488.
(28) Agarwal, P. K.; Genetti, W. E.; Lee, Y. Y.; Prasad, S. N. Model for Drying during Fluidized-Bed Combustion of Wet Low-Rank Coals. *Fuel* **1984**, *63* (7), 1020–1027. https://doi.org/10.1016/0016-2361(84)90328-4.
(29) Komatina, M.; Manovic, V.; Saljnikov, A. A Model of Coal Particle Drying in Fluidized Bed Combustion Reactor. *Energy Sources, Part A: Recovery, Utilization, and Environmental Effects* **2007**, *29* (3), 239–250. https://doi.org/10.1080/00908310600688796.
(30) Bird, R. B.; Stewart, W. E.; Lightfoot, E. N. *Transport Phenomena*, 2nd ed.; Wiley&sons: New York, 2002.
(31) Winter, F.; Prah, M. E.; Hofbauer, H. Temperatures in a Fuel Particle Burning in a Fluidized Bed: The Effect of Drying, Devolatilization, and Char Combustion. *Combustion and Flame* **1997**, *108* (3), 302–314. https://doi.org/10.1016/S0010-2180(96)00140-X.
(32) Bryden, K. M.; Ragland, K. W.; Rutland, C. J. Modeling Thermally Thick Pyrolysis of Wood. *Biomass and Bioenergy* **2002**, *22* (1), 41–53. https://doi.org/10.1016/S0961-9534(01)00060-5.

(33) Thunman, H.; Davidsson, K.; Leckner, B. Separation of Drying and Devolatilization during Conversion of Solid Fuels. *Combustion and Flame* **2004**, *137* (1–2), 242–250. https://doi.org/10.1016/j.combustflame.2004.02.008.
(34) Alves, S. S.; Figueiredo, J. L. A Model for Pyrolysis of Wet Wood. *Chemical Engineering Science* **1989**, *44* (12), 2861–2869. https://doi.org/10.1016/0009-2509(89)85096-1.
(35) Di Blasi, C. Multi-Phase Moisture Transfer in the High-Temperature Drying of Wood Particles. *Chemical Engineering Science* **1998**, *53* (2), 353–366. https://doi.org/10.1016/S0009-2509(97)00197-8.
(36) Varnier, M.; Sauvat, N.; Ulmet, L.; Montero, C.; Dubois, F.; Gril, J. Influence of Temperature in a Mass Transfer Simulation: Application to Wood. *Wood Science and Technology*. Springer July 1, 2020, pp 943–962. https://doi.org/10.1007/s00226-020-01197-y.
(37) Sand, U.; Sandberg, J.; Larfeldt, J.; Bel Fdhila, R. Numerical Prediction of the Transport and Pyrolysis in the Interior and Surrounding of Dry and Wet Wood Log. *Applied Energy* **2008**, *85* (12), 1208–1224. https://doi.org/10.1016/j.apenergy.2008.03.001.
(38) Kung, K. S.; Ghoniem, A. F. Multi-Scale Analysis of Drying Thermally Thick Biomass for Bioenergy Applications. *Energy* **2019**, *187*, 115989. https://doi.org/10.1016/j.energy.2019.115989.
(39) Galgano, A.; Di Blasi, C. Modeling the Propagation of Drying and Decomposition Fronts in Wood. *Combustion and Flame* **2004**, *139* (1–2), 16–27. https://doi.org/10.1016/j.combustflame.2004.07.004.
(40) Bryden, K. M.; Hagge, M. J. Modeling the Combined Impact of Moisture and Char Shrinkage on the Pyrolysis of a Biomass Particle. *Fuel* **2003**, *82* (13), 1633–1644. https://doi.org/10.1016/S0016-2361(03)00108-X.
(41) Chan, W. C. R.; Kelbon, M.; Krieger, B. B. Modelling and Experimental Verification of Physical and Chemical Processes during Pyrolysis of a Large Biomass Particle. *Fuel* **1985**, *64* (11), 1505–1513. https://doi.org/10.1016/0016-2361(85)90364-3.
(42) Simal, S.; Femenia, A.; Garau, M. C.; Rosselló, C. Use of Exponential, Page's and Diffusional Models to Simulate the Drying Kinetics of Kiwi Fruit. *Journal of Food Engineering* **2005**, *66* (3), 323–328. https://doi.org/10.1016/j.jfoodeng.2004.03.025.
(43) Peters, B.; Bruch, C. Drying and Pyrolysis of Wood Particles: Experiments and Simulation. *Journal of Analytical and Applied Pyrolysis* **2003**, *70* (2), 233–250. https://doi.org/10.1016/S0165-2370(02)00134-1.
(44) Chen, X. D.; Putranto, A. Reaction Engineering Approach (REA) to Modeling Drying Problems: Recent Development and Implementations. *Drying Technology* **2015**, *33* (15–16), 1899–1910. https://doi.org/10.1080/07373937.2015.1069326.
(45) Kharaghani, A.; Hiep Le, K.; Thu Hang Tran, T.; Tsotsas, E. Reaction Engineering Approach for Modeling Single Wood Particle Drying at Elevated Air Temperature. *Chemical Engineering Science* **2019**. https://doi.org/10.1016/J.CES.2019.01.042.
(46) Gronli, M. G.; Melaaen, M. C. Mathematical Model for Wood Pyrolysis-Comparison of Experimental Measurements with Model Predictions. *Energy and Fuels* **2000**, *14* (4), 791–800. https://doi.org/10.1021/ef990176q.
(47) Le, K. H.; Tsotsas, E.; Kharaghani, A. Continuum-Scale Modeling of Superheated Steam Drying of Cellular Plant Porous Media. *International Journal of Heat and Mass Transfer* **2018**, *124*, 1033–1044. https://doi.org/10.1016/j.ijheatmasstransfer.2018.04.032.
(48) Mehrabian, R.; Zahirovic, S.; Scharler, R.; Obernberger, I.; Kleditzsch, S.; Wirtz, S.; Scherer, V.; Lu, H.; Baxter, L. L. A CFD Model for Thermal Conversion of Thermally Thick Biomass Particles. *Fuel Processing Technology* **2012**, *95*, 96–108. https://doi.org/10.1016/j.fuproc.2011.11.021.
(49) Gómez, M. A.; Porteiro, J.; Patiño, D.; Míguez, J. L. Fast-Solving Thermally Thick Model of Biomass Particles Embedded in a CFD Code for the Simulation of Fixed-Bed Burners. *Energy Conversion and Management* **2015**, *105*, 30–44. https://doi.org/10.1016/j.enconman.2015.07.059.

(50) Yang, Y. B.; Sharifi, V. N.; Swithenbank, J.; Ma, L.; Darvell, L. I.; Jones, J. M.; Pourkashanian, M.; Williams, A. Combustion of a Single Particle of Biomass. https://doi.org/10.1021/ef700305r.
(51) Lu, H.; Robert, W.; Peirce, G.; Ripa, B.; Baxter, L. L. Comprehensive Study of Biomass Particle Combustion. *Energy & Fuels* **2008**, *22* (4), 2826–2839. https://doi.org/10.1021/ef800006z.
(52) Li, T.; Thunman, H.; Ström, H. A Fast-Solving Particle Model for Thermochemical Conversion of Biomass. *Combustion and Flame* **2020**, *213*, 117–131. https://doi.org/10.1016/j.combustflame.2019.11.018.
(53) Kharaghani, A.; Hiep Le, K.; Thu Hang Tran, T.; Tsotsas, E.; Le, K. H.; Tran, T. T. H.; Tsotsas, E. Reaction Engineering Approach for Modeling Single Wood Particle Drying at Elevated Air Temperature. *Chemical Engineering Science* **2019**, *199*, 602–612. https://doi.org/10.1016/J.CES.2019.01.042.
(54) Biagini, E.; Barontini, F.; Tognotti, L. Devolatilization of Biomass Fuels and Biomass Components Studied by TG/FTIR Technique. **2006**. https://doi.org/10.1021/ie0514049.
(55) Grieco, E.; Baldi, G. Analysis and Modelling of Wood Pyrolysis. *Chemical Engineering Science* **2011**, *66* (4), 650–660. https://doi.org/10.1016/j.ces.2010.11.018.
(56) Ren, X.-Y.; Feng, X.-B.; Cao, J.-P.; Tang, W.; Wang, Z.-H.; Yang, Z.; Zhao, J.-P.; Zhang, L.-Y.; Wang, Y.-J.; Zhao, X.-Y. Catalytic Conversion of Coal and Biomass Volatiles: A Review. *Energy & Fuels* **2020**. https://doi.org/10.1021/acs.energyfuels.0c01432.
(57) Di Blasi, C.; Modeling Chemical and Physical Processes of Wood and Biomass Pyrolysis. *Progress in Energy and Combustion Science* **2008**, *34* (1), 47–90. https://doi.org/10.1016/j.pecs.2006.12.001.
(58) Anca-Couce, A. Reaction Mechanisms and Multi-Scale Modelling of Lignocellulosic Biomass Pyrolysis. *Progress in Energy and Combustion Science* **2016**, *53*, 41–79. https://doi.org/10.1016/j.pecs.2015.10.002.
(59) Wang, G.; Dai, Y.; Yang, H.; Xiong, Q.; Wang, K.; Zhou, J.; Li, Y.; Wang, S. A Review of Recent Advances in Biomass Pyrolysis. *Energy and Fuels*. American Chemical Society 2020. https://doi.org/10.1021/acs.energyfuels.0c03107.
(60) Chen, X.; Che, Q.; Li, S.; Liu, Z.; Yang, H.; Chen, Y.; Wang, X.; Shao, J.; Chen, H. Recent Developments in Lignocellulosic Biomass Catalytic Fast Pyrolysis: Strategies for the Optimization of Bio-Oil Quality and Yield. *Fuel Processing Technology* **2019**, *196*, 106180. https://doi.org/10.1016/j.fuproc.2019.106180.
(61) Fatehi, H.; Weng, W.; Li, Z.; Bai, X. S.; Aldén, M. Recent Development in Numerical Simulations and Experimental Studies of Biomass Thermochemical Conversion. *Energy and Fuels*. American Chemical Society 2021. https://doi.org/10.1021/acs.energyfuels.0c04139.
(62) Kaczor, Z.; Buliński, Z.; Werle, S. Modelling Approaches to Waste Biomass Pyrolysis: A Review. *Renewable Energy* **2020**, *159*, 427–443. https://doi.org/10.1016/j.renene.2020.05.110.
(63) Zhao, S.; Luo, Y. Multiscale Modeling of Lignocellulosic Biomass Thermochemical Conversion Technology: An Overview on the State-of-the-Art. *Energy & Fuels* **2020**, *34* (10), 11867–11886. https://doi.org/10.1021/acs.energyfuels.0c02247.
(64) Wang, S.; Dai, G.; Yang, H.; Luo, Z. Lignocellulosic Biomass Pyrolysis Mechanism: A State-of-the-Art Review. *Progress in Energy and Combustion Science* **2017**, *62*, 33–86. https://doi.org/10.1016/j.pecs.2017.05.004.
(65) Kostetskyy, P.; Broadbelt, L. J. Progress in Modeling of Biomass Fast Pyrolysis: A Review. *Energy & Fuels* **2020**, *34*, 15195–15216. https://doi.org/10.1021/acs.energyfuels.0c02295.
(66) Thunman, H.; Niklasson, F.; Johnsson, F.; Leckner, B. Composition of Volatile Gases and Thermochemical Properties of Wood for Modeling of Fixed or Fluidized Beds. *Energy and Fuels* **2001**, *15* (6), 1488–1497. https://doi.org/10.1021/ef010097q.

(67) Ranzi, E.; Cuoci, A.; Faravelli, T.; Frassoldati, A.; Migliavacca, G.; Pierucci, S.; Sommariva, S. Chemical Kinetics of Biomass Pyrolysis. *Energy & Fuels* **2008**, *22* (6), 4292–4300. https://doi.org/10.1021/ef800551t.
(68) Shafizadeh, F.; Chin, P. P. S. Thermal Deterioration of Wood. In *Wood Technology: Chemical Aspects*; ACS , 1977; pp 57–81. https://doi.org/10.1021/bk-1977-0043.ch005.
(69) Thurner, F.; Mann, U. Kinetic Investigation of Wood Pyrolysis. *Industrial and Engineering Chemistry Process Design and Development* **1981**, *20* (3), 482–488. https://doi.org/10.1021/i200014a015.
(70) Nunn, T. R.; Howard, J. B.; Longwell, J. P.; Peters, W. A. Product Compositions and Kinetics in the Rapid Pyrolysis of Sweet Gum Hardwood. *Industrial and Engineering Chemistry Process Design and Development* **1985**, *24* (3), 836–844. https://doi.org/10.1021/i200030a053.
(71) Wagenaar, B. M.; Prins, W.; van Swaaij, W. P. M. Flash Pyrolysis Kinetics of Pine Wood. *Fuel Processing Technology* **1993**, *36* (1–3), 291–298. https://doi.org/10.1016/0378-3820(93)90039-7.
(72) Reina, J.; Velo, E.; Puigjaner, L. Kinetic Study of the Pyrolysis of Waste Wood. *Industrial and Engineering Chemistry Research* **1998**, *37* (11), 4290–4295. https://doi.org/10.1021/ie980083g.
(73) Di Blasi, C.; Branca, C. Kinetics of Primary Product Formation from Wood Pyrolysis. *Industrial & Engineering Chemistry Research* **2001**, *40* (23), 5547–5556. https://doi.org/10.1021/ie000997e.
(74) Berčič, G. The Universality of Friedman's Isoconversional Analysis Results in a Model-Less Prediction of Thermodegradation Profiles. *Thermochimica Acta* **2017**, *650*, 1–7. https://doi.org/10.1016/j.tca.2017.01.011.
(75) Liu, L.; Guo, Q.-X. Isokinetic Relationship, Isoequilibrium Relationship, and Enthalpy−Entropy Compensation. *Chemical Reviews* **2001**, *101* (3), 673–696. https://doi.org/10.1021/cr990416z.
(76) Zhang, Z.; Duan, H.; Zhang, Y.; Guo, X.; Yu, X.; Zhang, X.; Rahman, Md. M.; Cai, J. Investigation of Kinetic Compensation Effect in Lignocellulosic Biomass Torrefaction: Kinetic and Thermodynamic Analyses. *Energy* **2020**, *207*, 118290. https://doi.org/10.1016/j.energy.2020.118290.
(77) Xu, D.; Chai, M.; Dong, Z.; Rahman, Md. M.; Yu, X.; Cai, J. Kinetic Compensation Effect in Logistic Distributed Activation Energy Model for Lignocellulosic Biomass Pyrolysis. *Bioresource Technology* **2018**, *265*, 139–145. https://doi.org/10.1016/j.biortech.2018.05.092.
(78) Mui, E. L. K.; Cheung, W. H.; Lee, V. K. C.; McKay, G. Compensation Effect during the Pyrolysis of Tyres and Bamboo. *Waste Management* **2010**, *30* (5), 821–830. https://doi.org/10.1016/j.wasman.2010.01.014.
(79) Liden, A. G.; Berruti, F.; Scott, D. S. A Kinetic Model for the Production of Liquids from the Flash Pyrolysis of Biomass. *Chemical Engineering Communications* **1988**, *65* (1), 207–221. https://doi.org/10.1080/00986448808940254.
(80) Janvijitsakul, K.; Kuprianov, V. I. Polycyclic Aromatic Hydrocarbons in Coarse Fly Ash Particles Emitted from Fluidized-Bed Combustion of Thai Rice Husk. **2007**, 9.
(81) Grass, S. W.; Jenkins, B. M. Biomass Fueled Fluidized Bed Combustion: Atmospheric Emissions, Emission Control Devices and Environmental Regulations. *Biomass and Bioenergy* **1994**, *6* (4), 243–260. https://doi.org/10.1016/0961-9534(94)90064-7.
(82) Walker, J. C. F. *Primary Wood Processing: Principle and Practice*; Chapman & Hall: London, 1993.
(83) Ward, S. M.; Braslaw, J. Experimental Weight Loss Kinetics of Wood Pyrolysis under Vacuum. *Combustion and Flame* **1985**, *61* (3), 261–269. https://doi.org/10.1016/0010-2180(85)90107-5.
(84) Shafizadeh, F. Pyrolytic Reactions and Products of Biomass. In *Fundamentals of biomass thermochemical conversion*; Overend, R. P., Milne, T. A., Mudge, L. K., Eds.; Elsevier: London, 1985; pp 183–217.

(85) Grønli, M. G.; Várhegyi, G.; Di Blasi, C. Thermogravimetric Analysis and Devolatilization Kinetics of Wood. *Industrial and Engineering Chemistry Research* **2002**, *41* (17), 4201–4208. https://doi.org/10.1021/ie0201157.
(86) Müller-Hagedorn, M.; Bockhorn, H.; Krebs, L.; Müller, U. A Comparative Kinetic Study on the Pyrolysis of Three Different Wood Species. In *Journal of Analytical and Applied Pyrolysis*; Elsevier, 2003; Vol. 68–69, pp 231–249. https://doi.org/10.1016/S0165-2370(03)00065-2.
(87) Miller, R. S.; Bellan, J. A Generalized Biomass Pyrolysis Model Based on Superimposed Cellulose, Hemicellulose and Lignin Kinetics. *Combustion Science and Technology* **1997**, *126*, 97–137. https://doi.org/10.1080/00102209708935670.
(88) Sheng, C.; Azevedo, J. L. T. Modeling Biomass Devolatilization Using the Chemical Percolation Devolatilization Model for the Main Components. *Proceedings of the Combustion Institute* **2002**, *29* (1), 407–414. https://doi.org/10.1016/S1540-7489(02)80054-2.
(89) Zhang, J.; Zheng, S.; Chen, C.; Wang, X.; ur Rahman, Z.; Tan, H. Kinetic Model Study on Biomass Pyrolysis and CFD Application by Using Pseudo-Bio-CPD Model. *Fuel* **2021**, *293*, 120266. https://doi.org/10.1016/j.fuel.2021.120266.
(90) Banyasz, J. L.; Li, S.; Lyons-Hart, J.; Shafer, K. H. Gas Evolution and the Mechanism of Cellulose Pyrolysis. *Fuel* **2001**, *80* (12), 1757–1763. https://doi.org/10.1016/S0016-2361(01)00060-6.
(91) Wang, Q.; Song, H.; Pan, S.; Dong, N.; Wang, X.; Sun, S. Initial Pyrolysis Mechanism and Product Formation of Cellulose: An Experimental and Density Functional Theory(DFT) Study. *Scientific Reports* **2020**, *10* (1), 3626. https://doi.org/10.1038/s41598-020-60095-2.
(92) Cai, J.; Wu, W.; Liu, R. An Overview of Distributed Activation Energy Model and Its Application in the Pyrolysis of Lignocellulosic Biomass. *Renewable and Sustainable Energy Reviews* **2014**, *36*, 236–246. https://doi.org/10.1016/j.rser.2014.04.052.
(93) Scott, S. A.; Dennis, J. S.; Davidson, J. F.; Hayhurst, A. N. An Algorithm for Determining the Kinetics of Devolatilisation of Complex Solid Fuels from Thermogravimetric Experiments. *Chemical Engineering Science* **2006**, *61* (8), 2339–2348. https://doi.org/10.1016/J.CES.2005.11.002.
(94) Anthony, D. B.; Howard, J. B.; Hottel, H. C.; Meissner, H. P. Rapid Devolatilization and Hydrogasification of Bituminous Coal. *Fuel* **1976**, *55* (2), 121–128. https://doi.org/10.1016/0016-2361(76)90008-9.
(95) Braun, R. L.; Burnham, A. K. *Analysis of Chemical Reaction Kinetics Using a Distribution of Activation Energies and Simpler Models*; 1987; Vol. 1.
(96) Burnham, A. K.; Braun, R. L. Global Kinetic Analysis of Complex Materials. *Energy and Fuels* **1999**, *13* (1), 1–22. https://doi.org/10.1021/ef9800765.
(97) Wang, S.; Lin, H.; Ru, B.; Sun, W.; Wang, Y.; Luo, Z. Comparison of the Pyrolysis Behavior of Pyrolytic Lignin and Milled Wood Lignin by Using TG-FTIR Analysis. *Journal of Analytical and Applied Pyrolysis* **2014**, *108*, 78–85. https://doi.org/10.1016/j.jaap.2014.05.014.
(98) Fletcher, T. H. Review of 30 Years of Research Using the Chemical Percolation Devolatilization Model. *Energy and Fuels*. American Chemical Society December 19, 2019, pp 12123–12153. https://doi.org/10.1021/acs.energyfuels.9b02826.
(99) Scott, S. A. A.; Davidson, J. F. F.; Dennis, J. S. S.; Hayhurst, A. N. N. The Devolatilisation of Particles of a Complex Fuel (Dried Sewage Sludge) in a Fluidised Bed. *Chemical Engineering Science* **2007**, *62* (1–2), 584–598. https://doi.org/10.1016/j.ces.2006.09.023.
(100) Bensidhom, G.; Ben Hassen Trabelsi, A.; mahmood, M. A.; Ceylan, S. Insights into Pyrolytic Feedstock Potential of Date Palm Industry Wastes: Kinetic Study and Product Characterization. *Fuel* **2021**, *285*, 119096. https://doi.org/10.1016/j.fuel.2020.119096.
(101) Soria-Verdugo, A.; Goos, E.; Morato-Godino, A.; García-Hernando, N.; Riedel, U. Pyrolysis of Biofuels of the Future: Sewage Sludge and Microalgae – Thermogravimetric Analysis and Modelling of the Pyrolysis under Different Temperature

Conditions. *Energy Conversion and Management* **2017**, *138*, 261–272. https://doi.org/10.1016/j.enconman.2017.01.059.
(102) Ma, J.; Liu, J.; Jiang, X.; Zhang, H. A Two-Dimensional Distributed Activation Energy Model for Pyrolysis of Solid Fuels. *Energy* **2021**, *230*, 120860. https://doi.org/10.1016/j.energy.2021.120860.
(103) Ranzi, E.; Debiagi, P. E. A.; Frassoldati, A. Mathematical Modeling of Fast Biomass Pyrolysis and Bio-Oil Formation. Note I: Kinetic Mechanism of Biomass Pyrolysis. *ACS Sustainable Chemistry & Engineering* **2017**, *5* (4), 2867–2881. https://doi.org/10.1021/acssuschemeng.6b03096.
(104) Debiagi, P.; Gentile, G.; Cuoci, A.; Frassoldati, A.; Ranzi, E.; Faravelli, T. A Predictive Model of Biochar Formation and Characterization. *Journal of Analytical and Applied Pyrolysis* **2018**, *134*, 326–335. https://doi.org/10.1016/j.jaap.2018.06.022.
(105) Hu, B.; Zhang, B.; Xie, W.; Jiang, X.; Liu, J.; Lu, Q. Recent Progress in Quantum Chemistry Modeling on the Pyrolysis Mechanisms of Lignocellulosic Biomass. *Energy & Fuels* **2020**, *34* (9), 10384–10440. https://doi.org/10.1021/acs.energyfuels.0c01948.
(106) Bharadwaj, A.; Baxter, L. L.; Robinson, A. L. Effects of Intraparticle Heat and Mass Transfer on Biomass Devolatilization: Experimental Results and Model Predictions. **2004**. https://doi.org/10.1021/ef0340357.
(107) Pyle, D. L.; Zaror, C. A. Models for the Low Temperature Pyrolysis of Wood Particles. In *Thermochemical Processing of Biomass*; Bridgwater, A. V., Ed.; Butterworths: London, 1984; pp 201–216.
(108) Blackshear, P. L. On the Combustion of Wood II: The Influence of Internal Convection on the Transient Pyrolysis of Cellulose. *COMBUSTION SCIENCE AND TECHNOLOGY* **1970**, *2* (1), 5–9. https://doi.org/10.1080/00102207008952230.
(109) Liu, X.; Wang, G.; Pan, G.; Wen, Z. Numerical Analysis of Heat Transfer and Volatile Evolution of Coal Particle. *Fuel* **2013**, *106*, 667–673. https://doi.org/10.1016/j.fuel.2012.10.072.
(110) Di Blasi, C. Modeling Intra- and Extra-Particle Processes of Wood Fast Pyrolysis. *AIChE Journal* **2002**, *48* (10), 2386–2397. https://doi.org/10.1002/aic.690481028.
(111) Chern, J.-S. S.; Hayhurst, A. N. A Model for the Devolatilization of a Coal Particle Sufficiently Large to Be Controlled by Heat Transfer. *Combustion and Flame* **2006**, *146* (3), 553–571. https://doi.org/10.1016/j.combustflame.2006.04.011.
(112) Chern, J. S.; Hayhurst, A. N. Fluidised Bed Studies of: (I) Reaction-Fronts inside a Coal Particle during Its Pyrolysis or Devolatilisation, (Ii) the Combustion of Carbon in Various Coal Chars. *Combustion and Flame* **2012**, *159* (1), 367–375. https://doi.org/10.1016/j.combustflame.2011.07.005.
(113) Hayhurst, A. N. The Kinetics of the Pyrolysis or Devolatilisation of Sewage Sludge and Other Solid Fuels. *Combustion and Flame* **2013**, *160* (1), 138–144. https://doi.org/10.1016/j.combustflame.2012.09.003.
(114) Jiang, X.; Chen, D.; Ma, Z.; Yan, J. Models for the Combustion of Single Solid Fuel Particles in Fluidized Beds: A Review. *Renewable and Sustainable Energy Reviews* **2017**, *68*, 410–431. https://doi.org/10.1016/j.rser.2016.10.001.
(115) Porteiro, J.; Granada, E.; Collazo, J.; Patiño, D.; Morán, J. C. A Model for the Combustion of Large Particles of Densified Wood. https://doi.org/10.1021/ef0701891.
(116) Ding, Y.; Zhang, J.; He, Q.; Huang, B.; Mao, S. The Application and Validity of Various Reaction Kinetic Models on Woody Biomass Pyrolysis. *Energy* **2019**. https://doi.org/10.1016/J.ENERGY.2019.05.021.
(117) Johansen, J. M.; Jensen, P. A.; Glarborg, P.; Mancini, M.; Weber, R.; Mitchell, R. E. Extension of Apparent Devolatilization Kinetics from Thermally Thin to Thermally Thick Particles in Zero Dimensions for Woody Biomass. *Energy* **2016**, *95*, 279–290. https://doi.org/10.1016/j.energy.2015.11.025.
(118) Agarwal, P. K.; Genetti, W. E.; Lee, Y. Y. Coupled Drying and Devolatilization of Wet Coal in Fluidized Beds. *Chemical Engineering Science* **1986**, *41* (9), 2373–2383. https://doi.org/10.1016/0009-2509(86)85087-4.

(119) Galgano, A.; Di Blasi, C. Modeling Wood Degradation by the Unreacted-Core-Shrinking Approximation. *Industrial and Engineering Chemistry Research* **2003**, *42* (10), 2101–2111. https://doi.org/10.1021/ie020939o.
(120) Ström, H.; Thunman, H. CFD Simulations of Biofuel Bed Conversion: A Submodel for the Drying and Devolatilization of Thermally Thick Wood Particles. *Combustion and Flame* **2013**, *160* (2), 417–431. https://doi.org/10.1016/j.combustflame.2012.10.005.
(121) Scala, F.; Salatino, P. Modelling Fluidized Bed Combustion of High-Volatile Solid Fuels. *Chemical Engineering Science* **2002**, *57* (7), 1175–1196. https://doi.org/10.1016/S0009-2509(02)00004-0.
(122) Fiorentino, M.; Marzocchella, A.; Salatino, P. Segregation of Fuel Particles and Volatile Matter during Devolatilization in a Fluidized Bed Reactor—II. Experimental. *Chemical Engineering Science* **1997**, *52* (12), 1909–1922. https://doi.org/10.1016/S0009-2509(97)00019-5.
(123) Salatino, P.; Solimene, R. Mixing and Segregation in Fluidized Bed Thermochemical Conversion of Biomass. *Powder Technology* **2017**, *316*, 29–40. https://doi.org/10.1016/j.powtec.2016.11.058.
(124) Hayhurst, A. N.; Tucker, R. F. The Combustion of Carbon Monoxide in a Two-Zone Fluidized Bed. *Combustion and Flame* **1990**, *79* (2), 175–189. https://doi.org/10.1016/0010-2180(90)90042-P.
(125) Dennis, J. S.; Hayhurst, A. N.; Mackley, I. G. The Ignition and Combustion of Propane/Air Mixtures in a Fluidised Bed. *Symposium (International) on Combustion* **1982**, *19* (1), 1205–1212. https://doi.org/10.1016/S0082-0784(82)80297-X.
(126) Chadeesingh, D. R.; Hayhurst, A. N. The Combustion of a Fuel-Rich Mixture of Methane and Air in a Bubbling Fluidised Bed of Silica Sand at 700°C and Also with Particles of Fe2O3 or Fe Present. *Fuel* **2014**, *127*, 169–177. https://doi.org/10.1016/j.fuel.2013.07.121.
(127) Baron, J.; Bulewicz, E. M.; Kandefer, S.; Pilawska, M.; Żukowski, W.; Hayhurst, A. N. Combustion of Hydrogen in a Bubbling Fluidized Bed. *Combustion and Flame* **2009**, *156* (5), 975–984. https://doi.org/10.1016/j.combustflame.2008.11.014.
(128) Hayhurst, A. N.; Parmar, M. S. Does Solid Carbon Burn in Oxygen to Give the Gaseous Intermediate CO or Produce CO2 Directly? Some Experiments in a Hot Bed of Sand Fluidized by Air. *Chemical Engineering Science* **1998**, *53* (3), 427–438. https://doi.org/10.1016/S0009-2509(97)00334-5.
(129) Müller, D.; Plankenbühler, T.; Karl, J. A Methodology for Measuring the Heat Release Efficiency in Bubbling Fluidised Bed Combustors. *Energies* **2020**, *13* (10), 2420. https://doi.org/10.3390/en13102420.
(130) Li, X.; Lyngfelt, A.; Mattisson, T. An Experimental Study of a Volatiles Distributor for Solid Fuels Chemical-Looping Combustion Process. *Fuel Processing Technology* **2021**, *220*, 106898. https://doi.org/10.1016/j.fuproc.2021.106898.
(131) Patil, K. N.; Huhnke, R. L.; Bellmer, D. D. Influence of Internal Baffles on Mixing Characteristics of Biomass in a Fluidized Sand Bed. *International Commission of Agricultural Engineering* **2007**, *9*.
(132) Dounit, S.; Hemati, M.; Andreux, R. Modelling and Experimental Validation of a Fluidized-Bed Reactor Freeboard Region: Application to Natural Gas Combustion. *Chemical Engineering Journal* **2008**, *140* (1), 457–465. https://doi.org/10.1016/j.cej.2007.11.033.
(133) Wu, W.; Dellenback, P. A.; Agarwal, P. K.; Haynes, H. W. Combustion of Isolated Bubbles in an Elevated-Temperature Fluidized Bed. *Combustion and Flame* **2005**, *140* (3), 204–221. https://doi.org/10.1016/j.combustflame.2004.11.010.
(134) Phounglamcheik, A.; Wang, L.; Romar, H.; Kienzl, N.; Broström, M.; Ramser, K.; Skreiberg, Ø.; Umeki, K. Effects of Pyrolysis Conditions and Feedstocks on the Properties and Gasification Reactivity of Charcoal from Woodchips. *Energy Fuels* **2020**, *34* (7), 8353–8365. https://doi.org/10.1021/acs.energyfuels.0c00592.
(135) McDonald-Wharry, J.; Manley-Harris, M.; Pickering, K. Carbonisation of Biomass-Derived Chars and the Thermal Reduction of a Graphene Oxide Sample Studied Using

Raman Spectroscopy. *Carbon* **2013**, *59*, 383–405. https://doi.org/10.1016/j.carbon.2013.03.033.
(136) Kwong, K. Y.; Mao, R.; Scott, S. A.; Dennis, J. S.; Marek, E. J. Analysis of the Rate of Combustion of Biomass Char in a Fluidised Bed of CLOU Particles. *Chemical Engineering Journal* **2020**, 127942. https://doi.org/10.1016/j.cej.2020.127942.
(137) Scala, F. A New Technique for the Measurement of the Product CO/CO2 Ratio at the Surface of Char Particles Burning in a Fluidized Bed. *Proceedings of the Combustion Institute* **2009**, *32* (2), 2021–2027. https://doi.org/10.1016/J.PROCI.2008.06.047.
(138) Scala, F. Fluidized-Bed Combustion of Single Coal Char Particles: An Analysis of the Burning Rate and of the Primary CO/CO $_2$ Ratio. *Energy & Fuels* **2011**, *25* (3), 1051–1059. https://doi.org/10.1021/ef101182s.
(139) Hu, W.; Marek, E.; Donat, F.; Dennis, J. S.; Scott, S. A. A Thermogravimetric Method for the Measurement of CO/CO2ratio at the Surface of Carbon during Combustion. *Proceedings of the Combustion Institute* **2018**, *000*, 1–7. https://doi.org/10.1016/j.proci.2018.05.040.
(140) Hurt, R. H.; Calo, J. M. Semi-Global Intrinsic Kinetics for Char Combustion Modeling. *Combustion and Flame* **2001**, *125* (3), 1138–1149. https://doi.org/10.1016/S0010-2180(01)00234-6.
(141) Bews, I. M.; Hayhurst, A. N.; Richardson, S. M.; Taylor, S. G. The Order, Arrhenius Parameters, and Mechanism of the Reaction between Gaseous Oxygen and Solid Carbon. *Combustion and Flame* **2001**, *124* (1–2), 231–245. https://doi.org/10.1016/S0010-2180(00)00199-1.
(142) Haynes, B. S. A Turnover Model for Carbon Reactivity I. Development. *Combustion and Flame* **2001**, *126* (1–2), 1421–1432. https://doi.org/10.1016/S0010-2180(01)00263-2.
(143) Fennell, P. S.; Dennis, J. S.; Hayhurst, A. N. The Order with Respect to Oxygen and the Activation Energy for the Burning of an Anthracitic Char in O2 in a Fluidised Bed, as Measured Using a Rapid Analyser for CO and CO2. *Proceedings of the Combustion Institute* **2009**, *32 II* (2), 2051–2058. https://doi.org/10.1016/j.proci.2008.06.097.
(144) Hayhurst, A. N. Does Carbon Monoxide Burn inside a Fluidized Bed? A New Model for the Combustion of Coal Char Particles in Fluidized Beds. *Combustion and Flame* **1991**, *85* (1–2), 155–168. https://doi.org/10.1016/0010-2180(91)90184-D.
(145) Arthur, J. R. Reactions between Carbon and Oxygen. *Transactions of the Faraday Society* **1951**, *47* (0), 164. https://doi.org/10.1039/tf9514700164.
(146) Rossberg, M. Experimentelle Ergebnisse Über Die Primärreaktionen Bei Der Kohlenstoffverbrennung. *Zeitschrift für Elektrochemie, Berichte der Bunsengesellschaft für physikalische Chemie* **1956**, *60* (9-10), 952–956. https://doi.org/10.1002/BBPC.19560600905.
(147) Linjewile, T. M.; Gururajan, V. S.; Agarwal, P. K. The COCO2 Product Ratio from the Combustion of Single Petroleum Coke Spheres in an Incipiently Fluidized Bed. *Chemical Engineering Science* **1995**, *50* (12), 1881–1888. https://doi.org/10.1016/0009-2509(95)00018-Z.
(148) Tognotti, L.; Longwell, J. P.; Sarofim, A. F. The Products of the High Temperature Oxidation of a Single Char Particle in an Electrodynamic Balance. *Symposium (International) on Combustion* **1991**, *23* (1), 1207–1213. https://doi.org/10.1016/S0082-0784(06)80382-6.
(149) Cerciello, F.; Coppola, A.; Lacovig, P.; Senneca, O.; Salatino, P. Characterization of Surface-Oxides on Char under Periodically Changing Oxidation/Desorption Conditions. *Renewable and Sustainable Energy Reviews* **2020**, 110453. https://doi.org/10.1016/j.rser.2020.110453.
(150) Mao, R. The Investigation of Aspects of Chemical Looping Combustion in Fluidised Beds, University of Cambridge, 2018.
(151) Scala, F. Mass Transfer around Freely Moving Active Particles in the Dense Phase of a Gas Fluidized Bed of Inert Particles. *Chemical Engineering Science* **2007**, *62* (16), 4159–4176. https://doi.org/10.1016/J.CES.2007.04.040.

(152) Anca-Couce, A.; Sommersacher, P.; Shiehnejadhesar, A.; Mehrabian, R.; Hochenauer, C.; Scharler, R. CO/CO 2 Ratio in Biomass Char Oxidation. *Energy Procedia* **2017**, *120*, 11. https://doi.org/10.1016/j.egypro.2017.07.170.
(153) Morin, M.; Pécate, S.; Hémati, M. Kinetic Study of Biomass Char Combustion in a Low Temperature Fluidized Bed Reactor. *Chemical Engineering Journal* **2018**, *331*, 265–277. https://doi.org/10.1016/j.cej.2017.08.063.
(154) Peterson, C. A.; Brown, R. C. Oxidation Kinetics of Biochar from Woody and Herbaceous Biomass. *Chemical Engineering Journal* **2020**, *401*, 126043. https://doi.org/10.1016/j.cej.2020.126043.
(155) Barnard, J. A.; Bradley, J. N. *Flame and Combustion*, 2nd ed.; Chapman & Hall: London, 1985.
(156) Wu, X.; Radovic, L. R. Catalytic Oxidation of Carbon/Carbon Composite Materials in the Presence of Potassium and Calcium Acetates. *Carbon* **2005**, *43* (2), 333–344. https://doi.org/10.1016/j.carbon.2004.09.025.
(157) Otterbein, M.; Bonnetain, L. Combustion d'un Carbone Vitreux Sous Basses Pressions d'oxygene. *Carbon* **1968**, *6* (6), 877–885. https://doi.org/10.1016/0008-6223(68)90072-9.
(158) Prins, W. Fluidized Bed Combustion of a Single Carbon Particle, University of Twente, Enschede, Netherlands, 1987.
(159) Linjewile, T. M.; Agarwal, P. K. The Influence of Product COCO2 Ratio on the Ignition and Temperature History of Petroleum Coke Particles in Incipiently Gas-Fluidized Beds. *Fuel* **1995**, *74* (1), 12–16. https://doi.org/10.1016/0016-2361(94)P4323-T.
(160) Du, Z.; Sarofim, A. F.; Longwell, J. P.; Mims, C. A. Kinetic Measurement and Modeling of Carbon Oxidation. *Energy & Fuels* **1991**, *5*, 214. https://doi.org/10.1021/ef00025a035.
(161) Zeng, T.; Fu, W. B. The Ratio CO/CO2 of Oxidation on a Burning Carbon Surface. *Combustion and Flame* **1996**, *107* (3), 197–210. https://doi.org/10.1016/S0010-2180(96)00071-5.
(162) Zou, R.; Luo, G.; Cao, L.; Jiang, L.; Li, X.; Yao, H. Surface CO/CO2 Ratio of Char Combustion Measured by Thermogravimetry and Differential Scanning Calorimetry. *Fuel* **2018**, *233*, 480–485. https://doi.org/10.1016/j.fuel.2018.06.072.
(163) Kwong, K. Y.; Mleczko, L.; Moujar-Bakhti, W.; Marek, E. J. Prediction of Combustion Burnout Times of Particles of Biomass Char Using Experimentally-Determined CO/CO2 Ratios. In *1st FERIA*; Nimmo, W., Ed.; Elsevier: Nottingham, 2021.
(164) Phillips, R.; Vastola, F. J.; Walker, P. L. Factors Affecting the Product Ratio of the Carbon-Oxygen Reaction—II. Reaction Temperature. *Carbon* **1970**, *8* (2), 205–210. https://doi.org/10.1016/0008-6223(70)90115-6.
(165) Shaddix, C. R.; Holzleithner, F.; Geier, M.; Haynes, B. S. Numerical Assessment of Tognotti Determination of CO2/CO Production Ratio during Char Oxidation. *Combustion and Flame* **2013**, *160* (9), 1827–1834. https://doi.org/10.1016/j.combustflame.2013.03.019.
(166) Geier, M.; Shaddix, C. R.; Holzleithner, F. A Mechanistic Char Oxidation Model Consistent with Observed CO2/CO Production Ratios. *Proceedings of the Combustion Institute* **2013**, *34* (2), 2411–2418. https://doi.org/10.1016/J.PROCI.2012.07.009.
(167) Haugen, N. E. L.; Mitchell, R. E.; Tilghman, M. B. A Comprehensive Model for Char Particle Conversion in Environments Containing O2 and CO2. *Combustion and Flame* **2015**, *162* (4), 1455–1463. https://doi.org/10.1016/J.COMBUSTFLAME.2014.11.015.
(168) Campbell, P. A. A.; Mitchell, R. E. E. The Impact of the Distributions of Surface Oxides and Their Migration on Characterization of the Heterogeneous Carbon–Oxygen Reaction. *Combustion and Flame* **2008**, *154* (1–2), 47–66.
(169) Campbell, P. A. Investigation into the Roles of Surface Oxide Complexes and Their Distributions in the Carbon-Oxygen Heterogenous Reaction Mechanism, Stanford University, 2005.

(170) Radovic, L. R. Active Sites in Graphene and the Mechanism of CO 2 Formation in Carbon Oxidation. *Journal of the American Chemical Society* **2009**, *131* (47), 17166–17175. https://doi.org/10.1021/ja904731q.
(171) Smith, I. W. The Intrinsic Reactivity of Carbons to Oxygen. *Fuel* **1978**, *57* (7), 409–414. https://doi.org/10.1016/0016-2361(78)90055-8.
(172) Hurt, R.; Sun, J. K.; Lunden, M. A Kinetic Model of Carbon Burnout in Pulverized Coal Combustion. *Combustion and Flame* **1998**, *113* (1–2), 181–197. https://doi.org/10.1016/S0010-2180(97)00240-X.
(173) Dai, P.; Dennis, J. S.; Scott, S. A. Using an Experimentally-Determined Model of the Evolution of Pore Structure for the Gasification of Chars by $CO_2$. *Fuel* **2016**, *171*, 29–43. https://doi.org/10.1016/j.fuel.2015.12.041.
(174) Campbell, P. A.; Mitchell, R. E.; Ma, L. Characterization of Coal Char and Biomass Char Reactivities to Oxygen. *Proceedings of the Combustion Institute* **2002**, *29* (1), 519–526. https://doi.org/10.1016/S1540-7489(02)80067-0.
(175) Di Blasi, C.; Buonanno, F.; Branca, C. Reactivities of Some Biomass Chars in Air. *Carbon* **1999**, *37* (8), 1227–1238. https://doi.org/10.1016/S0008-6223(98)00319-4.
(176) Shen, D. K.; Gu, S.; Luo, K. H.; Bridgwater, A. V.; Fang, M. X. Kinetic Study on Thermal Decomposition of Woods in Oxidative Environment. *Fuel* **2009**, *88* (6), 1024–1030. https://doi.org/10.1016/j.fuel.2008.10.034.
(177) Scala, F.; Solimene, R.; Montagnaro, F. Conversion of Solid Fuels and Sorbents in Fluidized Bed Combustion and Gasification. In *Fluidized Bed Technologies for Near-Zero Emission Combustion and Gasification*; Scala, F., Ed.; Woodhead Publishing: Oxford, Cambridge, Philadelphia, New Delhi, 2013; pp 319–387. https://doi.org/10.1533/9780857098801.2.319.
(178) Al-Qayim, K.; Nimmo, W.; Hughes, K.; Pourkashanian, M. Kinetic Parameters of the Intrinsic Reactivity of Woody Biomass and Coal Chars via Thermogravimetric Analysis. *Fuel* **2017**, *210*, 811–825. https://doi.org/10.1016/j.fuel.2017.09.010.
(179) Várhegyi, G.; Sebestyén, Z.; Czégény, Z.; Lezsovits, F.; Könczöl, S. Combustion Kinetics of Biomass Materials in the Kinetic Regime. *Energy and Fuels* **2012**, *26* (2), 1323–1335. https://doi.org/10.1021/ef201497k.
(180) Recari, J.; Berrueco, C.; Abelló, S.; Montané, D.; Farriol, X. Effect of Temperature and Pressure on Characteristics and Reactivity of Biomass-Derived Chars. *Bioresource Technology* **2014**, *170*, 204–210. https://doi.org/10.1016/j.biortech.2014.07.080.
(181) Morin, M.; Pécate, S.; Hémati, M.; Kara, Y. Pyrolysis of Biomass in a Batch Fluidized Bed Reactor: Effect of the Pyrolysis Conditions and the Nature of the Biomass on the Physicochemical Properties and the Reactivity of Char. *Journal of Analytical and Applied Pyrolysis* **2016**, *122*, 511–523. https://doi.org/10.1016/j.jaap.2016.10.002.
(182) Antal, M. J.; Grønli, M. The Art, Science, and Technology of Charcoal Production. *Industrial and Engineering Chemistry Research*. American Chemical Society April 16, 2003, pp 1619–1640. https://doi.org/10.1021/ie0207919.
(183) Mian, I.; Li, X.; Dacres, O. D.; Wang, J.; Wei, B.; Jian, Y.; Zhong, M.; Liu, J.; Ma, F.; Rahman, N. Combustion Kinetics and Mechanism of Biomass Pellet. *Energy* **2020**, *205*, 117909. https://doi.org/10.1016/j.energy.2020.117909.
(184) Vallejos-Burgos, F.; Díaz-Pérez, N.; Silva-Villalobos, Á.; Jiménez, R.; García, X.; Radovic, L. R. On the Structural and Reactivity Differences between Biomass- and Coal-Derived Chars. *Carbon* **2016**, *109*, 253–263. https://doi.org/10.1016/j.carbon.2016.08.012.
(185) Parmar, M. S.; Hayhurst, A. N. The Heat Transfer Coefficient for a Freely Moving Sphere in a Bubbling Fluidised Bed. *Chemical Engineering Science* **2002**, *57* (17), 3485–3494. https://doi.org/10.1016/S0009-2509(02)00259-2.
(186) Di Natale, F.; Nigro, R.; Scala, F. Heat and Mass Transfer in Fluidised Bed Combustion and Gasification Systems. In *Fludised bed technologies for near-zero emission combustion and gasification*; Scala, F., Ed.; Woodhead Publishing: Oxford, Cambridge, Philadelphia, New Delhi, Cambridge, Philadelphia, New Delhi, 2013; pp 177–252.

(187) Abdelmotalib, H. M.; Youssef, M. A. M.; Hassan, A. A.; Youn, S. B.; Im, I. T. Heat Transfer Process in Gas–Solid Fluidized Bed Combustors: A Review. *International Journal of Heat and Mass Transfer* **2015**, *89*, 567–575. https://doi.org/10.1016/J.IJHEATMASSTRANSFER.2015.05.085.
(188) Botterill, J. S. M. *Fluid-Bed Heat Transfer*, 1st ed.; Academic Press Inc.: New York, 1975.
(189) Scott, S. A. The Gasification and Combustion of Sewage Sludge in a Fluidised Bed, University of Cambridge, 2004.
(190) Agarwal, P. K. Transport Phenomena in Multi-Particle Systems-IV. Heat Transfer to a Large Freely Moving Particle in Gas Fluidized Bed of Smaller Particles. *Chemical Engineering Science* **1991**, *46* (4), 1115–1127. https://doi.org/10.1016/0009-2509(91)85104-6.
(191) Mickley, H. S.; Fairbanks, D. F. Mechanism of Heat Transfer to Fluidized Beds. *AIChE Journal* **1955**, *1* (3), 374–384. https://doi.org/10.1002/aic.690010317.
(192) Ross, I. B.; Patel, M. S.; Davidson, J. F. The Temperature of Burning Carbon in Fluidised Beds. *Trans. Inst. Chem. Eng.* **1981**, *59*, 84–88.
(193) Tamarin, A. I.; Galershtein, D. M.; Shuklina, V. M. Heat Transfer and the Combustion Temperature of Coke Particles in a Fluidized Bed. *Journal of Engineering Physics* **1982**, *42* (1), 14–19. https://doi.org/10.1007/BF00824983.
(194) Scott, S. A.; Davidson, J. F.; Dennis, J. S.; Hayhurst, A. N. Heat Transfer to a Single Sphere Immersed in Beds of Particles Supplied by Gas at Rates above and below Minimum Fluidization. *Industrial and Engineering Chemistry Research* **2004**, *43* (18), 5632–5644. https://doi.org/10.1021/ie0307380.
(195) Chao, J.; Lu, J.; Yang, H.; Zhang, M.; Liu, Q. Experimental Study on the Heat Transfer Coefficient between a Freely Moving Sphere and a Fluidized Bed of Small Particles. *International Journal of Heat and Mass Transfer* **2015**, *80*, 115–125. https://doi.org/10.1016/j.ijheatmasstransfer.2014.08.049.
(196) von Berg, L.; Soria-Verdugo, A.; Hochenauer, C.; Scharler, R.; Anca-Couce, A. Evaluation of Heat Transfer Models at Various Fluidization Velocities for Biomass Pyrolysis Conducted in a Bubbling Fluidized Bed. *International Journal of Heat and Mass Transfer* **2020**, *160*, 120175. https://doi.org/10.1016/j.ijheatmasstransfer.2020.120175.
(197) Anca-Couce, A.; Sommersacher, P.; Scharler, R. Online Experiments and Modelling with a Detailed Reaction Scheme of Single Particle Biomass Pyrolysis. *Journal of Analytical and Applied Pyrolysis* **2017**, *127*, 411–425. https://doi.org/10.1016/j.jaap.2017.07.008.
(198) Collier, A. R.; Hayhurst, A. N.; Richardson, J. L.; Scott, S. A. The Heat Transfer Coefficient between a Particle and a Bed (Packed or Fluidised) of Much Larger Particles. *Chemical Engineering Science* **2004**, *59* (21), 4613–4620. https://doi.org/10.1016/j.ces.2004.07.029.
(199) Leckner, B. Heat and Mass Transfer to/from Active Particles in a Fluidized Bed—An Analysis of the Baskakov-Palchonok Correlation. *International Journal of Heat and Mass Transfer* **2021**, *168*, 120860. https://doi.org/10.1016/j.ijheatmasstransfer.2020.120860.
(200) Garcia-Gutierrez, L. M.; Hernández-Jiménez, F.; Cano-Pleite, E.; Soria-Verdugo, A. Experimental Evaluation of the Convection Heat Transfer Coefficient of Large Particles Moving Freely in a Fluidized Bed Reactor. *International Journal of Heat and Mass Transfer* **2020**, *153*, 119612. https://doi.org/10.1016/j.ijheatmasstransfer.2020.119612.
(201) Prins, W.; Casteleijn, T. P.; Draijer, W.; van Swaaij, W. P. M. Mass Transfer from a Freely Moving Single Sphere to the Dense Phase of a Gas Fluidized Bed of Inert Particles. *Chemical Engineering Science* **1985**, *40* (3), 481–497. https://doi.org/10.1016/0009-2509(85)85109-5.
(202) Agarwal, P. K.; La Nauze, R. D. Transfer Processes Local to the Coal Particle: A Review of Drying, Devolatilization and Mass Transfer in Fluidised Bed Combustion. *Chemical*

*Engineering Research and Design* **1989**, *67*, 457–480. https://doi.org/10.1016/S0076-6879(08)03802-0.
(203) Hayhurst, A. N. The Mass Transfer Coefficient for Oxygen Reacting with a Carbon Particle in a Fluidized or Packed Bed. *Combustion and Flame* **2000**, *121* (4), 679–688. https://doi.org/10.1016/S0010-2180(99)00178-9.
(204) Förtsch, D.; Schnell, U.; Hein, K. R. G.; Essenhigh, R. H. The Mass Transfer Coefficient for the Combustion of Pulverized Carbon Particles. *Combustion and Flame* **2001**, *126* (3), 1662–1668. https://doi.org/10.1016/S0010-2180(01)00275-9.
(205) Scala, F. Calculation of the Mass Transfer Coefficient for the Combustion of a Carbon Particle. *Combustion and Flame* **2010**, *157* (1), 137–142. https://doi.org/10.1016/j.combustflame.2009.06.002.
(206) Sit, S. P.; Grace, J. R. Effect of Bubble Interaction on Interphase Mass Transfer in Gas Fluidized Beds. *Chemical Engineering Science* **1981**, *36* (2), 327–335. https://doi.org/10.1016/0009-2509(81)85012-9.
(207) Yates, J. G. *Fundamentals of Fluidized-Bed Chemical Processes*, 1st ed.; Mullin, J. W., Ed.; Butterworths: London, 1983.
(208) Wu, W.; Agarwal, P. K. The Effect of Bed Temperature on Mass Transfer between the Bubble and Emulsion Phases in a Fluidized Bed. *The Canadian Journal of Chemical Engineering* **2008**, *81* (5), 940–948. https://doi.org/10.1002/cjce.5450810503.
(209) Medrano, J. A.; Gallucci, F.; Boccia, F.; Alfano, N.; van Sint Annaland, M. Determination of the Bubble-to-Emulsion Phase Mass Transfer Coefficient in Gas-Solid Fluidized Beds Using a Non-Invasive Infra-Red Technique. *Chemical Engineering Journal* **2017**, *325*, 404–414. https://doi.org/10.1016/j.cej.2017.05.089.
(210) Davidson, J. F.; Harrison, D. *Fluidised Particles*, 1st ed.; Cambridge University Press: Cambridge, 1963.
(211) Wu, W.; Dellenback, P.; Agarwal, P.; Haynes Jr, H. Combustion of Isolated Bubbles in an Elevated-Temperature Fluidized Bed. *Combustion and Flame* **2005**, *140* (3), 204–221. https://doi.org/10.1016/j.combustflame.2004.11.010.
(212) Zhang, K.; Wang, S.; Wu, Q.; Wang, T.; He, Y. Investigation of Bubble-to-Emulsion Phase Mass Transfer at Non-Isothermal Conditions via a Coupled CFD-DEM Approach. *Chemical Engineering Science* **2021**, *231*, 116284. https://doi.org/10.1016/j.ces.2020.116284.
(213) Redko, T.; Volford, A.; Marek, E. J.; Scott, S. A.; Hayhurst, A. N. Measurement of the Times for Pyrolysis and the Thermal Diffusivity of a Pyrolysing Particle of Wood and Also of the Resulting Char. *Combustion and Flame* **2020**, *212*, 510–518. https://doi.org/10.1016/j.combustflame.2019.10.024.
(214) Yan, J.; Oyedeji, O.; Leal, J. H.; Donohoe, B. S.; Semelsberger, T. A.; Li, C.; Hoover, A. N.; Webb, E.; Bose, E. A.; Zeng, Y.; Williams, C. L.; Schaller, K. D.; Sun, N.; Ray, A. E.; Tanjore, D. Characterizing Variability in Lignocellulosic Biomass: A Review. *ACS Sustainable Chemistry & Engineering* **2020**. https://doi.org/10.1021/acssuschemeng.9b06263.
(215) Gentile, G.; Debiagi, P. E. A.; Cuoci, A.; Frassoldati, A.; Ranzi, E.; Faravelli, T. A Computational Framework for the Pyrolysis of Anisotropic Biomass Particles. *Chemical Engineering Journal* **2017**, *321*, 458–473. https://doi.org/10.1016/j.cej.2017.03.113.
(216) Lester, E.; Avila, C.; Pang, C. H.; Williams, O.; Perkins, J.; Gaddipatti, S.; Tucker, G.; Barraza, J. M.; Trujillo-Uribe, M. P.; Wu, T. A Proposed Biomass Char Classification System. *Fuel* **2018**, *232*, 845–854. https://doi.org/10.1016/j.fuel.2018.05.153.
(217) Henriksen, U.; Hindsgaul, C.; Qvale, B.; Fjellerup, J.; Jensen, A. D. Investigation of the Anisotropic Behavior of Wood Char Particles during Gasification. *Energy Fuels* **2006**, *20* (5), 2233–2238. https://doi.org/10.1021/ef060140f.
(218) Pang, C. H.; Lester, E.; Wu, T. Influence of Lignocellulose and Plant Cell Walls on Biomass Char Morphology and Combustion Reactivity. *Biomass and Bioenergy* **2018**, *119*, 480–491. https://doi.org/10.1016/j.biombioe.2018.10.011.

(219) Liang, D.; Singer, S. Pore-Resolving Simulations to Study the Impacts of Char Morphology on Zone II Combustion and Effectiveness Factor Models. *Combustion and Flame* **2021**, *229*, 111405. https://doi.org/10.1016/j.combustflame.2021.111405.
(220) Barr, M. R.; Jervis, R.; Zhang, Y.; Bodey, A. J.; Rau, C.; Shearing, P. R.; Brett, D. J. L.; Titirici, M.-M.; Volpe, R. Towards a Mechanistic Understanding of Particle Shrinkage during Biomass Pyrolysis via Synchrotron X-Ray Microtomography and in-Situ Radiography. *Sci Rep* **2021**, *11* (1), 2656. https://doi.org/10.1038/s41598-020-80228-x.
(221) Davidsson, K. O.; Pettersson, J. B. C. Birch Wood Particle Shrinkage during Rapid Pyrolysis. *Fuel* **2002**, *81* (3), 263–270. https://doi.org/10.1016/S0016-2361(01)00169-7.
(222) Holmgren, P.; Wagner, D. R.; Strandberg, A.; Molinder, R.; Wiinikka, H.; Umeki, K.; Broström, M. Size, Shape, and Density Changes of Biomass Particles during Rapid Devolatilization. *Fuel* **2017**, *206*, 342–351. https://doi.org/10.1016/j.fuel.2017.06.009.
(223) Paulauskas, R.; Džiugys, A.; Striūgas, N. Experimental Investigation of Wood Pellet Swelling and Shrinking during Pyrolysis. *Fuel* **2015**, *142*, 145–151. https://doi.org/10.1016/j.fuel.2014.11.023.
(224) Huang, Q. X.; Wang, R. P.; Li, W. J.; Tang, Y. J.; Chi, Y.; Yan, J. H. Modeling and Experimental Studies of the Effects of Volume Shrinkage on the Pyrolysis of Waste Wood Sphere. *Energy and Fuels* **2014**, *28* (10), 6398–6406. https://doi.org/10.1021/ef501504k.
(225) Sreekanth, M.; Prasad, B. V. S. S. S.; Kolar, A. K.; Thunman, H.; Leckner, B. Stresses in a Cylindrical Wood Particle Undergoing Devolatilization in a Hot Bubbling Fluidized Bed. *Energy Fuels* **2008**, *22* (3), 1549–1559. https://doi.org/10.1021/ef700658k.
(226) S. Mettler, M.; G. Vlachos, D.; J. Dauenhauer, P. Top Ten Fundamental Challenges of Biomass Pyrolysis for Biofuels. *Energy & Environmental Science* **2012**, *5* (7), 7797–7809. https://doi.org/10.1039/C2EE21679E.
(227) Pallarès, D.; Johnsson, F. Modeling of Fuel Mixing in Fluidized Bed Combustors. *Chemical Engineering Science* **2008**, *63* (23), 5663–5671. https://doi.org/10.1016/j.ces.2008.07.035.
(228) Qin, K.; Thunman, H.; Leckner, B. Mass Transfer under Segregation Conditions in Fluidized Beds. *Fuel* **2017**, *195*, 105–112. https://doi.org/10.1016/j.fuel.2017.01.021.
(229) Köhler, A.; Rasch, A.; Pallarès, D.; Johnsson, F. Experimental Characterization of Axial Fuel Mixing in Fluidized Beds by Magnetic Particle Tracking. *Powder Technology* **2017**, *316*, 492–499. https://doi.org/10.1016/j.powtec.2016.12.093.
(230) Köhler, A.; Pallarès, D.; Johnsson, F. Modeling Axial Mixing of Fuel Particles in the Dense Region of a Fluidized Bed. *Energy and Fuels* **2020**. https://doi.org/10.1021/acs.energyfuels.9b04194.
(231) Olsson, J.; Pallarès, D.; Johnsson, F. Lateral Fuel Dispersion in a Large-Scale Bubbling Fluidized Bed. *Chemical Engineering Science* **2012**, *74*, 148–159. https://doi.org/10.1016/J.CES.2012.02.027.
(232) Bruni, G.; Solimene, R.; Marzocchella, A.; Salatino, P.; Yates, J. G.; Lettieri, P.; Fiorentino, M. Self-Segregation of High-Volatile Fuel Particles during Devolatilization in a Fluidized Bed Reactor. *Powder Technology* **2002**, *128* (1), 11–21. https://doi.org/10.1016/S0032-5910(02)00149-3.
(233) Halow, J.; Holsopple, K.; Crawshaw, B.; Daw, S.; Finney, C. Observed Mixing Behavior of Single Particles in a Bubbling Fluidized Bed of Higher-Density Particles. *Industrial and Engineering Chemistry Research* **2012**, *51* (44), 14566–14576. https://doi.org/10.1021/ie301517w.
(234) Sette, E.; Berdugo Vilches, T.; Pallarès, D.; Johnsson, F. Measuring Fuel Mixing under Industrial Fluidized-Bed Conditions - A Camera-Probe Based Fuel Tracking System. *Applied Energy* **2016**, *163*, 304–312. https://doi.org/10.1016/j.apenergy.2015.11.024.
(235) Bond, Z. W. M.; Dennis, J. S. Behaviour of Devolatilising Biomass Particles in Fluidised Beds; 2018; pp 1–18.

(236) Martinez Castilla, G.; Larsson, A.; Lundberg, L.; Johnsson, F.; Pallarès, D. A Novel Experimental Method for Determining Lateral Mixing of Solids in Fluidized Beds – Quantification of the Splash-Zone Contribution. *Powder Technology* **2020**, *370*, 96–103. https://doi.org/10.1016/j.powtec.2020.05.036.
(237) Köhler, A.; Pallarès, D.; Johnsson, F. Magnetic Tracking of a Fuel Particle in a Fluid-Dynamically down-Scaled Fluidised Bed. *Fuel Processing Technology* **2017**, *162*, 147–156. https://doi.org/10.1016/j.fuproc.2017.03.018.
(238) Solimene, R.; Marzocchella, A.; Salatino, P. Hydrodynamic Interaction between a Coarse Gas-Emitting Particle and a Gas Fluidized Bed of Finer Solids. *Powder Technology* **2003**, *133* (1–3), 79–90. https://doi.org/10.1016/S0032-5910(03)00080-9.
(239) Fiorentino, M.; Marzocchella, A.; Salatino, P. Segregation of Fuel Particles and Volatile Matter during Devolatilization in a Fluidized Bed Reactor—I. Model Development. *Chemical Engineering Science* **1997**, *52* (12), 1893–1908. https://doi.org/10.1016/S0009-2509(97)00018-3.
(240) Kuba, M.; Skoglund, N.; Öhman, M.; Hofbauer, H. A Review on Bed Material Particle Layer Formation and Its Positive Influence on the Performance of Thermo-Chemical Biomass Conversion in Fluidized Beds. *Fuel*. Elsevier Ltd May 1, 2021, p 120214. https://doi.org/10.1016/j.fuel.2021.120214.
(241) Nascimento, F. R. M.; González, A. M.; Silva Lora, E. E.; Ratner, A.; Escobar Palacio, J. C.; Reinaldo, R. Bench-Scale Bubbling Fluidized Bed Systems around the World - Bed Agglomeration and Collapse: A Comprehensive Review. *International Journal of Hydrogen Energy* **2021**, *46* (36), 18740–18766. https://doi.org/10.1016/j.ijhydene.2021.03.036.
(242) He, H.; Ji, X.; Boström, D.; Backman, R.; Öhman, M. Mechanism of Quartz Bed Particle Layer Formation in Fluidized Bed Combustion of Wood-Derived Fuels. *Energy and Fuels* **2016**, *30* (3), 2227–2232. https://doi.org/10.1021/acs.energyfuels.5b02891.
(243) He, H.; Skoglund, N.; Öhman, M. Time-Dependent Crack Layer Formation in Quartz Bed Particles during Fluidized Bed Combustion of Woody Biomass. *Energy and Fuels* **2017**, *31* (2), 1672–1677. https://doi.org/10.1021/acs.energyfuels.6b02980.
(244) Imtiaz, Q.; Armutlulu, A.; Donat, F.; Naeem, M. A.; Müller, C. R. Preventing Agglomeration of CuO-Based Oxygen Carriers for Chemical Looping Applications. *ACS Sustainable Chemistry & Engineering* **2021**, *9* (17), 5972–5980. https://doi.org/10.1021/acssuschemeng.1c00560.
(245) Corcoran, A.; Knutsson, P.; Lind, F.; Thunman, H. Mechanism for Migration and Layer Growth of Biomass Ash on Ilmenite Used for Oxygen Carrier Aided Combustion. *Energy & Fuels* **2018**, *32* (8), 8845–8856. https://doi.org/10.1021/acs.energyfuels.8b01888.
(246) Moradian, F.; Pettersson, A.; Richards, T. Bed Agglomeration Characteristics during Cocombustion of Animal Waste with Municipal Solid Waste in a Bubbling Fluidized-Bed Boiler—A Thermodynamic Modeling Approach. *Energy & Fuels* **2014**, *28* (3), 2236–2247. https://doi.org/10.1021/ef402455h.
(247) Gatternig, B.; Karl, J. A Discrete Element Cohesive Particle Collision Model for the Prediction of Ash-Induced Agglomeration. *International Journal of Ambient Energy* **2019**, *0* (0), 1–9. https://doi.org/10.1080/01430750.2019.1594367.
(248) Liliedahl, T.; Sjöström, K.; Engvall, K.; Rosén, C. Defluidisation of Fluidised Beds during Gasification of Biomass. *Biomass and Bioenergy* **2011**, *35*, S63–S70. https://doi.org/10.1016/j.biombioe.2011.05.006.
(249) Morris, J. D.; Daood, S. S.; Chilton, S.; Nimmo, W. Mechanisms and Mitigation of Agglomeration during Fluidized Bed Combustion of Biomass: A Review. *Fuel* **2018**, *230*, 452–473. https://doi.org/10.1016/J.FUEL.2018.04.098.
(250) Bartels, M.; Lin, W.; Nijenhuis, J.; Kapteijn, F.; van Ommen, J. R. Agglomeration in Fluidized Beds at High Temperatures: Mechanisms, Detection and Prevention. *Progress in Energy and Combustion Science* **2008**, *34* (5), 633–666. https://doi.org/10.1016/j.pecs.2008.04.002.

(251) Ren, Q.; Li, L. Co-Combustion of Agricultural Straw with Municipal Sewage Sludge in a Fluidized Bed: Role of Phosphorus in Potassium Behavior. *Energy & Fuels* **2015**, *29* (7), 4321–4327. https://doi.org/10.1021/acs.energyfuels.5b00790.
(252) Vassilev, S. V.; Vassileva, C. G. Water-Soluble Fractions of Biomass and Biomass Ash and Their Significance for Biofuel Application. *Energy Fuels* **2019**, *33* (4), 2763–2777. https://doi.org/10.1021/acs.energyfuels.9b00081.
(253) Jand, N.; Foscolo, P. U. Decomposition of Wood Particles in Fluidized Beds. *Industrial and Engineering Chemistry Research* **2005**, *44* (14), 5079–5089. https://doi.org/10.1021/ie040170a.
(254) Bridgwater, A. V.; Toft, A. J.; Brammer, J. G. A Techno-Economic Comparison of Power Production by Biomass Fast Pyrolysis with Gasification and Combustion. *Renewable and Sustainable Energy Reviews*. Elsevier Ltd September 1, 2002, pp 181–246. https://doi.org/10.1016/S1364-0321(01)00010-7.
(255) Yassin, L.; Lettieri, P.; Simons, S. J. R.; Germanà, A. Techno-Economic Performance of Energy-from-Waste Fluidized Bed Combustion and Gasification Processes in the UK Context. *Chemical Engineering Journal* **2009**, *146* (3), 315–327. https://doi.org/10.1016/j.cej.2008.06.014.
(256) Kunii, D.; Levenspiel, O. *Fluidization Engineering*, 2nd ed.; Brenner, H., Ed.; Butterworth-Heinemann: Boston, 1991.
(257) Kunii, D.; Levenspiel, O. Bubbling Bed Model for Kinetic Processes in Fluidised Beds. Gas-Solid Mass and Heat Transfer and Catalytic Reactions. *Industrial & Engineering Chemistry Process Design and Development* **1963**, *7* (4), 1963.
(258) Kunii, D.; Levenspiel, O. Fluidized Reactor Models. 1. For Bubbling Beds of Fine, Intermediate, and Large Particles. 2. For the Lean Phase: Freeboard and Fast Fluidization. *Industrial and Engineering Chemistry Research* **1990**, *29* (7), 1226–1234. https://doi.org/10.1021/ie00103a022.
(259) Turnbull, E.; Kossakowski, E. R.; Davidson, J. F.; Hopes, R. B.; Blackshaw, H. W.; Goodyer, P. T. Y. Effect of Pressure on Combustion of Char in Fluidised Bed. *Transactions of the Institution of Chemical Engineers* **1984**, *62*, 223–234. https://doi.org/10.1016/b978-0-08-030537-0.50017-x.
(260) Porrazzo, R.; White, G.; Ocone, R. Techno-Economic Investigation of a Chemical Looping Combustion Based Power Plant. *Faraday Discussions*. Royal Society of Chemistry October 17, 2016, pp 437–457. https://doi.org/10.1039/c6fd00033a.
(261) Keller, M.; Kaibe, K.; Hatano, H.; Otomo, J. Techno-Economic Evaluation of BECCS via Chemical Looping Combustion of Japanese Woody Biomass. *International Journal of Greenhouse Gas Control* **2019**, *83*, 69–82. https://doi.org/10.1016/j.ijggc.2019.01.019.
(262) Di Blasi, C.; Branca, C.; Teislev, B. Development of a Novel Reactor for the Oxidative Degradation of Straw. *Bioresource Technology* **2004**, *91* (3), 263–271. https://doi.org/10.1016/S0960-8524(03)00200-1.
(263) Van Der Hoef, M. A.; Van, M.; Annaland, S.; Deen, N. G.; Kuipers, J. A. M. Numerical Simulation of Dense Gas-Solid Fluidized Beds: A Multiscale Modeling Strategy. *Annu. Rev. Fluid Mech* **2008**, *40*, 47–70. https://doi.org/10.1146/annurev.fluid.40.111406.102130.
(264) Bruchmüller, J.; van Wachem, B. G. M.; Gu, S.; Luo, K. H.; Brown, R. C. Modeling the Thermochemical Degradation of Biomass inside a Fast Pyrolysis Fluidized Bed Reactor. *AIChE Journal* **2012**, *58* (10), 3030–3042. https://doi.org/10.1002/aic.13705.
(265) Papadikis, K.; Bridgwater, A. V.; Gu, S. CFD Modelling of the Fast Pyrolysis of Biomass in Fluidised Bed Reactors, Part A: Eulerian Computation of Momentum Transport in Bubbling Fluidised Beds. *Chemical Engineering Science* **2008**, *63* (16), 4218–4227. https://doi.org/10.1016/j.ces.2008.05.045.
(266) Papadikis, K.; Gu, S.; Bridgwater, A. V. CFD Modelling of the Fast Pyrolysis of Biomass in Fluidised Bed Reactors. Part B. Heat, Momentum and Mass Transport in Bubbling Fluidised Beds. *Chemical Engineering Science* **2009**, *64* (5), 1036–1045. https://doi.org/10.1016/j.ces.2008.11.007.

(267) Lu, L.; Gao, X.; Shahnam, M.; Rogers, W. A. Bridging Particle and Reactor Scales in the Simulation of Biomass Fast Pyrolysis by Coupling Particle Resolved Simulation and Coarse Grained CFD-DEM. *Chemical Engineering Science* **2020**, *216*, 115471. https://doi.org/10.1016/j.ces.2020.115471.
(268) Mu, L.; Buist, K. A.; Kuipers, J. A. M.; Deen, N. G. Scaling Method of CFD-DEM Simulations for Gas-Solid Flows in Risers. *Chemical Engineering Science: X* **2020**, *6*, 100054. https://doi.org/10.1016/j.cesx.2019.100054.
(269) Xie, J.; Zhong, W.; Shao, Y.; Li, K. Coupling of CFD-DEM and Reaction Model for 3D Fluidized Beds. *Powder Technology* **2019**, *353*, 72–83. https://doi.org/10.1016/j.powtec.2019.05.001.
(270) Zhang, J.; Li, T.; Ström, H.; Løvås, T. Grid-Independent Eulerian-Lagrangian Approaches for Simulations of Solid Fuel Particle Combustion. *Chemical Engineering Journal* **2020**, *387*, 123964. https://doi.org/10.1016/j.cej.2019.123964.
(271) Xie, J.; Zhong, W.; Shao, Y. Study on the Char Combustion in a Fluidized Bed by CFD-DEM Simulations: Influences of Fuel Properties. *Powder Technology* **2021**, *394*, 20–34. https://doi.org/10.1016/j.powtec.2021.08.018.
(272) Xie, J.; Zhong, W.; Shao, Y. Study on the Char Combustion in a Fluidized Bed by CFD-DEM Simulations: Influences of Fuel Properties. *Powder Technology* **2021**. https://doi.org/10.1016/J.POWTEC.2021.08.018.
(273) Geng, Y.; Che, D. An Extended DEM–CFD Model for Char Combustion in a Bubbling Fluidized Bed Combustor of Inert Sand. *Chemical Engineering Science* **2011**, *66* (2), 207–219. https://doi.org/10.1016/j.ces.2010.10.011.
(274) Wang, S.; Luo, K.; Fan, J. CFD-DEM Coupled with Thermochemical Sub-Models for Biomass Gasification: Validation and Sensitivity Analysis. *Chemical Engineering Science* **2020**, 115550. https://doi.org/10.1016/j.ces.2020.115550.
(275) Patil, A. V.; Peters, E. A. J. F.; Kuipers, J. A. M. Comparison of CFD–DEM Heat Transfer Simulations with Infrared/Visual Measurements. *Chemical Engineering Journal* **2015**, *277*, 388–401. https://doi.org/10.1016/J.CEJ.2015.04.131.
(276) Liu, X.; Deen, N. G.; Tang, Y. On the Treatment of Bed-to-Wall Heat Transfer in CFD-DEM Simulations of Gas-Fluidized Beds. *Chemical Engineering Science* **2021**, *236*, 116492. https://doi.org/10.1016/J.CES.2021.116492.
(277) Wei, J.; Guo, Q.; Ding, L.; Gong, Y.; Yu, J.; Yu, G. Understanding the Effect of Different Biomass Ash Additions on Pyrolysis Product Distribution, Char Physicochemical Characteristics, and Char Gasification Reactivity of Bituminous Coal. *Energy & Fuels* **2019**. https://doi.org/10.1021/acs.energyfuels.9b00064.
(278) Agarwal, U. P. Analysis of Cellulose and Lignocellulose Materials by Raman Spectroscopy: A Review of the Current Status. *Molecules* **2019**, *24* (9), 1659. https://doi.org/10.3390/molecules24091659.
(279) Xu, J.; He, Q.; Xiong, Z.; Yu, Y.; Zhang, S.; Hu, X.; Jiang, L.; Su, S.; Hu, S.; Wang, Y.; Xiang, J. Raman Spectroscopy as a Versatile Tool for Investigating Thermochemical Processing of Coal, Biomass, and Wastes: Recent Advances and Future Perspectives. *Energy & Fuels* **2021**, *35* (4), 2870–2913. https://doi.org/10.1021/acs.energyfuels.0c03298.
(280) Smith, M. W.; Dallmeyer, I.; Johnson, T. J.; Brauer, C. S.; McEwen, J.-S.; Espinal, J. F.; Garcia-Perez, M. Structural Analysis of Char by Raman Spectroscopy: Improving Band Assignments through Computational Calculations from First Principles. *Carbon* **2016**, *100*, 678–692. https://doi.org/10.1016/j.carbon.2016.01.031.
(281) Miyafuji, H.; Komai, K.; Kanbayashi, T. Development of Quantification Method for Lignin Content in Woody Biomass by Raman Micro-Spectroscopy. *Vibrational Spectroscopy* **2017**, *88*, 9–13. https://doi.org/10.1016/j.vibspec.2016.10.011.
(282) Cuesta, A.; Dhamelincourt, P.; Laureyns, J.; Martínez-Alonso, A.; Tascón, J. M. D. Raman Microprobe Studies on Carbon Materials. *Carbon* **1994**, *32* (8), 1523–1532. https://doi.org/10.1016/0008-6223(94)90148-1.
(283) Sadezky, A.; Muckenhuber, H.; Grothe, H.; Niessner, R.; Pöschl, U. Raman Microspectroscopy of Soot and Related Carbonaceous Materials: Spectral Analysis and

Structural Information. *Carbon* **2005**, *43* (8), 1731–1742. https://doi.org/10.1016/j.carbon.2005.02.018.
(284) Zaida, A.; Bar-Ziv, E.; Radovic, L. R.; Lee, Y.-J. Further Development of Raman Microprobe Spectroscopy for Characterization of Char Reactivity. *Proceedings of the Combustion Institute* **2007**, *31* (2), 1881–1887. https://doi.org/10.1016/j.proci.2006.07.011.
(285) Guizani, C.; Haddad, K.; Limousy, L.; Jeguirim, M. New Insights on the Structural Evolution of Biomass Char upon Pyrolysis as Revealed by the Raman Spectroscopy and Elemental Analysis. *Carbon* **2017**, *119*, 519–521. https://doi.org/10.1016/j.carbon.2017.04.078.
(286) Yu, J.; Guo, Q.; Ding, L.; Gong, Y.; Yu, G. Studying Effects of Solid Structure Evolution on Gasification Reactivity of Coal Chars by In-Situ Raman Spectroscopy. *Fuel* **2020**, *270*, 117603. https://doi.org/10.1016/j.fuel.2020.117603.
(287) Yu, J.; Guo, Q.; Ding, L.; Gong, Y.; Yu, G. Study on the Effect of Inherent AAEM on Char Structure Evolution during Coal Pyrolysis by In-Situ Raman and TG. *Fuel* **2021**, *292*, 120406. https://doi.org/10.1016/j.fuel.2021.120406.
(288) Jones, K.; Ramakrishnan, G.; Uchimiya, M.; Orlov, A. New Applications of X-Ray Tomography in Pyrolysis of Biomass: Biochar Imaging. *Energy Fuels* **2015**, *29* (3), 1628–1634. https://doi.org/10.1021/ef5027604.
(289) Jorgensen, S.; Singer, S. Micro-CT-Based Approaches for Quantifying the Morphology of Pulverized Char Particles. *Energy and Fuels* **2019**, *33* (6), 4826–4834. https://doi.org/10.1021/acs.energyfuels.9b00437.
(290) Boigné, E.; Bennett, N. R.; Wang, A.; Mohri, K.; Ihme, M. Simultaneous In-Situ Measurements of Gas Temperature and Pyrolysis of Biomass Smoldering via X-Ray Computed Tomography. *Proceedings of the Combustion Institute* **2021**, *38* (3), 3899–3907. https://doi.org/10.1016/j.proci.2020.06.070.
(291) Smith, M.; Scudiero, L.; Espinal, J.; McEwen, J.-S.; Garcia-Perez, M. Improving the Deconvolution and Interpretation of XPS Spectra from Chars by Ab Initio Calculations. *Carbon* **2016**, *110*, 155–171. https://doi.org/10.1016/j.carbon.2016.09.012.
(292) Perry, D. L.; Grint, A. Application of XPS to Coal Characterization. *Fuel* **1983**, *62* (9), 1024–1033. https://doi.org/10.1016/0016-2361(83)90135-7.
(293) Nishimiya, K.; Hata, T.; Imamura, Y.; Ishihara, S. Analysis of Chemical Structure of Wood Charcoal by X-Ray Photoelectron Spectroscopy. *J Wood Sci* **1998**, *44* (1), 56–61. https://doi.org/10.1007/BF00521875.
(294) Levi, G.; Senneca, O.; Causà, M.; Salatino, P.; Lacovig, P.; Lizzit, S. Probing the Chemical Nature of Surface Oxides during Coal Char Oxidation by High-Resolution XPS. *Carbon* **2015**, *90*, 181–196. https://doi.org/10.1016/j.carbon.2015.04.003.
(295) Levi, G.; Causà, M.; Lacovig, P.; Salatino, P.; Senneca, O. Mechanism and Thermochemistry of Coal Char Oxidation and Desorption of Surface Oxides. *Energy Fuels* **2017**, *31* (3), 2308–2316. https://doi.org/10.1021/acs.energyfuels.6b02324.
(296) Chandrasekera, T. C.; Wang, A.; Holland, D. J.; Marashdeh, Q.; Pore, M.; Wang, F.; Sederman, A. J.; Fan, L. S.; Gladden, L. F.; Dennis, J. S. A Comparison of Magnetic Resonance Imaging and Electrical Capacitance Tomography: An Air Jet through a Bed of Particles. *Powder Technology* **2012**, *227*, 86–95. https://doi.org/10.1016/j.powtec.2012.03.005.
(297) Chandrasekera, T. C.; Li, Y.; Moody, D.; Schnellmann, M. A.; Dennis, J. S.; Holland, D. J. Measurement of Bubble Sizes in Fluidised Beds Using Electrical Capacitance Tomography. *Chemical Engineering Science* **2015**, *126*, 679–687. https://doi.org/10.1016/j.ces.2015.01.011.
(298) Agrawal, V.; Shinde, Y. H.; Shah, M. T.; Utikar, R. P.; Pareek, V. K.; Joshi, J. B. Estimation of Bubble Properties in Bubbling Fluidized Bed Using ECVT Measurements. *Industrial & Engineering Chemistry Research* **2018**, *57* (24), 8319–8333. https://doi.org/10.1021/ACS.IECR.8B00349.

(299) Singh, B. K.; Roy, S.; Buwa, V. V. Bubbling/Slugging Flow Behavior in a Cylindrical Fluidized Bed: ECT Measurements and Two-Fluid Simulations. *Chemical Engineering Journal* **2019**, 123120. https://doi.org/10.1016/J.CEJ.2019.123120.

(300) Agu, C. E.; Tokheim, L.-A.; Pfeifer, C.; Moldestad, B. M. E. Behaviour of Biomass Particles in a Bubbling Fluidized Bed: A Comparison between Wood Pellets and Wood Chips. *Chemical Engineering Journal* **2019**. https://doi.org/10.1016/J.CEJ.2019.01.120.

(301) Guo, Y.; Zhao, Y.; Meng, S.; Feng, D.; Yan, T.; Wang, P.; Sun, S. Development of a Multistage in Situ Reaction Analyzer Based on a Micro Fluidized Bed and Its Suitability for Rapid Gas–Solid Reactions. *Energy and Fuels* **2016**, *30* (7), 6021–6033. https://doi.org/10.1021/ACS.ENERGYFUELS.6B00538.

(302) Qie, Z.; Alhassawi, H.; Sun, F.; Gao, J.; Zhao, G.; Fan, X. Characteristics and Applications of Micro Fluidized Beds (MFBs). *Chemical Engineering Journal* **2021**, 131330. https://doi.org/10.1016/J.CEJ.2021.131330.

(303) Yu, J.; Yao, C.; Zeng, X.; Geng, S.; Dong, L.; Wang, Y.; Gao, S.; Xu, G. Biomass Pyrolysis in a Micro-Fluidized Bed Reactor: Characterization and Kinetics. *Chemical Engineering Journal* **2011**, *168* (2), 839–847. https://doi.org/10.1016/j.cej.2011.01.097.

(304) Li, Y.; Wang, H.; Li, W.; Li, Z.; Cai, N. CO 2 Gasification of a Lignite Char in Microfluidized Bed Thermogravimetric Analysis for Chemical Looping Combustion and Chemical Looping with Oxygen Uncoupling. **2018**. https://doi.org/10.1021/acs.energyfuels.8b02909.

(305) Liu, L.; Li, Z.; Cai, N. Oxidization and Reduction Kinetics of a Manganese Oxygen Carrier Granulated with the Spray Drying Method at a Tonnage Scale for Chemical Looping Combustion. *Fuel* **2021**, *303*, 121267. https://doi.org/10.1016/j.fuel.2021.121267.

(306) Wang, H.; Li, Z.; Li, Y.; Cai, N. Reduced-Order Model for CaO Carbonation Kinetics Measured Using Micro-Fluidized Bed Thermogravimetric Analysis. *Chemical Engineering Science* **2021**, *229*, 116039. https://doi.org/10.1016/j.ces.2020.116039.

(307) Liu, L.; Li, Z. Z.; Li, Z. Z.; Larring, Y.; Cai, N. Heterogeneous Reaction Kinetics of a Perovskite Oxygen Carrier for Chemical Looping Combustion Coupled with Oxygen Uncoupling. *Chemical Engineering Journal* **2020**, 128054. https://doi.org/10.1016/j.cej.2020.128054.

(308) Geng, C.; Shao, Y.; Bian, Z.; Zhong, W. Experimental Study on Oxy-Fuel Combustion Behavior of Lignite Char and Carbon Transfer Mechanism with Isotopic Tracing Method. *Chemical Engineering Journal* **2020**, *386*, 123977. https://doi.org/10.1016/J.CEJ.2019.123977.

(309) Fuss, S.; Lamb, W. F.; Callaghan, M. W.; Hilaire, J.; Creutzig, F.; Amann, T.; Beringer, T.; de Oliveira Garcia, W.; Hartmann, J.; Khanna, T.; Luderer, G.; Nemet, G. F.; Rogelj, J.; Smith, P.; Vicente, J. L. V.; Wilcox, J.; del Mar Zamora Dominguez, M.; Minx, J. C. Negative Emissions—Part 2: Costs, Potentials and Side Effects. *Environmental Research Letters* **2018**, *13* (6), 063002. https://doi.org/10.1088/1748-9326/aabf9f.

(310) Mendiara, T.; García-Labiano, F.; Abad, A.; Gayán, P.; de Diego, L. F.; Izquierdo, M. T.; Adánez, J. Negative CO2 Emissions through the Use of Biofuels in Chemical Looping Technology: A Review. *Applied Energy* **2018**, *232*, 657–684. https://doi.org/10.1016/J.APENERGY.2018.09.201.

(311) Bhave, A.; Taylor, R. H. S.; Fennell, P.; Livingston, W. R.; Shah, N.; Dowell, N. Mac; Dennis, J.; Kraft, M.; Pourkashanian, M.; Insa, M.; Jones, J.; Burdett, N.; Bauen, A.; Beal, C.; Smallbone, A.; Akroyd, J. Screening and Techno-Economic Assessment of Biomass-Based Power Generation with CCS Technologies to Meet 2050 CO2targets. *Applied Energy* **2017**, *190*, 481–489. https://doi.org/10.1016/j.apenergy.2016.12.120.

(312) Jensen, W. B.; Senning, A. Chemical Education Today The Origin of the Brin Process for the Manufacture of Oxygen. *Journal of Chemical Education* • **2009**, *86* (11).

(313) Lewis, W.; Gilliland, E. Production of Pure Carbon Dioxide. US2665972A, November 13, 1950.

(314) Ishida, M.; Zheng, D.; Akehata, T. Evaluation of a Chemical-Looping-Combustion Power-Generation System by Graphic Exergy Analysis. *Energy* **1987**, *12* (2), 147–154. https://doi.org/10.1016/0360-5442(87)90119-8.
(315) Ishida, M.; Jin, H. A New Advanced Power-Generation System Using Chemical-Looping Combustion. *Energy* **1994**, *19* (4), 415–422. https://doi.org/10.1016/0360-5442(94)90120-1.
(316) Adanez, J.; Abad, A.; Garcia-Labiano, F.; Gayan, P.; de Diego, L. F. Progress in Chemical-Looping Combustion and Reforming Technologies. *Progress in Energy and Combustion Science* **2012**, *38* (2), 215–282. https://doi.org/10.1016/J.PECS.2011.09.001.
(317) Ströhle, J.; Orth, M.; Epple, B. Design and Operation of a 1 MWth Chemical Looping Plant. *Applied Energy* **2014**, *113*, 1490–1495. https://doi.org/10.1016/J.APENERGY.2013.09.008.
(318) Adánez-Rubio, I.; Abad, A.; Gayán, P.; De Diego, L. F.; García-Labiano, F.; Adánez, J. Biomass Combustion with CO2capture by Chemical Looping with Oxygen Uncoupling (CLOU). *Fuel Processing Technology* **2014**, *124*, 104–114. https://doi.org/10.1016/j.fuproc.2014.02.019.
(319) Lyngfelt, A.; Leckner, B. A 1000 MWth Boiler for Chemical-Looping Combustion of Solid Fuels – Discussion of Design and Costs. *Applied Energy* **2015**, *157*, 475–487. https://doi.org/10.1016/J.APENERGY.2015.04.057.
(320) Abad, A.; Adánez, J.; Gayán, P.; de Diego, L. F.; García-Labiano, F.; Sprachmann, G. Conceptual Design of a 100 MWth CLC Unit for Solid Fuel Combustion. *Applied Energy* **2015**, *157*, 462–474. https://doi.org/10.1016/j.apenergy.2015.04.043.
(321) Lyngfelt, A. Chemical-Looping Combustion – Status and Development Challenges. *Energy & Fuels* **2020**. https://doi.org/10.1021/acs.energyfuels.0c01454.
(322) Lyngfelt, A.; Brink, A.; Langørgen, Ø.; Mattisson, T.; Rydén, M.; Linderholm, C. 11,000 h of Chemical-Looping Combustion Operation—Where Are We and Where Do We Want to Go? *International Journal of Greenhouse Gas Control* **2019**, *88*, 38–56. https://doi.org/10.1016/J.IJGGC.2019.05.023.
(323) Marek, E. J.; Zheng, Y.; Scott, S. A. Enhancement of Char Gasification in $CO_2$ during Chemical Looping Combustion. *Chemical Engineering Journal* **2018**, *354*, 137–148. https://doi.org/10.1016/j.cej.2018.07.215.
(324) Mattisson, T.; Lyngfelt, A.; Leion, H. Chemical-Looping with Oxygen Uncoupling for Combustion of Solid Fuels. *International Journal of Greenhouse Gas Control* **2009**, *3* (1), 11–19. https://doi.org/10.1016/j.ijggc.2008.06.002.
(325) Mei, D.; Mendiara, T.; Abad, A.; de Diego, L. F.; García-Labiano, F.; Gayán, P.; Adánez, J.; Zhao, H. Evaluation of Manganese Minerals for Chemical Looping Combustion. *Energy & Fuels* **2015**, *29* (10), 6605–6615. https://doi.org/10.1021/acs.energyfuels.5b01293.
(326) Adánez-Rubio, I.; Pérez-Astray, A.; Mendiara, T.; Izquierdo, M. T.; Abad, A.; Gayán, P.; de Diego, L. F.; García-Labiano, F.; Adánez, J. Chemical Looping Combustion of Biomass: CLOU Experiments with a Cu-Mn Mixed Oxide. *Fuel Processing Technology* **2018**, *172*, 179–186. https://doi.org/10.1016/J.FUPROC.2017.12.010.
(327) Adánez, J.; Abad, A.; Mendiara, T.; Gayán, P.; de Diego, L. F.; García-Labiano, F. Chemical Looping Combustion of Solid Fuels. *Progress in Energy and Combustion Science* **2018**, *65*, 6–66. https://doi.org/10.1016/j.pecs.2017.07.005.
(328) Thunman, H.; Lind, F.; Breitholtz, C.; Berguerand, N.; Seemann, M. Using an Oxygen-Carrier as Bed Material for Combustion of Biomass in a 12-MWth Circulating Fluidized-Bed Boiler. *Fuel* **2013**, *113*, 300–309. https://doi.org/10.1016/J.FUEL.2013.05.073.
(329) Stenberg, V.; Rydén, M.; Mattisson, T.; Lyngfelt, A. Experimental Investigation of Oxygen Carrier Aided Combustion (OCAC) with Methane and PSA Off-Gas. *Applied Sciences* **2021**, *11* (1), 210. https://doi.org/10.3390/app11010210.
(330) Staničić, I.; Mattisson, T.; Backman, R.; Cao, Y.; Rydén, M. Oxygen Carrier Aided Combustion (OCAC) of Two Waste Fuels - Experimental and Theoretical Study of the

Interaction between Ilmenite and Zinc, Copper and Lead. *Biomass and Bioenergy* **2021**, *148*, 106060. https://doi.org/10.1016/j.biombioe.2021.106060.
(331) Rydén, M.; Hanning, M.; Lind, F. Oxygen Carrier Aided Combustion (OCAC) of Wood Chips in a 12 MWth Circulating Fluidized Bed Boiler Using Steel Converter Slag as Bed Material. *Applied Sciences* **2018**, *8* (12), 2657. https://doi.org/10.3390/app8122657.
(332) Rydén, M.; Hanning, M.; Corcoran, A.; Lind, F.; Rydén, M.; Hanning, M.; Corcoran, A.; Lind, F. Oxygen Carrier Aided Combustion (OCAC) of Wood Chips in a Semi-Commercial Circulating Fluidized Bed Boiler Using Manganese Ore as Bed Material. *Applied Sciences* **2016**, *6* (11), 347. https://doi.org/10.3390/app6110347.
(333) Fennell, P.; Anthony, B. *Calcium and Chemical Looping Technology for Power Generation and Carbon Dioxide (CO2) Capture*, 1st ed.; Fennell, P., Anthony, B., Eds.; Woodhead Publishing, 2015.
(334) Breault, R. W. *Handbook of Chemical Looping Technology*, 1st ed.; Breault, R. W., Ed.; Wiley-VCH, 2019.
(335) Adánez, J.; Abad, A. Chemical-Looping Combustion: Status and Research Needs. *Proceedings of the Combustion Institute* **2019**, *37* (4), 4303–4317. https://doi.org/10.1016/j.proci.2018.09.002.
(336) Song, T.; Shen, L. Review of Reactor for Chemical Looping Combustion of Solid Fuels. *International Journal of Greenhouse Gas Control*. Elsevier Ltd September 1, 2018, pp 92–110. https://doi.org/10.1016/j.ijggc.2018.06.004.
(337) Imtiaz, Q.; Hosseini, D.; Müller, C. R. Review of Oxygen Carriers for Chemical Looping with Oxygen Uncoupling (CLOU): Thermodynamics, Material Development, and Synthesis. *Energy Technology* **2013**, *1* (11), 633–647. https://doi.org/10.1002/ente.201300099.
(338) Mattisson, T. Materials for Chemical-Looping with Oxygen Uncoupling. *ISRN Chemical Engineering* **2013**, *2013*, 1–19. https://doi.org/10.1155/2013/526375.
(339) Whitty, K. J.; Lighty, J. S.; Mattisson, T. Chemical Looping with Oxygen Uncoupling (CLOU) Processes. In *Handbook of Chemical Looping Technology*; Breault, R. W., Ed.; Wiley-VCH: Weinheim, Germany, 2019; pp 93–122.
(340) Zhao, X.; Zhou, H.; Sikarwar, V. S.; Zhao, M.; Park, A.-H. A.; Fennell, P. S.; Shen, L.; Fan, L.-S. Biomass-Based Chemical Looping Technologies: The Good, the Bad and the Future. *Energy & Environmental Science* **2017**, *10* (9), 1885–1910. https://doi.org/10.1039/C6EE03718F.
(341) Gogolev, I.; Linderholm, C.; Gall, D.; Schmitz, M.; Mattisson, T.; Pettersson, J. B. C.; Lyngfelt, A. Chemical-Looping Combustion in a 100 kW Unit Using a Mixture of Synthetic and Natural Oxygen Carriers – Operational Results and Fate of Biomass Fuel Alkali. *International Journal of Greenhouse Gas Control* **2019**, *88*, 371–382. https://doi.org/10.1016/J.IJGGC.2019.06.020.
(342) Xing, J.; Luo, K.; Wang, H.; Gao, Z.; Fan, J. A Comprehensive Study on Estimating Higher Heating Value of Biomass from Proximate and Ultimate Analysis with Machine Learning Approaches. *Energy* **2019**, *188*, 116077. https://doi.org/10.1016/j.energy.2019.116077.
(343) Xing, J.; Luo, K.; Wang, H.; Jin, T.; Fan, J. A Novel Sensitivity Study for Biomass Directional Devolatilization by Random Forest Models. *Energy & Fuels* **2020**. https://doi.org/10.1021/acs.energyfuels.0c00822.
(344) Gulyurtlu, I.; Pinto, F.; Abelha, P.; Lopes, H.; Crujeira, A. T. 9 - Pollutant Emissions and Their Control in Fluidised Bed Combustion and Gasification. In *Fluidized Bed Technologies for Near-Zero Emission Combustion and Gasification*; Scala, F., Ed.; Woodhead Publishing Series in Energy; Woodhead Publishing, 2013; pp 435–480. https://doi.org/10.1533/9780857098801.2.435.
(345) Scala, F.; Chirone, R.; Salatino, P. 6 - Attrition Phenomena Relevant to Fluidized Bed Combustion and Gasification Systems. In *Fluidized Bed Technologies for Near-Zero Emission Combustion and Gasification*; Scala, F., Ed.; Woodhead Publishing Series in Energy; Woodhead Publishing, 2013; pp 254–315. https://doi.org/10.1533/9780857098801.1.254.

(346) Scala, F.; Chirone, R.; Salatino, P. Combustion and Attrition of Biomass Chars in a Fluidized Bed. **2006**. https://doi.org/10.1021/ef050102g.
(347) Bates, R. B.; Altantzis, C.; Ghoniem, A. F. Modeling of Biomass Char Gasification, Combustion, and Attrition Kinetics in Fluidized Beds. *Energy & Fuels* **2016**, *30* (1), 360–376. https://doi.org/10.1021/acs.energyfuels.5b02120.
(348) Hecht, E. S.; Shaddix, C. R.; Geier, M.; Molina, A.; Haynes, B. S. Effect of CO2 and Steam Gasification Reactions on the Oxy-Combustion of Pulverized Coal Char. *Combustion and Flame* **2012**, *159* (11), 3437–3447. https://doi.org/10.1016/j.combustflame.2012.06.009.
(349) Marek, E.; Świątkowski, B. Experimental Studies of Single Particle Combustion in Air and Different Oxy-Fuel Atmospheres. *Applied Thermal Engineering* **2014**, *66* (1), 35–42. https://doi.org/10.1016/j.applthermaleng.2014.01.070.

## *TOC Graphic*

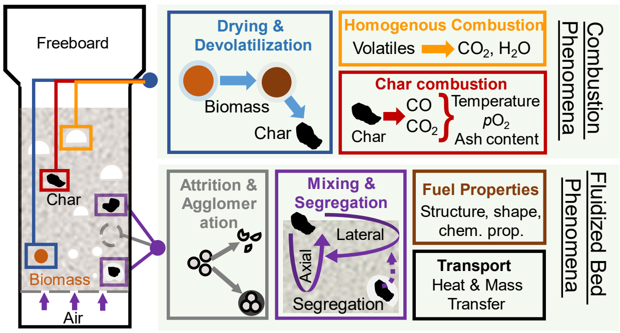

Freeboard
Char
Biomass
Air
Drying & Devolatilization
Biomass
Char
Homogenous Combustion
Volatiles $CO_2$, $H_2O$
Char combustion
Char
CO
$CO_2$
Temperature
$pO_2$
Ash content
Combustion Phenomena
Attrition & Agglomeration
Mixing & Segregation
Lateral
Axial
Segregation
Fuel Properties
Structure, shape, chem. prop.
Transport
Heat & Mass Transfer
Fluidized Bed Phenomena